Evaluation of nutritional modes of orchids associate with rhizoctonia: testing and application of stable isotope analysis

八木, 龍太

(Degree)
博士（理学）

(Date of Degree)
2024-09-25

(Date of Publication)
2025-09-01

(Resource Type)
doctoral thesis

(Report Number)
甲第8998号

(URL)
https://hdl.handle.net/20.500.14094/0100492507

博士論文

Evaluation of nutritional modes of orchids associate with rhizoctonia: testing and application of stable isotope analysis

リゾクトニアと共生するラン科植物の栄養摂取様式：

安定同位体分析を用いた推定手法の検証と応用

令和 6 年 7 月

神戸大学大学院理学研究科

八木龍太

Ryuta YAGI

Contents

Abstract

全ての陸上植物の 90%以上が菌根共生を行ない，自らの光合成産物を菌類から受け取る土壌の水や無機塩類と交換している．しかしラン科植物では，共生相手である菌類を有機物源として利用する菌従属栄養性が進化しており，少なくとも全ての種が発芽時に菌従属栄養性を示す．

1 章では，菌根共生系とラン科植物の菌従属栄養性に関する概観を述べた．ラン科植物は 28000 種以上からなる多様な分類群であり，その大部分は「リゾクトニア」と呼ばれる菌類と菌根共生するが，一部の種はリゾクトニア以外の外生菌根菌や木材腐朽菌などとも共生する．また，それら非リゾクトニア菌と共生するラン科植物はほぼ例外なく，葉を持つ成熟期にも菌への寄生性を示す（部分的菌従属栄養）か，あるいは光合成を完全にやめて菌類に有機物を依存する（完全菌従属栄養）ことが知られている．系統解析によって，このような進化はラン科の中で少なくとも 17 回以上独立に起こったことが示唆されており，また非リゾクトニア菌との共生は，リゾクトニアの共生より派生的な生態形質であることが示されている．以上よりラン科では，様々な系統の菌類の利用やより多くの栄養を獲得することが可能となる進化が，種の多様化に伴って段階的に起こってきたと考えられている．成熟期の菌従属栄養の進化が段階的に起こったことを考慮すると，非リゾクトニア菌への共生菌シフトが起こる以前に，リゾクトニアと共生するラン科植物においても広く部分的菌従属栄養性が獲得されていた可能性が考えられる．しかし，リゾクトニアと共生するラン科植物の栄養摂取様式は炭素・窒素安定同位体比によって調べられてきたが，菌からの炭素獲得を直接的に示す炭素同位体比の分離能が低いことから，その実態は議論の対象となっている．そこで本章では，リゾクトニアと共生するラン科植物においては，安定同位体分析の菌従属栄養性の推定手法としての妥当性を検証したうえで，複数系統のラン科植物への適用を行なう重要性を指摘した．

2 章では，水素安定同位体分析がラン科植物の栄養摂取様式推定に有効であるかを，交換性水素の影響に着目して検討した．リゾクトニアと共生するラン科植物においては，特に炭素同位体比の分離能の低さに起因する栄養摂取様式推定の難しさを受けて，近年水素安定同位体を利用した手法の活用が提唱された．しかし，それらの先行研究では推定結果に影響を与えうる交換性水素に関する考慮がなされていないという問題があった．そこで本章では，交換性水素画分を操作したサンプルを用いて，交

換性水素の存在が推定結果に与える影響を調査した．それにより，交換性水素は推定に大きな影響を与えず，簡便なバルクサンプルを用いた分析方法の有効性が示された．

3章では，複数系統のラン科植物の菌根菌相と栄養摂取様式を，特に研究例が不足している亜熱帯・暖温帯アジア圏の種を対象に調査した．ラン科植物のほとんどは菌根菌相が未解明であることから，対象とした 13 種のラン科植物の菌根菌相を次世代シーケンサーによる DNA バーコーディングを行なうことで，リゾクトニアと共生するランであることを確認した．そのうえで，2章で示された水素安定同位体分析の有効性に基づき，ランの炭素，窒素，水素安定同位体分析比を分析し，独立栄養植物の値と比較した．その結果，7種のラン科植物において部分的菌従属栄養性が示唆された．リゾクトニアと共生するラン科植物において広く部分的菌従属栄養性が獲得されていることが示唆されたことは，比較的祖先的なラン科植物における部分的菌従属栄養性が，複数系統において共生菌のシフトを伴う菌への依存度の上昇が起こる上での前適応として働いたことを示唆している．また，アジア圏に分布するラン科植物において幅広く部分的菌従属栄養性が獲得されていることを示した本研究は，温暖・湿潤な当該地域において，腐朽菌を利用した菌従属栄養性が進化しやすいとした先行研究の予想に合致する結果といえる．

4章では，各章の結果をまとめ，ラン科植物の栄養摂取様式研究における今後の方向性について議論した．ラン科植物の炭素同位体比が独立栄養植物と比べて差がみられなくとも菌由来有機物の獲得は否定されないことから，リゾクトニアと共生するラン科植物の栄養摂取様式の推定は，炭素同位体比の後に窒素，水素同位体比を比較するといった段階を分けて実施することが有効だと考えられる．この手法を利用することにより，ラン科という多様な系統内でどのように部分的菌従属栄養性が分布しているかを詳細に明らかにし，菌従属栄養性の進化過程を理解することが可能となると考えられる．

Chapter 1

General introduction

Mycorrhizal symbiosis

Land plants are well known for their close interaction with fungi in their natural habitats, exchanging nutritional resources with fungi through a symbiotic interface in the plant roots. This interaction, known as mycorrhizal symbiosis, is generally considered a mutualistic nutrient trade in which plants provide photosynthates to their mycorrhizal partners, while mycorrhizal fungi supply water and mineral nutrients from the surrounding soil to the plants (Smith *et al.*, 2009).

Mycorrhizal symbiosis is a widespread mutualistic relationship found in over 90% of land plants, excluding non-mycorrhizal species like Brassicaceae or Cyperaceae (Merckx, 2013). A phylogenetically wide range of fungi also associates with plants, including arbuscular mycorrhizal fungi (Glomeromycota), which form distinctive structures called arbuscules and vesicles in the root cells of various plants. Some Basidiomycota fungi also form ectomycorrhizae with trees such as Fagaceae and Pinaceae, where fungal hyphae surround but do not penetrate into plant root cells. Additionally, ericoid mycorrhiza, observed in ericaceous plants, is formed by various Ascomycota fungi.

Mycoheterotrophy

Mycorrhizal symbiosis is commonly considered a mutualistic interaction. However, some plants exploit fungal partners for both organic and inorganic nutrients, a nutritional strategy known as mycoheterotrophy (Leake, 1994). Researchers categorize mycoheterotrophy based on the degree of carbon dependence (Hynson *et al.*, 2013),

ranging from initial mycoheterotrophy (plants utilize fungal carbon only during the germination stage) to partial mycoheterotrophy (plants acquire carbon from both photosynthesis and mycorrhizal fungi), and full mycoheterotrophy (plants rely entirely on fungi for organic and inorganic nutrition). Full mycoheterotrophy has independently evolved in plant lineages at least 47 times (Merckx *et al.*, 2013b), leading to a wide range of plants, including liverworts, monocots, and eudicots, exhibiting this nutritional strategy.

Mycoheterotrophy in Orchidaceae

Orchidaceae is a highly diverse plant family, comprising over 28,000 species (Givnish *et al.*, 2015). Mycoheterotrophy has notably evolved in this family; all orchids lack nutrient storage in their seeds and rely on fungal carbon during germination. Some green species are reported to be partially mycoheterotrophic, utilizing both photosynthetic and fungal carbon during the adult stage (e.g. Gebauer & Meyer, 2003). Full or nearly full mycoheterotrophy, in which plants entirely depend on their carbon demand on fungi, has independently evolved in Orchidaceae at least 17 times, resulting in about 235 species (Merckx *et al.*, 2013a; Wang *et al.*, 2021).

In orchid mycorrhiza, fungal hyphae penetrate orchid root cells and form a coiling structure known as pelotons (Rasmussen & Rasmussen, 2009). Orchids associate with diverse fungi, primarily saprotrophic (SAP) rhizoctonia (Ceratobasidiaceae and Tulasnellaceae from Canthallerales, and Serendipitaceae from Sebacinales). Orchids also associate with ectomycorrhizal fungi, as well as non-rhizoctonia SAP fungi that do not usually form mycorrhizal relationships with plants (reviewed in (Ogura-Tsujita *et al.*,

2021).

An intriguing aspect of the evolutionary process in Orchidaceae is that fungal partner switches during shifts in trophic modes. Phylogenetic analysis based on fungal functional guilds revealed that the association of orchids with rhizoctonia is an ancestral ecological trait, while the association with ectomycorrhizal or non-rhizoctonia SAP fungi is derivative. Additionally, orchids associate with ectomycorrhizal/non-rhizoctonia SAP fungi are arguably mycoheterotrophic during their adult stage (Gebauer & Meyer, 2003; Yagame *et al.*, 2012; Ogura-Tsujita *et al.*, 2021; Suetsugu *et al.*, 2022a). This may suggest that rhizoctonia-associated orchids have already acquired the ability to exploit fungal carbon in their developed stage (i.e., partial mycoheterotrophy), which may serve as a preadaptation for the evolutionary shift toward full mycoheterotrophy.

Although the nutritional modes of orchids have been studied using a stable isotope approach for over two decades, the nutritional modes of orchids associated with rhizoctonia remain poorly understood, primarily due to the low resolution of estimates from carbon and nitrogen stable isotope ($\delta^{13}C$, $\delta^{15}N$) analysis, as detailed in Chapter 2. Understanding their nutritional strategy is important for elucidating the evolutionary process of mycoheterotrophy in the Orchidaceae, providing fundamental insights into how the ability to exploit fungi has evolved within this plant family.

Issues addressed in this thesis

In this thesis, I aimed to comprehend the nutritional strategy of orchids associated with rhizoctonia fungi.

In Chapter 2, I investigated the efficacy of hydrogen stable isotope analysis for assessing plant nutritional modes. While traditional stable isotope analysis struggles to accurately evaluate the nutritional strategy of rhizoctonia-associated orchids due to low discrimination ability in carbon stable isotope ratio, recent studies propose hydrogen stable isotope (δ^2H) analysis as a promising alternative (Gebauer *et al.*, 2016). However, previous research has often overlooked the impact of exchangeable hydrogens on estimation accuracy. This chapter addresses this oversight and confirms δ^2H analysis as a useful method for estimating plant nutritional modes.

In Chapter 3, I estimated the nutritional modes of various orchid species from the subtropical region of Japan, given that such warm and humid environmental conditions in the region are believed to drive the evolution of mycoheterotrophy dependent on saprotrophic fungi like rhizoctonia. Selecting orchid species likely associated with rhizoctonia based on phylogenetic data within the Orchidaceae (Wang *et al.*, 2021), I identified their mycorrhizal fungi using high-throughput sequencing. Building upon the effectiveness of hydrogen isotope analysis suggested in the previous chapter, I conducted comprehensive δ^{13}C, δ^{15}N, and δ^2H stable isotope analysis. Subsequently, I discussed their nutritional modes based on mycorrhizal information and stable isotope ratios.

In Chapter 4, based on the insights described in Chapters 2 and 3, I discussed the following points: (1) the effectiveness of δ^2H analysis and the potential driver of ^{2}H enrichment in orchids, (2) the nutritional strategy of orchidaceous plants investigated in this study, based on their taxonomic groups and the environmental conditions of their habitat, and (3) future directions in the research fields of plant nutritional modes.

Chapter 2

Do exchangeable hydrogens affect the evaluation of partial mycoheterotrophy in orchids?: Insights from δ^2H analysis in bulk, α-cellulose, and cellulose nitrate samples

Introduction

The plant family, Orchidaceae, is present on all continents except Antarctica and comprises over 28,000 species (Givnish *et al.*, 2015). These highly successful plants have a notable ecological trait known as mycoheterotrophy (Leake, 1994; Bidartondo, 2005, Merckx 2013), through which they obtain organic resources from mycorrhizal fungi. Mycoheterotrophy is observed in all orchids, at least during their germination stage, because of their small seed size, referred to as dust seeds, which lack endosperm or cotyledons for storing nutrients required for germination. During their developmental stages, each orchid species exhibits various nutritional modes. While most green-leaved orchids are considered autotrophic, some orchids show partial mycoheterotrophy (or mixotrophy, Hynson *et al.*, 2013), utilizing photosynthetic and fungal carbon sources. Additionally, certain orchids exhibit full mycoheterotrophy, losing their photosynthetic ability and relying entirely on mycorrhizal fungi for their carbon supply.

Fully mycoheterotrophic orchids can be readily discerned by the absence of normal leaves, unequivocally signifying their distinctive nutritional strategy. However, determining the nutritional mode of most chlorophyllous orchids solely based on their appearance is challenging. Consequently, stable isotope analysis has frequently been used to estimate the nutritional mode of green-leaved orchids, since partially mycoheterotrophic orchids show higher stable isotope ratios than obligate autotrophic plants, reflecting the acquisition of fungal organic compounds enriched in heavy stable isotopes. Through this method, some orchids, such as *Cephalanthera falcata* (Gebauer & Meyer, 2003; Sakamoto *et al.*, 2016), reportedly exhibit partial mycoheterotrophy despite

their relatively broad leaves. Conversely, *Goodyera repens*, which has somewhat small leaves, is identified as an autotrophic plant, based on its ^{13}C and ^{15}N abundances (Hynson *et al.*, 2009; Liebel *et al.*, 2015). Indeed, radioactive tracer experiments demonstrated the autotrophy of *G. repens* under cultivated conditions (Cameron *et al.,* 2006, 2008).

Orchids associate with various mycorrhizal fungi. The most common symbionts are Basidiomycota fungi known as 'rhizoctonia' from Ceratobasidiaceae, Tulasnellaceae (Cantharellales), and Serendipitaceae (Sebacinales, Dearnaley *et al.*, 2012). These fungi exhibit various functional traits, including saprotrophy (SAP), formation of ectomycorrhiza with trees (ECM), and plant endophyte (Dearnaley *et al.*, 2012). In contrast, some orchids associate with ECM-forming rhizoctonia and non-rhizoctonia ECM fungi, which typically form ectomycorrhizas with trees. For example, *Cephalanthera* spp. reportedly associates with diverse ECM fungi (Bidartondo *et al.*, 2004). *Platanthera bifolia* and *Apostasia nipponica* have also been reported to be associated with ECM-forming rhizoctonia (Ceratobasidiaceae, Yagame *et al.*, 2012; Suetsugu & Matsubayashi, 2021). Additionally, some previous studies suggest that non-rhizoctonia SAP fungi can be recruited as orchid mycorrhizal fungi in at least nine orchid clades (Ogura-Tsujita *et al.*, 2021).

Many previous studies have indicated that most chlorophyllous orchids associated with ECM or non-rhizoctonia SAP fungi arguably exhibit partial mycoheterotrophy, based on their high $\delta^{13}C$ and $\delta^{15}N$ compared with their surrounding autotrophic plants (Gebauer & Meyer, 2003; Ogura-Tsujita *et al.*, 2012; Sakamoto *et al.*, 2016; Suetsugu *et al.*, 2021b; Suetsugu & Matsubayashi, 2021b,a; Suetsugu *et al.*, 2022). In contrast, it

remains elusive whether orchids associated with SAP rhizoctonia fungi exhibit partial mycoheterotrophy based on ^{13}C abundance. Albino mutants of some SAP rhizoctonia-associated orchids have been discovered within their natural habitats (Suetsugu *et al.*, 2019, 2021c). These mutants exhibit higher $\delta^{13}C$ and $\delta^{15}N$ than the neighboring autotrophic plants, indicating the ability to exploit fungi. Moreover, some rhizoctonia-associated orchids have been proposed to be partially mycoheterotrophic based on consistently high $\delta^{13}C$ and $\delta^{15}N$, even under natural light conditions (Suetsugu *et al.*, 2021c; Suetsugu & Matsubayashi, 2022; Yagi *et al.*, 2022). However, for most SAP rhizoctonia-associated orchids, the nutritional mode remains unclear because these orchids occasionally exhibit elevated nitrogen content and $\delta^{15}N$, and maintain similar or even lower $\delta^{13}C$ than autotrophic plants (Hynson *et al.*, 2013). Orchids displaying such stable isotope signatures and nitrogen content are referred to as 'cryptic mycoheterotrophs,' presumed to be partially mycoheterotrophic; however, the evidence is inconclusive (Hynson *et al.*, 2013).

To address this limitation, researchers have used hydrogen stable isotope ratio ($\delta^{2}H$) analysis as an alternative to that of $\delta^{13}C$ to assess the nutritional mode of orchids associated with SAP rhizoctonia fungi (Gebauer *et al.*, 2016). This approach is based on the model proposed by Yakir (1992), which suggests that secondary heterotrophic organic compounds, such as those derived from fungi, exhibit ^{2}H enrichment. This method has enabled estimating the nutritional mode of SAP rhizoctonia-associated orchid species that do not exhibit ^{13}C enrichment. The $\delta^{2}H$ analysis has suggested that several SAP rhizoctonia-associated orchids are partially mycoheterotrophic (Schiebold *et al.*, 2018;

Schweiger *et al.*, 2018, 2019). Partial mycoheterotrophy *sensu lato (s.l.)* is defined as the condition in which plants obtain carbon from fungi (Merckx, 2013), including scenarios of bidirectional carbon movement between the plant and fungi (carbon exchangers) (Lallemand *et al.*, 2017). There is ongoing debate regarding the feasibility of using hydrogen isotope measurements to estimate partial mycoheterotrophy, particularly because it can be challenging to ascertain the net direction of carbon flow (Lallemand *et al.*, 2017; Jacquemyn *et al.*, 2021). Nonetheless, given that secondary heterotrophic organic compounds derived from fungi typically show ^{2}H enrichment (Yakir, 1992), this enrichment probably serves as an indicator of plants obtaining carbon from fungi, even when the precise dynamics of new carbon flow are unclear. Therefore, similar to other recent studies (Gebauer *et al.*, 2016; Schiebold *et al.*, 2018; Schweiger *et al.*, 2018, 2019; Giesemann *et al.*, 2020; Zahn *et al.*, 2023), we consider plants with significant enrichment in ^{2}H plausible candidates for partial mycoheterotrophy *s.l.*

Although the application of $\delta^{2}H$ analysis has provided possible new insights into the nutritional modes of SAP rhizoctonia-associated orchids, previous studies did not sufficiently address two analytical challenges. First, nitrogen-containing compounds can form hydrogen cyanide under the thermal conversion elemental analyzer (TC/EA) conditions, causing fractionation of ^{2}H. To mitigate this concern, it is recommended to use a chromium (Cr) reactor for $\delta^{2}H$ analysis of nitrogen-containing organic compounds (Gehre *et al.*, 2015). Second, exchangeable hydrogen, represented by the H atom in hydroxyl (OH) groups, is readily exchanged with the H atoms in atmospheric water vapor, affecting the $\delta^{2}H$ of samples.

As the contribution of the OH fraction to total hydrogen differs among standard reference materials or plant species, this inter-sample difference can cause inconsistent hydrogen exchangeability (Epstein *et al.*, 1976). Therefore, studies that involve analyzing plant δ^2H are conducted using two primary methods to address this heterogeneity. One commonly used method involves synthesizing cellulose nitrate from plant cellulose (e.g., Epstein *et al.*, 1976; Sternberg *et al.*, 1984). This process allows for the determination of the δ^2H of non-exchangeable hydrogen by replacing -OH with -O-NO_2. Another approach is to equilibrate the exchangeable hydrogen in samples with standard water of known isotope composition and calculate the δ^2H of non-exchangeable hydrogen (e.g., Filot *et al.*, 2006; Wassenaar *et al.*, 2015).

The limitation of previous studies that involved assessing δ^2H in heterotrophic plants (Gebauer *et al.*, 2016; Schiebold *et al.*, 2018; Schweiger *et al.*, 2018, 2019; Giesemann *et al.*, 2020; Zahn *et al.*, 2023) was that they primarily relied on the δ^2H of bulk samples (excluding Cormier *et al.*, 2019), leading to some uncertainty in their data. Measuring bulk δ^2H is more cost-effective because the extraction and nitration of cellulose are time-consuming. While the equilibrium method can address the difference in exchangeable hydrogen fractions between bulk samples and standard materials, it is also time-consuming or requires specific systems that enable rapid sample equilibration (Filot *et al.*, 2006; Wassenaar *et al.*, 2015; Schuler *et al.*, 2022). Therefore, if the bulk δ^2H analysis aligns well with other analytical methods, it can aid in interpreting data from previous studies and accelerate the progress of those of the future.

Considering these factors, we collected orchids and their reference autotrophs

and manipulated the exchangeable hydrogen fractions of these samples in three ways: non-manipulation (bulk), single compound extraction (α-cellulose), and elimination (cellulose nitrate). By analyzing the δ^2H of these samples, we aimed to determine whether the manipulations of exchangeable hydrogen would exert a discernible influence on the estimation of the nutritional strategies of these plants.

Material and Methods

Sampling scheme

Plant samples were collected from the wild habitats of a temperate forest floor in Chiba (June 13th, 2019) and Hyogo (September 21st, 2021) Prefectures, Japan (Table 1). We established 1 × 1 m sampling plots in these habitats and collected orchids and their reference autotrophs (Table 1). Briefly, we selected two orchid species, *Calanthe discolor* (associates with SAP fungi, (Jae-Young *et al.*, 2012), and putatively is a 'cryptic mycoheterotroph') and *Gastrodia pubilabiata* (associates with saprotrophic Agaricales fungi such as *Mycena* and Marasmiaceae, Kinoshita *et al.*, 2016), to represent rhizoctonia-associated and fully mycoheterotrophic orchids, respectively. We specifically collected present-year leaves at the same height to reduce the sampling bias caused by environmental heterogeneity (Gebauer & Meyer, 2003). However, for *G. pubilabiata*, which is leafless, we collected the whole plant body except for the roots. The collected samples were dried at 65 °C overnight, ground with an agate mortar and pestle, and stored

in glass vials until analysis.

Sample pretreatment for stable isotope analysis

The samples underwent three pretreatment forms: bulk, α-cellulose, and cellulose nitrate. The bulk treatment involved grinding dry leaves with an agate mortar and pestle and contained exchangeable hydrogens with various fractions. Although the extracted α-cellulose contained exchangeable hydrogens, we can exclude differences in its inter-sample fractions. To extract α-cellulose from bulk samples, we modified the Jayme–Wise method from previous studies (Green, 1963; Gaudinski *et al.*, 2005). Briefly, we used glass SPE reservoirs (GL Science, Tokyo, Japan) equipped with glass filters as alternatives to Soxhlet thimbles described by Loader *et al.* (1997). Samples were placed into these reservoirs and simmered with deionized water at 80 °C to remove water-soluble compounds; this was repeated until the discarded water became transparent. Subsequently, samples were treated with sodium hypochlorite four times at 75 °C to remove lignin. Next, delignified samples were processed with a 2:1 toluene/ethanol mixture overnight to remove lipids. Finally, the acquired holocellulose was treated with 17.5% NaOH three times, followed by neutralization with acetic acid and thorough rinsing with deionized water.

The δ^2H of cellulose nitrate is derived from non-exchangeable hydrogens since it lacks a hydroxyl group. Extracted α-cellulose was subsampled and nitrated according to the method of Alexander & Mitchell (1949). We prepared an acid mixture of 64% HNO_3, 26% H_3PO_4, 10% P_2O_5 and added it into the glass reservoir, allowing nitration for 24 h at

-5 °C. Nitrated samples were washed with 50 % (v/v) acetic acid, neutralized with $NaCO_3$, and stabilized with deionized water and methanol. The nitrated product was purified by dissolving it in acetone (5 ml) and separating it in a large volume (at least 50 ml) of deionized water. Bulk, α-cellulose, and cellulose nitrate products were stored in glass vials and redried overnight at 50 °C just before weighing.

Selection of standard reference materials for calibrating δ^2H

The C and N isotopic ratios were calibrated using laboratory standards: CERKU-02 (*L*-alanine, δ^{13}C = −19.04‰, δ^{15}N = 22.71‰), CERKU-03 (glycine, δ^{13}C = −34.92‰, δ^{15}N = 2.18‰) and CERKU-05 (threonine, δ^{13}C = −9.45‰, δ^{15}N = −2.88‰), which are traceable to international standards (Tayasu *et al.*, 2011).

As mentioned in the introduction, the inter-sample difference in OH fraction causes different hydrogen exchangeability. Therefore, we carefully selected three reference materials, IAEA-CH-7 (polyethylene film, δ^2H = −100.3‰, IAEA, 2007), USGS61 (caffeine, δ^2H = 96.9‰, Coplen, 2019) and USGS62 (caffeine, δ^2H = −156.1‰, Coplen, 2019), to calibrate the δ^2H of cellulose nitrate. We used both nitrogen-free (IAEA-CH-7) and nitrogen-containing compounds (USGS61-62) to confirm the effect of the Cr method (Gehre *et al.*, 2015). Since cellulose nitrate lacks OH groups, its accurate δ^2H can be calibrated using the selected standard reference materials that also lack exchangeable hydrogen.

Calibrating bulk δ^2H with standard reference materials that lack exchangeable hydrogens is challenging due to the different exchangeable hydrogen fractions. Despite

this, we calibrated bulk δ^2H using IAEA-CH-7 and USGS61-62 to facilitate the discussions of previous studies where calibration was conducted with reference standards containing only non-exchangeable hydrogens. Additionally, we selected USGS54 (Canadian lodgepole pine, δ^2H = 150.4‰, Qi *et al.*, 2016) and USGS55 (Mexican ziricote, δ^2H = −28.2‰, Qi *et al.*, 2016) as standard reference materials to calibrate bulk samples (but only for *C. discolor* and its references owing to the limited quantity of *G. pubilabiata* samples). These standards are designed for calibrating isotopically unknown whole wood samples and contain exchangeable hydrogens, although their fraction presumably differs from those of bulk leaf samples because of the difference in chemical composition.

Stable isotope analysis for δ^{13}C, δ^{15}N, and δ^2H

All stable isotope ratio and nitrogen concentration measurements were conducted at the Research Institute for Humanity and Nature (Kyoto, Japan). For δ^{13}C and δ^{15}N analyses, approximately 0.3–3 mg of bulk samples were weighed into tin capsules. The relative abundances of ^{13}C and ^{15}N and the nitrogen concentrations were measured using the Delta V Advantage mass spectrometer connected to a Flash EA 1112 elemental analyzer via the ConFlo IV interface (all Thermo Fisher Scientific, Waltham, Massachusetts, USA).

The equilibration with ambient vapor for exchangeable hydrogen was performed based on the method of Gebauer *et al.* (2016) with slight modifications. Samples (approximately 0.2 mg for bulk and α-cellulose and 0.5 mg for cellulose nitrate) were weighed into silver capsules. These capsules were wrapped loosely to allow water vapor to enter but prevent the loss of sample material. Subsequently, the weighed capsules were

freeze-dried overnight, and the exchangeable hydrogens within the samples were equilibrated. To approximate conditions similar to those of previous studies that did not achieve equilibrium, we conducted equilibration with atmospheric water vapor for one week, instead of using the hot vapor method. The equilibrated samples underwent freeze-drying overnight again and were quickly set to the Costech Zero Blank Autosampler (Pelican Scientific Ltd., Alford, UK), which was coupled to TC/EA. Because post-wrapping bias caused by atmospheric vapor cannot be perfectly eliminated, orchids and their respective autotrophic references were analyzed together, as much as possible, in the same batches.

Hydrogen stable isotope ratios were analyzed using a Delta V Advantage mass spectrometer coupled to a pyrolysis elemental analyzer TC/EA via the ConFlo IV interface (all Thermo Fisher Scientific, Waltham, Massachusetts, USA). We used the Cr reactor method to avoid the bias of δ^2H caused by nitrogen or halogen in organic samples (Gehre *et al.*, 2015, Fig. S1). The temperatures of the gas chromatography column and Cr reactor were set to 90°C and 1250 °C, respectively. Each sample was analyzed only once in the batches, unlike Gebauer *et al*. (2016) and Cormier *et al*. (2019), who analyzed each sample three times because our preliminary experiments did not show a noticeable memory bias of δ^2H derived from previous samples (Olsen *et al.*, 2006) under our experimental conditions.

The relative abundances of the stable isotopes were calculated as δ^{13}C, δ^{15}N or δ^2H $= (R_{sample}/R_{standard} - 1) \times 1000$ [‰], where R_{sample} represents the $^{13}C/^{12}C$, $^{15}N/^{14}N$, or $^{2}H/^{1}H$ ratio of the sample, and $R_{standard}$ represents the $^{13}C/^{12}C$ ratio of Vienna Pee Dee Belemnite,

the $^{15}N/^{14}N$ ratio of atmospheric N_2, or the $^{2}H/^{1}H$ ratio of Vienna Standard Mean Ocean Water (VSMOW). The analytical standard deviation of international standard materials is presented in Table S6.

In addition, enrichment factors (ε) *sensu* Preiss and Gebauer (2008) were calculated from the δ values of each plant group based on $\varepsilon X = \delta X_S - \delta X_{REF}$, where δX_S represents $\delta^{13}C$, $\delta^{15}N$, or the $\delta^{2}H$ of bulk, α-cellulose, or cellulose nitrate prepared from *C. discolor* or *G. pubilabiata,* and δX_{REF} represents the mean $\delta^{13}C$, $\delta^{15}N$, or $\delta^{2}H$ of all autotrophic reference plants from a specific sampling plot.

Statistical analysis

All statistical analyses described below were performed using R v.4.3.1 (R Development Core Team, 2023). We conducted multiple comparisons of the relative abundances of bulk ^{13}C and ^{15}N and the nitrogen concentration between orchids and their autotrophic references using the lmer function (implemented in the lme4 package), including 'plot' as the random effect of our model. *P*-values were calculated using a post-hoc *t*-test with Satterthwaite's approximation using the R package lmerTest (Kuznetsova 2015). Similarly, the $\delta^{2}H$ calibrated using the IAEA-CH-7 and USGS 61-62 standard sets derived from each treatment were compared.

The comparison of bulk $\delta^{2}H$ corrected using different standard sets (IAEA-CH-7, USGS 61-62, or USGS54-55 set) was conducted to confirm the effect of the hydrogen exchangeability of international standard materials. We assigned 'standard set' as explanatory variables and fitted linear mixed models, including 'plot' and 'species' as

random effects. Furthermore, we compared δ^2H calibrated using the USGS54-55 set based on the sample type (orchid vs. autotrophs), with 'plot' included as a random effect, in order to test whether the -OH fraction of standard materials significantly alters the estimation results.

Additionally, we assessed the ability of δ^{13}C, δ^{15}N, δ^2H derived from each treatment and nitrogen concentration to discriminate among plant nutritional modes. This evaluation was conducted based on the regression coefficients calculated using the lmer function from z-score normalized response variables (i.e., δ^{13}C, δ^{15}N, N mmol/g, δ^2H of bulk (δ^2H_{bulk}), α-cellulose ($\delta^2H_{cellulose}$), or cellulose nitrate ($\delta^2H_{nitrate}$) due to the differing ranges of these values. The closer the regression coefficient is to 0, the lower the discrimination ability of the nutritional mode; the further above from 0, the better the nutritional mode is discriminated.

Results

δ^{13}C, δ^{15}N, and nitrogen concentration of bulk samples

The mean ± SD and results of the lmer function for δ^{13}C and δ^{15}N and the nitrogen concentrations of all plant species collected in this study are summarized in Table 2. *Calanthe discolor* showed significantly higher δ^{15}N ($p < 0.003$) and nitrogen concentration ($p = 0.032$; Fig. 1, Table 2) than autotrophic plants. However, the δ^{13}C of *C. discolor* was significantly lower than those of autotrophs ($p = 0.003$; Fig. 1, Table 2). The mean enrichment factors of *C. discolor* were as follows: $\varepsilon^{13}C = -1.8 \pm 0.5$ ‰, ε^{15}N

= 3.6 ± 0.8 ‰ (Table S3).

In contrast, *G. pubilabiata* exhibited significantly higher $\delta^{13}C$ ($p < 0.001$) and $\delta^{15}N$ ($p = 0.006$) and nitrogen concentrations ($p = 0.025$) than those of autotrophic reference plants (Fig. 1, Table 2). The mean enrichment factors of *G. pubilabiata* were as follows: $\varepsilon^{13}C$ = 9.3 ± 1.2 ‰, $\varepsilon^{15}N$ = 2.3 ± 1.1 ‰ (Table S3).

Stable hydrogen isotope ratios of bulk, α-cellulose, and cellulose nitrate

The mean $\delta^{2}H$ ± SD of *C. discolor*, *G. pubilabiata*, and their autotrophic reference species for each treatment are summarized in Fig. 2 and Table 2. The $\delta^{2}H$ of *C. discolor* was significantly higher than those of autotrophic references in all treatments (bulk; $p < 0.001$, α-cellulose; $p = 0.003$, cellulose nitrate; $p < 0.001$, Table 2). Similarly, *G. pubilabiata* showed significantly higher $\delta^{2}H$ than autotrophs (bulk; $p < 0.001$, α-cellulose; $p < 0.001$, cellulose nitrate; $p < 0.001$, Table 2).

The $\varepsilon^{2}H$ of *C. discolor* were as follows: for bulk; 22.8 ± 4.2‰, for α-cellulose; 42.0 ± 25.1‰, and for cellulose nitrate; 45.9 ± 27.3‰ respectively. Similarly, $\varepsilon^{2}H$ values for *G. pubilabiata* vs. autotrophic references were as follows; 68.4 ± 8.9‰ for bulk samples, 56.1 ± 18.8‰ for α-cellulose samples, and 67.0 ± 4.2‰ for cellulose nitrate samples, respectively.

Comparison of calibrated $\delta^{2}H$ values using international standards with or without exchangeable hydrogens

The mean $\delta^{2}H$ ± SD of all bulk samples calibrated using IAEA-CH-7 and USGS 61−62

was −71.2 ± 12.2‰, significantly differing ($p < 0.001$, Table 3) from the −78.3 ± 12.8‰ calibrated with the wood standard materials USGS 54−55.

The comparison of δ^2H, calibrated using the USGS 54−55 set indicated that *C. discolor* shows significantly higher δ^2H than autotrophs (−59.2 ± 4.8 ‰ vs −83.1 ± 9.1 ‰, $p < 0.001$, Table 3, Table S2). Therefore, the estimation aligns with the comparison of bulk δ^2H calibrated using the IAEA-CH-7 and USGS 61−62 set.

Discrimination abilities of δ^{13}C, δ^{15}N, δ^2H, and nitrogen concentrations for plant nutritional mode

The regression coefficients for all standardized response variables are presented in Table 4. All response variables, except for δ^{13}C in *C. discolor,* were greater than 1. The coefficient of δ^2H in both orchids demonstrated a high discrimination ability across all pretreatments (ranging from 1.705 to 2.130). In *C. discolor*, the coefficient for δ^{15}N (2.028) was comparable to that of δ^2H. However, for *G. pubilabiata*, the coefficient for δ^{15}N (1.129) was lower than that of δ^2H.

Discussion

The stable isotopic signatures and nitrogen concentrations observed in this study align with those reported in previous studies. Many studies have indicated that in orchids associated with rhizoctonia, the δ^{15}N and nitrogen concentrations are usually higher than those in autotrophs, whereas the δ^{13}C of such orchids do not differ significantly or are even lower than those of autotrophs (Hynson *et al.*, 2013; Gebauer *et al.*, 2016; Schiebold

et al., 2017, 2018; Schweiger *et al.*, 2018; Suetsugu *et al.*, 2021c). Our results also reveal that *C. discolor*, a rhizoctonia-associated orchid species (Jae-Young *et al.*, 2012), exhibited higher $\delta^{15}N$ and nitrogen concentrations but lower $\delta^{13}C$ than autotrophic references. Therefore, *C. discolor* is classified as a 'cryptic mycoheterotroph' according to Hynson *et al.* (2013).

Assuming that *C. discolor* is partially mycoheterotrophic, the lack of ^{13}C enrichment is somewhat enigmatic; however, this is likely due to fungi exhibiting significantly lower ^{13}C values compared to non-saprotrophic fungi. Pelotons extracted from rhizoctonia-associated orchids show notably low ^{13}C enrichments than pelotons of ectomycorrhizal fungi, ranging from 1.4–2.4‰ (Gomes *et al.*, 2023; Zahn *et al.*, 2023). Consequently, the minimal ^{13}C enrichment observed (< 3‰) probably limits the utility of ^{13}C enrichment as a nutritional indicator for assessing mycoheterotrophic carbon acquisition in rhizoctonia-associated orchids (Gomes *et al.*, 2023; Zahn *et al.*, 2023). The low ^{13}C enrichment of rhizoctonias is likely attributable to the somewhat endophytic niches they occupy (Selosse & Martos, 2014; Suetsugu *et al.*, 2019, 2021a). This hypothesis is supported by the tendency of endophytic associations to result in decreased ^{13}C levels (Halbwachs *et al.*, 2013; Selosse & Martos, 2014), as well as the frequent transitions from saprotrophy to endophytism observed in Veldre *et al.* (2013).

In contrast to *C. discolor*, $\delta^{13}C$, $\delta^{15}N$, and nitrogen concentrations of *G. pubilabiata* were higher than those of autotrophic references. Species of the genus *Gastrodia* are fully mycoheterotrophic, evidenced by their leafless, achlorophyllous nature and previous reports of reduced plastome genomes (Yuan *et al.*, 2018). *Gastrodia* spp. associate with

various wood/litter-decaying fungi, such as Mycenaceae or Marasmiaceae (Kinoshita *et al.*, 2016). Our results further corroborate that *G. pubilabiata* is a fully mycoheterotrophic species exploiting non-rhizoctonia SAP fungi, displaying typical isotopic signatures of orchids associated with such fungi — significantly differing from autotrophs in δ^{15}N; however, the ε^{15}N (2.3 ± 1.1 ‰) is not high as in ε^{13}C (9.3 ± 1.2 ‰, Hynson *et al.*, 2013). Notably, green-leaved *C. discolor* exhibited higher ε^{15}N (3.6 ± 0.8‰) than leafless *G. pubilabiata* (2.3 ± 1.1‰). The lower ^{15}N enrichment in *G. pubilabiata* may be associated with non-selective nitrogen acquisition from fungal hyphae, given that fully mycoheterotrophic orchids probably digest the entire fungal hyphae including chitin (Bougoure *et al.*, 2014), which has a lower δ^{15}N compared to amino acids (Taylor *et al.*, 1997; Hobbie *et al.*, 2012). On the other hand, *C. discolor* may selectively acquire amino acids from fungi that are typically SAP or endophytes, as suggested by Fochi *et al.*, (2017), resulting in higher ε^{15}N than *G. pubilabiata*.

Both orchids exhibited significantly higher δ^{2}H than autotrophic plants in bulk, α-cellulose, and cellulose nitrate treatments. Considering the hydrogen exchangeability of each sample and the international standard materials, the most accurate δ^{2}H are likely derived from cellulose nitrate, as it lacks exchangeable hydrogens, allowing for precise calibration using no-OH-containing standard materials (IAEA-CH-7 and USGS 61-62). In contrast, δ^{2}H derived from OH-containing bulk and α-cellulose samples may lack precision if calibrated using non-OH-containing standards. USGS54-55, which contains OH groups similar to bulk and α-cellulose samples, may offer a better calibration for these samples. However, we note that the δ^{2}H might lack precision owing to the heterogeneity

of exchangeable hydrogen content in bulk leaf or α-cellulose, as these standards were originally designed for δ^2H calibration of whole wood samples (Qi *et al.*, 2016). Nevertheless, our comparison suggests that orchid hydrogen isotope ratios are consistently higher than those of autotrophs, regardless of pretreatment or calibrating reference materials. This suggests that variations in exchangeable hydrogen content do not significantly affect the estimations from comparing δ^2H in evaluating nutritional strategies in green plants, such as distinguishing between partial mycoheterotrophy and autotrophy.

The regression coefficients of the standardized response variables showed that the δ^2H derived from all treatments have a similar degree of discrimination ability. Although we noted missing data in α-cellulose and cellulose nitrate, these results also indicate that bulk δ^2H can be used for nutritional mode evaluation. Moreover, the coefficients of δ^2H showed similar degrees to those of δ^{15}N, suggesting that combining these two values would be a suitable indicator of partial mycoheterotrophy in rhizoctonia-associated orchids. Based on the ^{2}H and ^{15}N enrichment, the present study suggested, for the first time, a partially mycoheterotrophic species within the genus *Calanthe* (tribe Collabieae) (Xiang *et al.*, 2014).

On the other hand, we note that inter-laboratory comparisons of the ^{2}H enrichment factor in bulk samples may not be suitable for accurately estimating the proportion of carbon derived from mycorrhizal fungi. Isotopic bias among sampling sites in studies of green-leaved orchids is typically addressed by calculating enrichment factors (Preiss & Gebauer, 2008). Consequently, the ^{13}C enrichment factor is commonly used to estimate

the rate of organic carbon acquisition by orchids from fungi, using the enrichment factors of fully mycoheterotrophic orchids as a benchmark for a 100% endpoint in the linear two-source mixing model (Gebauer & Meyer, 2003; Hynson *et al.*, 2013). Even when the ^{2}H enrichment factor is applied, the presence of exchangeable hydrogens may potentially lead to inaccurate estimates of the quantity of organic matter received by orchids from fungi. In our study, the enrichment factor for both orchid species varied considerably among treatments, ranging from 22.8‰ to 45.9‰ for *C. discolor* and from 56.1‰ to 68.4‰ for *G. pubilabiata*. Therefore, the application of bulk $\delta^{2}H$ analysis should be limited to estimating nutritional modes, and using ^{2}H enrichment factors to estimate organic matter gain should be carefully considered. To ensure accurate and comparable data, it is advisable to exclude exchangeable hydrogen through nitration (Epstein *et al.*, 1976) or perform equilibrium adjustments to bulk or α-cellulose using water with known hydrogen isotope ratios (Filot *et al.*, 2006; Wassenaar *et al.*, 2015).

We also note that whether partial mycoheterotrophy can be estimated from hydrogen isotope measurements remains somewhat unclear (Lallemand *et al.*, 2017; Jacquemyn *et al.*, 2021), while the acquisition of ^{2}H-enriched compounds from fungi is at least one of the probable explanations for the high $\delta^{2}H$ observed in green orchids such as *C. discolor* (Gebauer *et al.*, 2016). Photosynthates in orchids are primarily directed to aboveground biomass, especially for fruit production (Gonneau *et al.*, 2014; Suetsugu *et al.*, 2018; Lallemand *et al.*, 2019), while fungal-derived compounds are utilized for subterranean growth and shoot formation (Gonneau *et al.*, 2014). *Calanthe discolor*, thriving on the dim forest floor, forms sprouts for the next year in a light-limited environment. Our

findings suggest that during this period, fungal organic compounds are incorporated into the structural carbohydrates of their leaves (Fig. 3). The high nitrogen concentration in *C. discolor* leaves also suggests that amino acid acquisition contributes to the observed high δ^2H_{bulk}. Although the specific impact of amino acids on $\delta^2H_{cellulose}$ or $\delta^2H_{nitrate}$ is not fully understood, the catabolism of amino acids as an energy source during shoot formation (Hilderbrandt *et al*., 2015) or their conversion to cellulose through gluconeogenesis (Eastmond *et al*., 2015; Cormier, 2019) likely influence the ^2H enrichment in cellulose and cellulose nitrate (Fig. 3). The high variability in $\delta^2H_{cellulose}$ and $\delta^2H_{nitrate}$ levels in *C. discolor* likely reflects variable heterotrophy among individuals, depending on environmental conditions such as irradiance (Preiss *et al.*, 2010).

Given that this study was conducted on a limited spatial scale (1 m × 1 m), environmental factors such as temperature, humidity, or δ^2H of source water absorbed by the roots likely have minimal impact on ^2H fractionation. Similarly, the influence of phylogenetic differences in transpiration rates on δ^2H may also be limited, as previous research strongly suggests that ^2H enrichment in green-leaved orchids is not predominantly due to transpiration rate differences, as simultaneously measured $\delta^{18}O$ does not show parallel enrichment patterns (Gebauer *et al.*, 2016; Schiebold *et al.*, 2018; Schweiger *et al.*, 2019). Parallel $\delta^{18}O$ patterns would be expected if isotopic effects on water (H_2O) molecules drove δ^2H patterns. Furthermore, although no data are available on whether dark respiration rates, which correlate positively with δ^2H of plant sugar (Holloway-Phillips *et al.*, 2022), differ between orchidaceous and non-orchidaceous plants, it is unlikely that the respiration rate in orchids causes ^2H enrichment, as plants in

dark environments would rather reduce their respiration rates to minimize carbon loss (Valladares & Niinemets, 2008; Leake & Cameron, 2010). Finally, while the heterotrophic use of the storage pool could influence δ^2H (Epstein *et al*., 1976; Lehmann *et al*., 2021; Vitali *et al*., 2022), this effect might be limited, as evidenced by one of our autotrophic reference plants, *Disporum sessile*, which relies entirely on the storage pool for cellulose synthesis at sprouting and shows a lower δ^2H than other autotrophic plants (Table S2). Nevertheless, there are possible explanations other than partial mycoheterotrophy for the increase in δ^2H in green orchids such as *C. discolor.* For instance, differences in the structure of photosynthetic enzymes could result in varied ^{2}H fractions during sugar synthesis among plant species (Fig. 3, Schuler *et al.*, 2023). Analyzing the isotopic fractionation between leaf water and sugars (Holloway-Phillips *et al.*, 2022) in orchids compared to other autotrophic plants may help further elucidate whether δ^2H in orchids is influenced by metabolic or physiological processes beyond mycoheterotrophy.

Overall, the current study utilized hydrogen, carbon, and nitrogen stable isotopes to explore mycoheterotrophy in orchids. Although measurements of hydrogen isotopes may introduce errors, as they encompass both exchangeable and non-exchangeable hydrogens, our results indicate that the discriminatory power of hydrogen isotope measurements remains consistent across different measurement approaches. This study supports previous research suggesting that many green orchids derive their carbon from mycorrhizal fungi, as evidenced by the significant ^{2}H and ^{15}N enrichment observed in bulk samples (Gebauer *et al.*, 2016; Schiebold *et al.*, 2018; Schweiger *et al.*, 2018, 2019).

However, the presence of exchangeable hydrogen can influence the absolute values of hydrogen enrichment factors, necessitating caution when using hydrogen isotope ratios to estimate the proportion of organic matter derived from mycorrhizal fungi. Additionally, further evidence may be needed to support the feasibility of using hydrogen isotope measurements to estimate partial mycoheterotrophy.

Figures

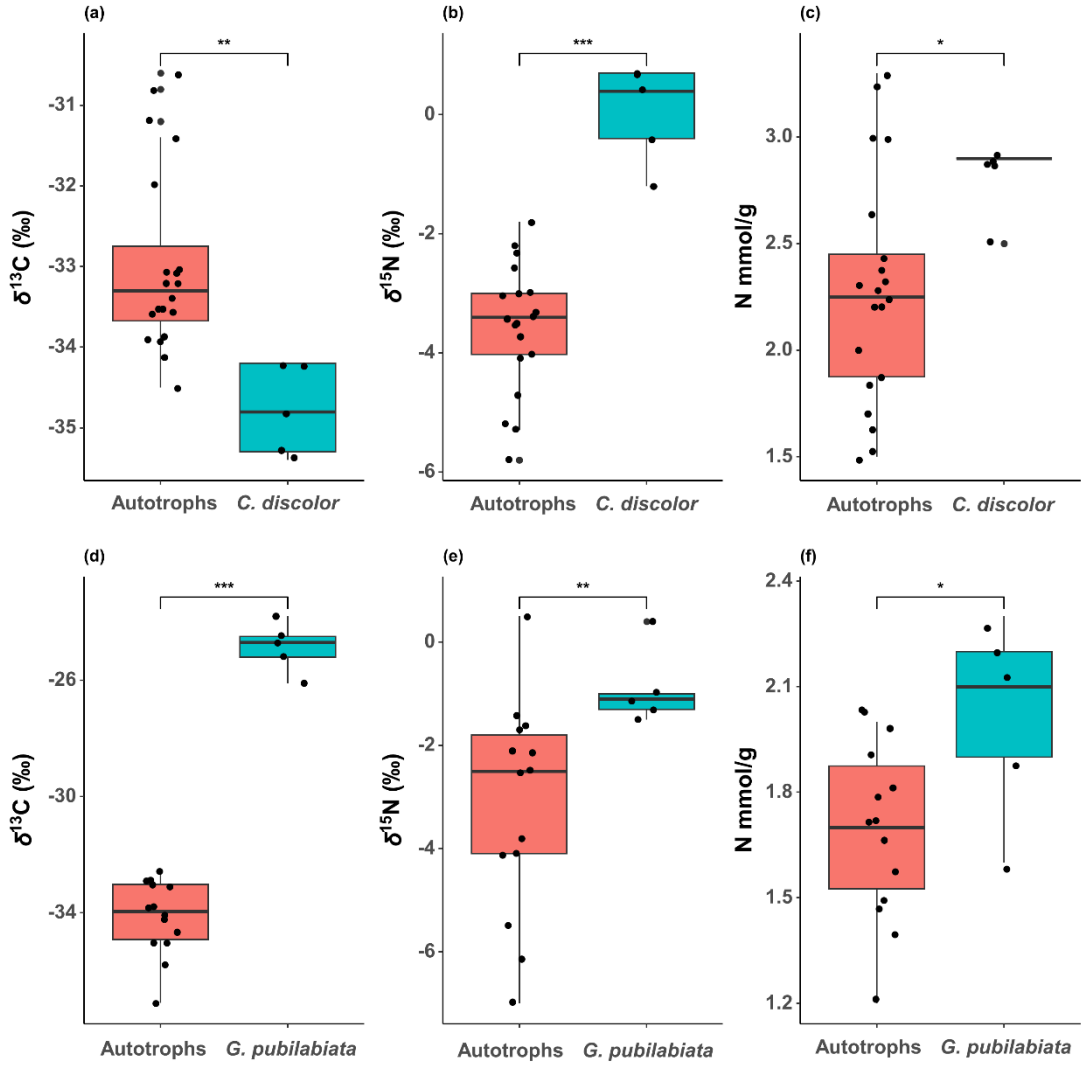

Figure 2.1 δ^{13}C, δ^{15}N, and nitrogen concentrations (mmol/g) of *Calanthe discolor* (a–c), *Gastrodia pubilabiata* (e–f), and their autotrophic references. The box is bounded by the 1st and 3rd quartiles (with the median indicated by the central line), and the whiskers represent 1.5 times the interquartile range. Stars indicate significance levels based on Linear Mixed Model (LMM) fitting with plot as a random effect, followed by post-hoc t-tests using Satterthwaite's approximation (*$p < 0.05$, **$p < 0.01$, ***$p < 0.001$).

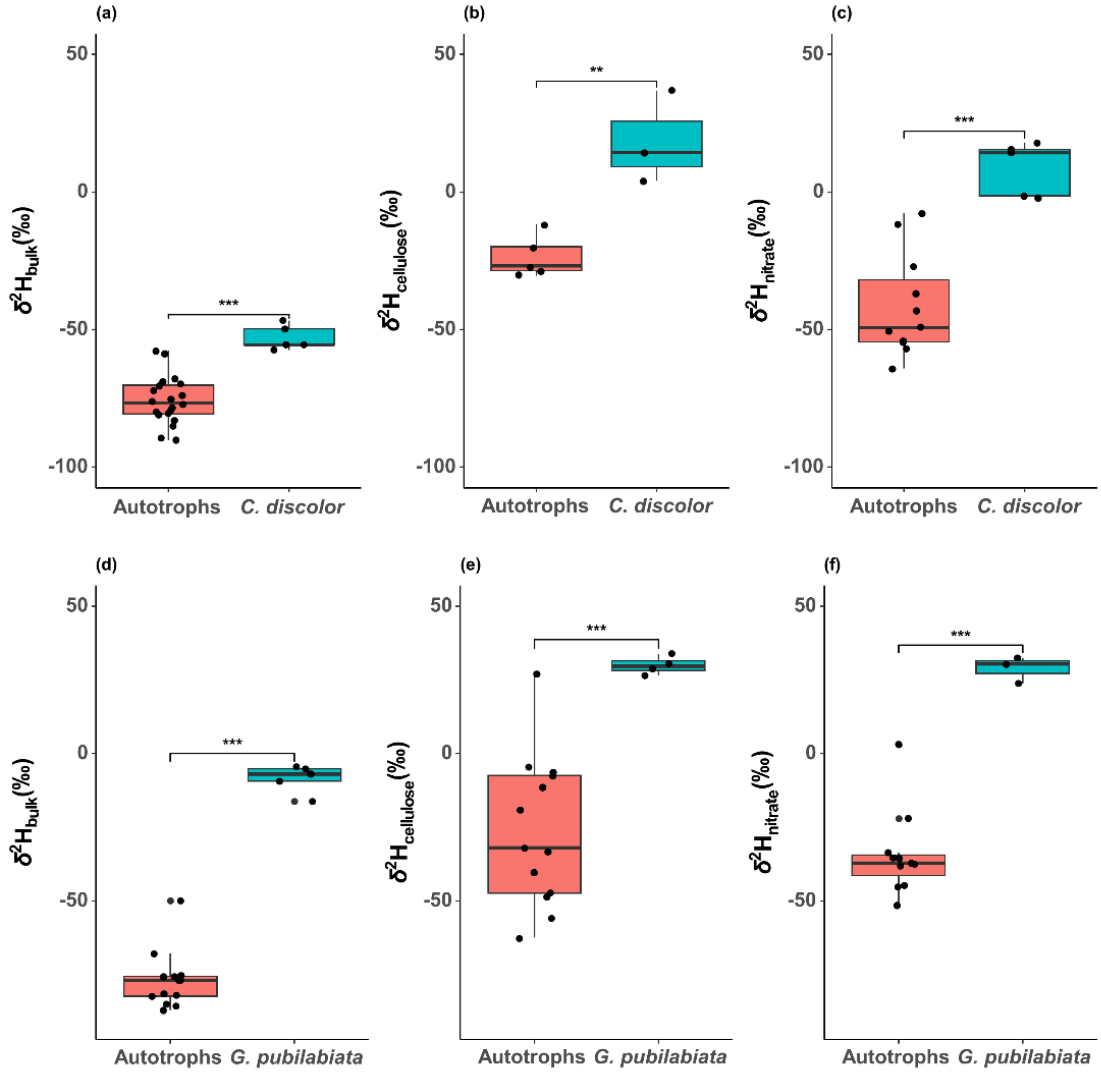

Figure 2.2 δ^2H of bulk, cellulose, and cellulose nitrate samples in *Calanthe discolor* (a–c), *Gastrodia pubilabiata* (e–f), and their autotrophic references. The box is bounded by the 1st and 3rd quartiles (with the median indicated by the central line), and the whiskers represent 1.5 times the interquartile range. Stars indicate significance levels based on Linear Mixed Model (LMM) fitting with plot as a random effect, followed by post-hoc t-tests using Satterthwaite's approximation (*$p < 0.05$, **$p < 0.01$, ***$p < 0.001$).

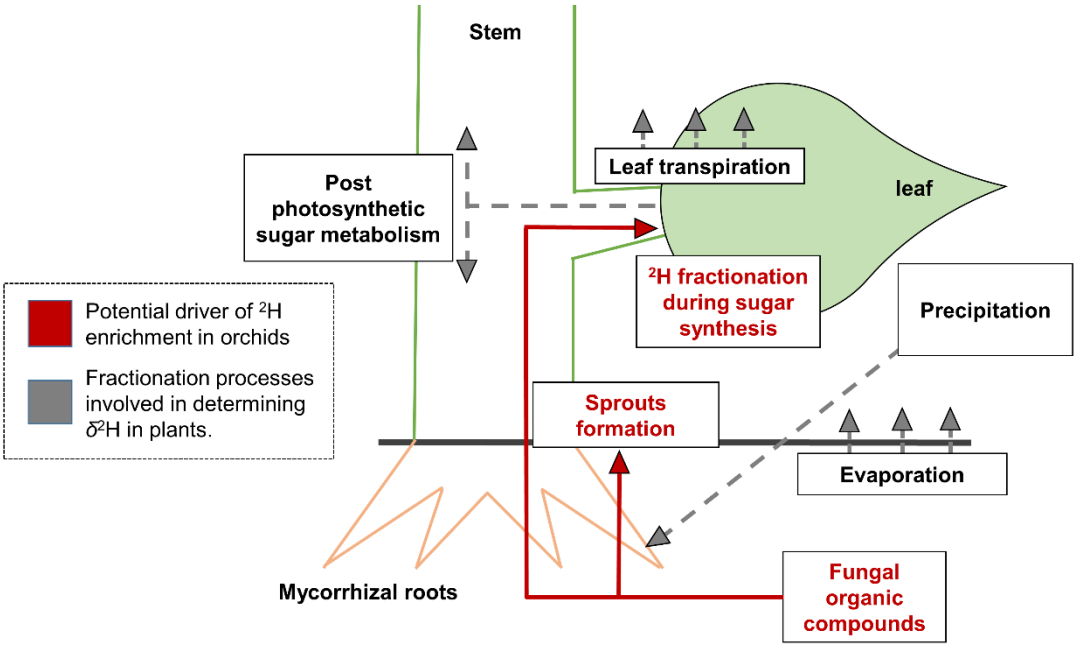

Figure 2.3 Conceptual diagram of a hypothetical ^{2}H enrichment process in orchids. The arrows and boxes indicate the hydrogen movement (as H_2O or organic compounds) and processes where ^{2}H fractionation occurs, respectively. The factors potentially driving ^{2}H enrichment in orchids are emphasized in red.

Tables

Table 2.1. Species and sample *n* collected in this study.

Samples from Sanmu City, Chiba Pref., Japan

Species	Plant type	Sample *n*
Calanthe discolor	Orchid	5
Houttuynia cordata	Autotroph	5
Dioscorea japonica	Autotroph	5
Rubus buergeri	Autotroph	5
Disporum sessile	Autotroph	5

Samples from Miki City, Hyogo Pref., Japan

Species	Plant type	Sample *n*
Gastrodia pubilabiata	Orchid	5
Chengiopanax sciadophylloides	Autotroph	5
Hedera rhombea	Autotroph	5
Quercus serrata	Autotroph	4

Table 2.2. Stable isotope ratios and nitrogen concentrations and brief summary of comparison between orchids and autotrophs. This comparison is based on Linear Mixed Model (LMM) fitting with plot as a random effect, and post-hoc *t*-tests using Satterthwaite's approximation. All δ^2H values were calibrated using the IAEA-CH-7 and USGS 61-62 standard set.

Orchid (*Calanthe discolor*) vs Autotrophs							
	Orchid	Autotrophs	Estimates	Std. Error	df	t	*p*-value
$\delta^{13}C$ (‰)	−34.8 ± 0.6	−33.0 ± 1.1	−1.8	0.5	23	−3.39	0.003
$\delta^{15}N$ (‰)	−0.0 ± 0.8	−3.6 ± 1.1	3.6	0.4	19	8.110	< 0.001
N mmol/g	2.8 ± 0.2	2.3 ± 0.5	0.6	0.2	23	2.215	0.032
δ^2H_{bulk} (‰)	−53.0 ± 4.5	−75.7 ± 8.6	22.8	4.0	23	5.637	< 0.001
$\delta^2H_{cellulose}$ (‰)	18.5 ± 16.8	−23.5 ± 7.7	41.9	8.4	6	4.965	0.003
$\delta^2H_{nitrate}$ (‰)	8.9 ± 9.7	−41.5 ± 18.6	50.3	9.0	14	5.623	< 0.001

Orchid (*Gastrodia pubilabiata*) vs Autotrophs							
	Orchid	Autotrophs	Estimates	Std. Error	df	t	*p*-value
$\delta^{13}C$ (‰)	−24.9 ± 0.9	−34.1 ± 1.3	9.3	0.6	12.966	16.010	< 0.001
$\delta^{15}N$ (‰)	−0.9 ± 0.8	−3.1 ± 2.1	1.1	0.3	13.116	3.269	0.006
N mmol/g	2.0 ± 0.3	1.7 ± 0.2	0.3	0.1	17	2.451	0.025
δ^2H_{bulk} (‰)	8.4 ± 4.7	−78.1 ± 10.1	68.9	3.1	12.876	22.110	< 0.001
$\delta^2H_{cellulose}$ (‰)	29.9 ± 3.1	−26.4 ± 25.4	56.3	12.9	12.645	4.349	< 0.001
$\delta^2H_{nitrate}$ (‰)	28.9 ± 4.5	−34.3 ± 14.5	63.4	8.7	11.346	7.309	< 0.001

Table 2.3. Results of comparison of δ^2H_{bulk} using linear mixed model and post-hoc t-test with Satterthwaite's approximation. (a) Comparison of all δ^2H_{bulk} values derived from Chiba Prefecture samples, calibrated with different standard sets (IAEA-CH-7 and USGS61-62 vs. USGS54-55). (b) Comparison of δ^2H_{bulk} between plant types (Orchid vs. Autotrophs), calibrated using USGS54-55.

(a) Standard set: IAEA-CH-7& USGS 61-62 vs USGS 55-56					
δ^2H_{bulk} (‰)					
Fixed effects	Estimates	Std. Error	df	t	p-value
(Intercept)	−71.2	5.9	4.384	−12.11	< 0.001
Standard set	−7.1	1.1	40	−6.593	< 0.001
Random effects	σ^2	N		Marginal R^2	0.066
Plot	2.546	5		AICc	308.506
Species	12.789	5		AICc (null model)	338.172

(b) Plant type: Orchid (*Calanthe discolor*) vs Autotrophs					
δ2H_{bulk} (‰, calibrated using USGS54－55)					
Fixed effects	Estimates	Std. Error	df	t	p-value
(Intercept)	−83.1	1.9	23	−43.906	< 0.001
Type	23.8	4.2	23	5.634	< 0.001
Random effects	σ^2	N		Marginal R^2	0.569
Plot	0	5		AICc	178.115
				AICc (null model)	200.777

Table 2.4. Regression coefficients for standardized stable isotope ratios and nitrogen concentrations.

	$\delta^{13}C$ (‰)	$\delta^{15}N$ (‰)	N mmol/g	$\delta^{2}H_{bulk}$ (‰)	$\delta^{2}H_{cellulose}$ (‰)	$\delta^{2}H_{nitrate}$ (‰)
Calanthe discolor vs autotrophs	−1.4138	2.028	1.027	1.866	1.732	1.739
Gastrodia pubilabiata vs autotrophs	2.135	1.106	1.129	2.103	1.705	2.125

Table S2.1. $\delta^{13}C$, $\delta^{15}H$, $\delta^{2}H$, and nitrogen concentrations of analysed bulk samples (Mean ± SD).

Samples from Sanmu City, Chiba Pref.

Species	Sample *n*	$\delta^{13}C$ (‰)	$\delta^{15}N$ (‰)	N mmol/g
Calanthe discolor	5	−34.8 ± 0.6	−0.0 ± 0.8	2.8 ± 0.2
All autotrophs	20	−33.0 ± 1.1	−3.6 ± 1.1	2.3 ± 0.5
Houttuynia cordata	5	−33.3 ± 0.2	−3.0 ± 0.6	2.3 ± 0.1
Dioscorea japonica	5	−33.5 ± 0.6	−4.1 ± 0.9	3.0 ± 0.3
Rubus buergeri	5	−31.2 ± 0.5	−4.2 ± 1.6	1.6 ± 0.1
Disporum sessile	5	−33.9 ± 0.2	−3.0 ± 0.7	2.1 ± 0.1

Samples from Miki City, Hyogo pref.

Species	Sample *n*	$\delta^{13}C$ (‰)	$\delta^{15}N$ (‰)	N mmol/g
Gastrodia pubilabiata	5	−24.9 ± 0.9	−0.9 ± 0.8	2.0 ± 0.3
All autotrophs	14	−34.1 ± 1.3	−3.1 ± 2.1	1.7 ± 0.2
Chengiopanax sciadophylloides	5	−34.0 ± 1.0	−2.9 ± 1.8	1.5 ± 0.2
Hedera rhombea	5	−33.7 ± 0.8	−4.5 ± 2.0	1.8 ± 0.3
Quercus serrata	4	−34.9 ± 2.0	−1.8 ± 1.8	1.8 ± 0.1

Table S2.2. Summary of hydrogen stable isotope ratios of bulk (δ^2H_{bulk}), α-cellulose ($\delta^2H_{cellulose}$) and cellulose nitrate ($\delta^2H_{nitrate}$) samples (Mean ± SD).

Samples from Sanmu City, Chiba Pref.				δ^2H calibrated using IAEA-CH-7 and USGS 61-62			δ^2H calibrated using USGS 54-55
Species	Sample n_{bulk}	Sample $n_{cellulose}$	Sample $n_{nitrate}$	δ^2H_{bulk} (‰)	$\delta^2H_{cellulose}$ (‰)	$\delta^2H_{nitrate}$ (‰)	δ^2H_{bulk} (‰)
Calanthe discolor	5	3	5	−53.0 ± 4.5	18.5 ± 16.8	8.9 ± 9.7	−59.2 ± 4.8
All autotrophs	20	5	11	−75.7 ± 8.6	−23.5 ± 7.7	−41.5 ± 18.6	−83.1 ± 9.1
Houttuynia cordata	5	0	3	−78.3 ± 2.1	NA	−51.9 ± 13.9	−85.7 ± 2.2
Dioscorea japonica	5	0	1	−74.2 ± 4.6	NA	−11.9 ± NA	−81.4 ± 4.8
Rubus buergeri	5	5	5	−65.1 ± 6.4	−23.5 ± 7.7	−37.7 ± 19.9	−72.0 ± 6.7
Disporum sessile	5	0	2	−85.4 ± 4.4	NA	−50.1 ± 9.6	−93.2 ± 4.7

Samples from Miki City, Hyogo Pref.				δ²H calibrated using IAEA−CH−7 and USGS 61−62		
Species	Sample n_{bulk}	Sample $n_{cellulose}$	Sample $n_{nitrate}$	δ^2H_{bulk} (‰)	$\delta^2H_{cellulose}$ (‰)	$\delta^2H_{nitrate}$ (‰)
Gastrodia pubilabiata	5	4	3	8.4 ± 4.7	29.9 ± 3.1	28.9 ± 4.5
All autotrophs	14	13	11	−78.1 ± 10.1	−26.4 ± 25.4	−34.3 ± 14.5
Chengiopanax sciadophylloides	5	5	3	−74.8 ± 14.3	−7.1 ± 21.9	−36.8 ± 1.4
Hedera rhombea	5	4	5	−77.4 ± 6.9	−50.1 ± 12.5	−29.9 ± 21.6

Quercus serrata	4	4	3	−83.1 ± 7.4	−26.7 ± 20.2	−39.2 ± 4.9

Table S2.3. Enrichment factors (ε^2H) of each analysed orchid sample.

Calanthe discolor

Plot	ε^{13}C (‰)	ε^{15}N (‰)	ε^2H_{bulk} (‰)	$\varepsilon^2H_{cellulose}$ (‰)	$\varepsilon^2H_{nitrate}$ (‰)
a	-2.2	2.8	20.9	44.9	66.9
b	-1.4	4.3	26.7	NA	60.2
c	-1.4	2.8	16.7	15.7	6.3
d	-2.4	3.8	26.8	NA	67.3
e	-1.7	4.3	22.8	65.6	28.6
Mean	-1.8	3.6	22.8	42.0	45.9
SD	0.5	0.8	4.2	25.1	27.3

Gastrodia pubilabiata

Plot	ε^{13}C (‰)	ε^{15}N (‰)	ε^2H_{bulk} (‰)	$\varepsilon^2H_{cellulose}$ (‰)	$\varepsilon^2H_{nitrate}$ (‰)
a	8.6	1.7	73.6	37.5	NA
b	8.7	1.9	69.0	NA	NA
c	9.1	4.1	68.6	76.9	69.6
d	11.5	1.2	77.0	66.8	62.1
e	8.8	2.5	53.7	43.3	69.2
Mean	9.3	2.3	68.4	56.1	67.0
SD	1.2	1.1	8.9	18.8	4.2

Table S2.4. Details of comparison of stable isotope ratios and nitrogen concentrations between plant type (orchid vs autotrophs) using linear mixed model and post-hoc t-test with Satterthwaite's approximation.

Calanthe discolor vs Autotrophs					
$\delta^{13}C$					
Fixed effects	Estimates	Std. Error	df	t	p-value
(Intercept)	−33.0	0.2	23	−138.47	< 0.001
type	−1.8	0.5	23	−3.39	0.003
Random effects	σ^2	N		Marginal R^2	0.326
plot	0	5		AICc	82.772
$\delta^{15}N$					
Fixed effects	Estimates	Std. Error	df	t	p-value
(Intercept)	−3.6	0.3	4.737	−11.47	< 0.001
type	3.6	0.4	19	8.110	< 0.001
Random effects	σ^2	N		Marginal R^2	0.668
plot	0.533	5		AICc	78.528
N mmol/g					
Fixed effects	Estimates	Std. Error	df	t	p-value
(Intercept)	2.3	0.1	23	20.446	< 0.001
type	0.6	0.2	23	2.215	0.032
Random effects	σ^2	N		Marginal R^2	0.170
plot	0	5		AICc	47.669

δ^2H_{bulk} (‰)					
Fixed effects	Estimates	Std. Error	df	t	p-value
(Intercept)	−75.7	1.8	23	−41.925	< 0.001
type	22.8	4.0	23	5.637	< 0.001
Random effects	σ^2	N		Marginal R^2	0.57
plot	0	5		AICc	175.977

$\delta^2H_{cellulose}$ (‰)					
Fixed effects	Estimates	Std. Error	df	t	p-value
(Intercept)	−23.5	5.2	6	−4.537	0.004
type	41.9	8.4	6	4.965	0.003
Random effects	σ^2	N		Marginal R^2	0.779
plot	0	5		AICc	70.443

$\delta^2H_{nitrate}$ (‰)					
Fixed effects	Estimates	Std. Error	df	t	p-value
(Intercept)	−41.5	5	14	−8.289	< 0.001
type	50.3	9	14	5.623	< 0.001
Random effects	σ^2	N		Marginal R^2	0.678
plot	0	5		AICc	134.034

Gastrodia pubilabiata vs Autotrophs					
$\delta^{13}C$					
Fixed effects	Estimates	Std. Error	df	t	p-value
(Intercept)	−34.2	0.4	5.607	−94.1	< 0.001
type	9.3	0.6	12.966	16.010	< 0.001
Random effects	σ^2	N		Marginal R^2	0.924
plot	0.461	5		AICc	69.031
$\delta^{15}N$					
Fixed effects	Estimates	Std. Error	df	t	p-value
(Intercept)	−0.3	0.3	4.708	−0.891	0.416
type	1.1	0.3	13.1159	3.269	0.006
Random effects	σ^2	N		Marginal R^2	0.230
plot	0.645	5		AICc	54.740
N mmol/g					
Fixed effects	Estimates	Std. Error	df	t	p-value
(Intercept)	1.7	0.1	17	25.378	< 0.001
type	0.3	0.1	17	2.451	0.025
Random effects	σ^2	N		Marginal R^2	0.250
plot	0	5		AICc	16.303

δ^2H_{bulk} (‰)					
Fixed effects	Estimates	Std. Error	df	t	p-value
(Intercept)	−77.3	3.8	4.248	−20.27	< 0.001
type	68.9	3.1	12.876	22.110	< 0.001
Random effects	σ^2	N		Marginal R^2	0.911
plot	7.730	5		AICc	132.054

$\delta^2H_{cellulose}$ (‰)					
Fixed effects	Estimates	Std. Error	df	t	p-value
(Intercept)	−26.3	6.4	6.336	−4.11	< 0.01
type	56.3	12.9	12.645	4.349	< 0.001
Random effects	σ^2	N		Marginal R^2	0.539
plot	2.784	5		AICc	151.585

$\delta^2H_{nitrate}$ (‰)					
Fixed effects	Estimates	Std. Error	df	t	p-value
(Intercept)	−34.4	4.1	5.012	−8.328	< 0.001
type	63.4	8.7	11.346	7.309	< 0.001
Random effects	σ^2	N		Marginal R^2	0.802
plot	2.312	5		AICc	112.250

Table S2.5. All stable isotope and nitrogen content data analysed in chapter 2.

Sanmu City, Chiba Pref., Japan, collected on 2019.6.13

species	plot	$\delta^{13}C$	$\delta^{15}N$	N mmol/g	$\delta^{2}H_{bulk}$	$\delta^{2}H_{cellulose}$	$\delta^{2}H_{nitrate}$	$\delta^{2}H$ (calibrated by wood STD)	Analysis date: $\delta^{13}C$ and nitrogen concentration	Analysis date: $\delta^{15}N$	Analysis date: $\delta^{2}H_{bulk}$	Analysis date: $\delta^{2}H_{cellulose}$	Analysis date: $\delta^{2}H_{nitrate}$	Analysis date: $\delta^{2}H_{wood}$	type
Calanthe discolor	A	−35.4	0.4	2.9	−57.4	14.5	14.3	−63.9	2019.08.28	2019.09.05	2022.11.15	2022.11.15	2022.11.15	2022.11.15	orchid
Rubus buergeri	A	−32	−2.6	1.8	−72.0	−30.4	−50.5	−79.2	2019.08.28	2019.09.05	2022.11.15	2022.11.15	2022.11.15	2022.11.15	autotroph
Dioscorea japonica	A	−33.6	−3.0	3.0	−73.8	NA	NA	−81.1	2019.08.28	2019.09.05	2022.11.15	NA	NA	2022.11.15	autotroph
Houttuynia cordata	A	−33.5	−2.2	2.4	−78.3	NA	−54.7	−85.8	2019.08.28	2019.09.05	2022.11.15	NA	2022.11.15	2022.11.15	autotroph
Disporum sessile	A	−33.6	−1.8	2.0	−89.2	NA	NA	−97.2	2019.08.28	2019.09.05	2022.11.15	NA	NA	2022.11.15	autotroph
Calanthe discolor	B	−34.2	0.7	2.5	−49.7	NA	15.4	−55.8	2019.08.28	2019.09.05	2022.11.15	NA	2022.11.15	2022.11.15	orchid
Rubus buergeri	B	−31.4	−4.1	1.5	−67.9	−26.8	−54.2	−74.9	2019.08.28	2019.09.05	2022.11.15	2022.11.15	2022.11.15	2022.11.15	autotroph
Dioscorea japonica	B	−33.1	−3.7	2.6	−70.3	NA	NA	−77.3	2019.08.28	2019.09.05	2022.11.15	NA	NA	2022.11.15	autotroph
Houttuynia cordata	B	−33.0	−3.5	2.3	−77.2	NA	−36.8	−84.6	2019.08.28	2019.09.05	2022.11.15	NA	2022.11.15	2022.11.15	autotroph
Disporum sessile	B	−33.9	−3.0	2.2	−90.2	NA	−43.3	−98.3	2019.08.28	2019.09.05	2022.11.15	NA	2022.11.15	2022.11.15	autotroph
Calanthe discolor	C	−34.2	−1.2	2.9	−55.5	4.0	−1.4	−61.9	2019.08.28	2019.09.05	2022.11.15	2022.11.15	2022.11.15	2022.11.15	orchid
Rubus buergeri	C	−30.6	−5.8	1.5	−58.8	−11.7	−7.7	−65.4	2019.08.28	2019.09.05	2022.11.15	2022.11.15	2022.11.15	2022.11.15	autotroph
Dioscorea japonica	C	−33.2	−4.0	3.2	−69.8	NA	NA	−76.8	2019.08.28	2019.09.05	2022.11.15	NA	NA	2022.11.15	autotroph
Houttuynia cordata	C	−33.5	−3.3	2.3	−80.6	NA	NA	−88.1	2019.08.28	2019.09.05	2022.11.15	NA	NA	2022.11.15	autotroph
Disporum sessile	C	−33.9	−3.0	1.9	−79.4	NA	NA	−86.9	2019.08.28	2019.09.05	2022.11.15	NA	NA	2022.11.15	autotroph
Calanthe discolor	D	−35.3	−0.4	2.9	−46.7	NA	18.0	−52.7	2019.08.28	2019.09.05	2022.11.15	NA	2022.11.15	2022.11.15	orchid
Rubus buergeri	D	−31.2	−5.2	1.7	−57.8	−19.8	−27.0	−64.3	2019.08.28	2019.09.05	2022.11.15	2022.11.15	2022.11.15	2022.11.15	autotroph
Dioscorea japonica	D	−33.1	−4.7	3.3	−76.0	NA	NA	−83.3	2019.08.28	2019.09.05	2022.11.15	NA	NA	2022.11.15	autotroph
Houttuynia cordata	D	−33.4	−3.4	2.4	−75.3	NA	−64.1	−82.6	2019.08.28	2019.09.05	2022.11.15	NA	2022.11.15	2022.11.15	autotroph
Disporum sessile	D	−33.9	−3.5	2.2	−84.9	NA	−56.9	−92.7	2019.08.28	2019.09.05	2022.11.15	NA	2022.11.15	2022.11.15	autotroph
Calanthe discolor	E	−34.8	0.7	2.9	−55.5	36.9	−2	−61.9	2019.08.28	2019.09.05	2022.11.15	2022.11.15	2022.11.15	2022.11.15	orchid
Rubus buergeri	E	−30.8	−3.4	1.6	−69.0	−28.6	−49.2	−76.1	2019.08.28	2019.09.05	2022.11.15	2022.11.15	2022.11.15	2022.11.15	autotroph
Dioscorea japonica	E	−34.5	−5.3	3.0	−81.0	NA	−11.9	−88.6	2019.08.28	2019.09.05	2022.11.15	NA	2022.11.15	2022.11.15	autotroph
Houttuynia cordata	E	−33.2	−2.3	2.3	−80.0	NA	NA	−87.6	2019.08.28	2019.09.05	2022.11.15	NA	NA	2022.11.15	autotroph
Disporum sessile	E	−34.1	−3.4	2.2	−83.1	NA	NA	−90.8	2019.08.28	2019.09.05	2022.11.15	NA	NA	2022.11.15	autotroph

Miki City, Hyogo Pref., Japan, collected on 2021.9.21

species	plot	$\delta^{13}C$	$\delta^{15}N$	N mmol/g	$\delta^{2}H_{bulk}$	$\delta^{2}H_{cellulose}$	$\delta^{2}H_{nitrate}$	$\delta^{2}H$ (calibrated by wood STD)	Analysis date: $\delta^{13}C$ and nitrogen concentration	Analysis date: $\delta^{15}N$	Analysis date: $\delta^{2}H_{bulk}$	Analysis date: $\delta^{2}H_{cellulose}$	Analysis date: $\delta^{2}H_{nitrate}$	Analysis date: $\delta^{2}H_{wood}$	type
Gastrodia pubilabiata	A	−24.5	−1.1	2.2	−4.4	30.6	NA	NA	2022.08.22	2022.08.22	2022.10.20	2023.06.01	NA	NA	orchid
Hedera rhombea	A	−33.0	−4.1	2.0	−75.7	NA	3.1	NA	2022.08.22	2022.08.22	2022.10.20	NA	2023.06.01	NA	autotroph
Chengiopanax sciadophylloides	A	−33.8	−2.5	1.5	−81.5	−6.4	−38.1	NA	2022.08.22	2022.08.22	2022.10.20	2023.06.01	2023.06.01	NA	autotroph
Quercus serrata	A	−32.6	−1.7	1.9	−76.9	−7.4	−35.5	NA	2022.08.22	2022.08.22	2022.10.20	2023.06.01	2023.06.01	NA	autotroph
Gastrodia pubilabiata	B	−24.7	−1.0	1.9	−6.9	NA	NA	NA	2022.08.22	2022.08.22	2022.10.20	NA	NA	NA	orchid
Hedera rhombea	B	−32.9	−4.1	2.0	−75.3	−33.4	−51.5	NA	2022.08.22	2022.08.22	2022.10.20	2023.06.01	2023.06.01	NA	autotroph
Chengiopanax sciadophylloides	B	−33.1	−2.5	1.5	−76.9	−4.7	−35.3	NA	2022.08.22	2022.08.22	2022.10.20	2023.06.01	2023.06.01	NA	autotroph
Quercus serrata	B	−34.2	−2.1	1.8	−76.9	−11.4	−37.5	NA	2022.08.22	2022.08.22	2022.10.20	2023.06.01	2023.06.01	NA	autotroph
Gastrodia pubilabiata	C	−25.2	−1.5	2.3	−16.2	33.8	30.4	NA	2022.08.22	2022.08.22	2022.10.20	2023.06.01	2023.07.25	NA	orchid
Hedera rhombea	C	−34.1	−7.0	1.4	−82.4	−62.5	−33.6	NA	2022.08.22	2022.08.22	2022.10.20	2023.06.01	2023.06.01	NA	autotroph
Chengiopanax sciadophylloides	C	−32.9	−6.1	1.2	−85.0	−19.3	NA	NA	2022.08.22	2022.08.22	2022.10.20	2023.06.01	NA	NA	autotroph
Quercus serrata	C	−35.8	−3.8	1.8	−87.1	−47.4	−44.7	NA	2022.08.22	2022.08.22	2022.10.20	2023.06.01	2023.06.01	NA	autotroph
Gastrodia pubilabiata	D	−23.8	0.4	2.1	−9.3	26.4	32.5	NA	2022.08.22	2022.08.22	2022.10.20	2023.06.01	2023.06.01	NA	orchid
Hedera rhombea	D	−33.8	−1.6	1.7	−85.6	−48.8	−22	NA	2022.08.22	2022.08.22	2022.10.20	2023.06.01	2023.06.01	NA	autotroph
Chengiopanax sciadophylloides	D	−35.0	−1.4	1.6	−81.9	−31.9	−37.1	NA	2022.08.22	2022.08.22	2022.10.20	2023.06.01	2023.06.01	NA	autotroph
Quercus serrata	D	−37.1	0.5	1.7	−91.5	−40.4	NA	NA	2022.08.22	2022.08.22	2022.10.20	2023.06.01	NA	NA	autotroph
Gastrodia pubilabiata	E	−26.1	−1.3	1.6	−5.2	28.8	23.9	NA	2022.08.22	2022.08.22	2022.10.20	2023.06.01	2023.06.01	NA	orchid
Hedera rhombea	E	−34.7	−5.5	2.0	−67.9	−55.8	−45.3	NA	2022.08.22	2022.08.22	2022.10.20	2023.06.01	2023.06.01	NA	autotroph
Chengiopanax sciadophylloides	E	−35.0	−2.1	1.7	−49.9	26.9	NA	NA	2022.08.22	2022.08.22	2022.10.20	2023.06.01	2022.11.15	NA	autotroph

Table S2.6. Analytical standard deviations and *n* of international reference materials used in this study.

CERKU-02

Date	SD_δ^{13}C	*n*_δ^{13}C	SD_δ^{15}N	*n*_δ^{15}N
2019.08.28	0.04	12	NA	NA

CERKU-03

Date	SD_δ^{13}C	*n*_δ^{13}C	SD_δ^{15}N	*n*_δ^{15}N
2019.08.28	0.05	12	NA	NA
2019.09.05	NA	NA	0.12	7
2022.08.22	0.07	23	0.08	12

CERKU-05

Date	SD_δ^{13}C	*n*_δ^{13}C	SD_δ^{15}N	*n*_δ^{15}N
2019.08.28	0.03	12	NA	NA
2019.09.05	NA	NA	0.07	9
2022.08.22	0.12	22	0.05	12

IAEA-CH-7

Date	SD_δ^{2}H	*n*_δ^{2}H
2022.10.20	1.17	8
2022.11.15	0.85	7
2023.06.01	0.70	7
2023.07.25	0.69	8

USGS61

Date	SD_δ^{2}H	*n*_δ^{2}H
2022.10.20	1.24	9
2022.11.15	0.68	8
2023.06.01	0.40	6
2023.07.25	0.85	8

USGS62

Date	SD_δ^{2}H	*n*_δ^{2}H
2022.10.20	1.24	9
2022.11.15	1.17	8
2023.06.01	1.01	7
2023.07.25	0.86	8

USGS54

Date	SD_δ^{2}H	n_δ^{2}H
2022.11.15	0.99	6

USGS55

Date	SD_δ^2H	n_δ^2H
2022.11.15	0.67	6

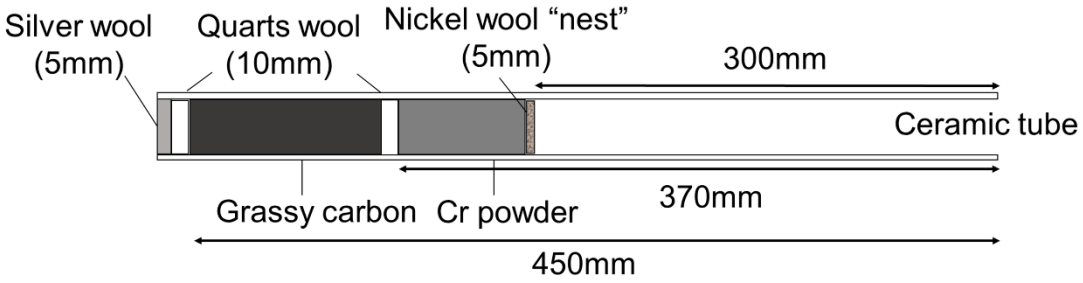

Figure S2.1. Schematic illustration of the CR reduction reactor system used in this study.

Chapter 3

Widespread occurrence of partial mycoheterotrophy in rhizoctonia-associated orchids in subtropical and temperate Japan: Evidence from a multi-element stable isotope approach

Introduction

Plant species in the Orchidaceae family are uniquely associated with fungi, diverging from many other plants that typically form symbiotic relationships with arbuscular mycorrhizal (AM) fungi (Glomeromycota). Instead, orchids predominantly engage with a diverse range of fungi from the phyla Basidiomycota and Ascomycota. Rhizoctonia fungi (Ceratobasidiaceae and Tulasnellaceae from Cantharellales, Serendipitaceae from Sebacinales) are among the most prevalent fungal symbionts of orchids. Weiss *et al*., 2016), are among the most prevalent fungal symbionts of orchids. While they are primarily considered to be saprotrophic (SAP), they also include ectomycorrhizal (ECM) and endophytic species (Dearnaley *et al.*, 2012). A wide range of Basidiomycota fungi other than rhizoctonia and Ascomycota fungi have also been detected from orchid mycorrhizal roots (Dearnaley *et al.*, 2012; Jacquemyn *et al.*, 2015, 2016).

Another distinguishing characteristic of orchids is initial mycoheterotrophy (Leake, 1994; Merckx & Merckx, 2013). While the vast majority of obligate autotrophic plants exchange their photosynthate for fungal mineral nutrition, orchids can exploit both organic carbon and mineral nutrition from mycorrhizal fungi. Mycoheterotrophy plays an essential role for all orchids to complete their life cycles (Bidartondo, 2005). Since all orchids have dust-like small seeds that almost lack carbon reserves for germination, they rely on their fungal partners for nutrients for the development of the early seedling stage (Hynson *et al.*, 2013). The nutritional strategy of adult orchids, however, varies by species. Parasitism on fungi at the adult stage is broadly classified into partial mycoheterotrophy (mixotrophic utilization of both photosynthetic and fungal-derived carbon) or full

mycoheterotrophy (loss of photosynthesis in favor of exclusively fungal-derived carbon) (Hynson *et al.*, 2013). Since full mycoheterotrophy in the adult stage has evolved independently, at least 30 times in the Orchidaceae (Merckx & Freudenstein, 2010), and often nested within partially mycoheterotrophic clades (Ogura-Tsujita *et al.*, 2012; Wang *et al.*, 2021), partial mycoheterotrophy is considered a preadaptation for full mycoheterotrophy.

Carbon and nitrogen stable isotope (δ^{13}C and δ^{15}N) analysis is an effective tool for estimating plant nutritional strategies. The natural abundance of stable isotope ratios in ecological compartments is affected by isotope effects caused by thermodynamic or biochemical processes (Hynson *et al.*, 2013). Because fungal carbon and nitrogen isotopic compositions are generally higher than those of autotrophic plants because fungi use different resources from plants, the isotopic signatures of mycoheterotrophic plants are similar to those of mycorrhizal fungi rather than obligate autotrophs, reflecting the acquisition of fungal organic matters enriched in heavy stable isotopes. This tool has been applied to many orchids and suggested that most green-leaved orchid species associated with ECM or non-rhizoctonia SAP fungi are arguably partially mycoheterotrophic based on their higher δ^{13}C and δ^{15}N values than those of obligate autotrophic plants (Gebauer & Meyer, 2003; Ogura-Tsujita *et al.*, 2012; Sakamoto *et al.*, 2016; Suetsugu & Matsubayashi, 2021a,b; Suetsugu *et al.*, 2022a).

On the other hand, there is limited evidence of partial mycoheterotrophy in orchids associated with non-ECM rhizoctonia (hereafter, I simply referred to as `rhizoctonia`) based only on δ^{13}C and δ^{15}N analysis (Roy *et al.*, 2009; Girlanda *et al.*, 2011; Suetsugu

et al., 2021c; Suetsugu & Matsubayashi, 2022; Yagi *et al.*, 2022). Because the association of orchids with rhizoctonia is a probable ancestral ecological trait compared to association with non-rhizoctonia fungi (Ogura-Tsujita *et al.*, 2012; Wang *et al.*, 2021), understanding the prevalence of partial mycoheterotrophy among rhizoctonia-associated orchid species is crucial for comprehending the evolutionary shifts in mycorrhizal associations and nutritional strategies within the Orchidaceae. However, the isotopic signatures of these orchids do not stand out as markedly as those associated with ECM or non-rhizoctonia SAP fungi; typically, there is no notable difference (or sometimes significantly lower) in $\delta^{13}C$, though $\delta^{15}N$ and total leaf nitrogen concentration are usually higher compared to autotrophs (Hynson *et al.*, 2009, 2013), making it difficult to estimate the nutritional modes of rhizoctonia-associated orchids. Although the reason for this ambiguity is not clearly understood, the isotopic signature of rhizoctonia hyphae, which shows relatively lower isotope enrichment than other fungi may explain this (Selosse & Martos, 2014; Gomes *et al.*, 2023; Zahn *et al.*, 2023).

Hence, stable hydrogen isotope (δ^2H) analysis has been adopted as a supplementary method to determine the nutritional strategies of orchids associated with rhizoctonia fungi (Gebauer *et al.*, 2016; Schiebold *et al.*, 2018; Schweiger *et al.*, 2018). This approach posits that the δ^2H value of an organic molecule increases through heterotrophic metabolism (Yakir, 1992), indicating that partial mycoheterotrophy might be more common among rhizoctonia-associated orchids than previously recognized (Gebauer *et al.*, 2016). Although measuring δ^2H of bulk samples is challenging to obtain accurate hydrogen isotope ratios due to the inter-sample heterogeneity of exchangeable hydrogens

(Epstein *et al.*, 1976), its accuracy is likely sufficient not to affect the estimation of nutritional strategies (Yagi *et al*. 2024). Consequently, combining the ^{2}H enrichment of bulk samples with another indirect evidence for mycoheterotrophy, particularly ^{15}N enrichment, likely serves as an indicator of partial mycoheterotrophy (Gebauer *et al.*, 2016; Schiebold *et al.*, 2018; Schweiger *et al.*, 2018, 2019).

Based on these backgrounds, I explored the potential for partial mycoheterotrophy in green Asian orchid species associated with rhizoctonia fungi, combining molecular identification of mycorrhizal fungi and $\delta^{13}C$, $\delta^{15}N$, $\delta^{2}H$, and nitrogen concertation analysis. I focused on orchid species from the two subfamilies Orchidoideae and Epidendroideae, for which mycorrhizal and stable isotope data were previously unavailable, to cover as wide a range systematically as possible. I primarily selected orchid species distributed in subtropical regions of Japan because, despite previous research on rhizoctonia-associated orchids being biased towards Europe (Gebauer *et al.*, 2016; Schiebold *et al.*, 2018; Schweiger *et al.*, 2018, 2019), the warm and humid environmental conditions in this region might be ideal for the growth of SAP fungi, potentially driving the evolution of mycoheterotrophy dependent on saprotrophic fungi, including rhizoctonia, at least with saprotrophic lifestyles (Lee *et al.*, 2015; Suetsugu *et al.*, 2021a).

Material and Methods

Sampling scheme

I selected 13 species of orchids distributed in subtropical or warm temperate regions, specifically from Shizuoka, Miyazaki, and Okinawa prefectures in Japan (Table 3.1). I chose orchids lacking mycorrhizal and stable isotope information but presumably associated with rhizoctonia fungi based on the phylogenetic data of orchids (Wang *et al.*, 2021). Specifically, I collected two species from Epidendroidaeae and 11 species from Orchidoideae. Within the subfamily Orchidoideae, one species was from Orchideae, one from Diurideae, and nine from Goodyerinae, Cranichideae. Although most orchids investigated in this study were collected from the forest floor, *Zeuxine strateumatica*, *Microtis unifolia*, and *Hemipilia lepida* were collected from grasslands.

I established sampling plots (1 × 1 m) containing orchids and 2 to 4 autotrophic reference species (see Table S3.1 for details). To minimize sampling bias due to environmental heterogeneity, I collected their current-year leaves, positioned at the same height (Gebauer & Meyer, 2003). Additionally, I collected mycorrhizal roots/rhizomes of orchids for the identification of their mycorrhizal partners.

Molecular identification of mycobionts

Mycorrhizal roots or rhizomes of orchids were carefully examined under a microscope to assess fungal colonization. Fragments measuring 2–3 mm were excised and stored at −20°C until DNA extraction. I used the cetyltrimethylammonium bromide (CTAB) method to extract DNA from these mycorrhizal fragments. The details of the sample type and number of mycorrhizal fragments for each orchid species are presented in Table 3.2.

The internal transcribed spacer 2 (ITS2) region of the nuclear ribosomal DNA was

amplified using the Q5 High-Fidelity DNA Polymerase kit (NEB, Ipswich, USA). For *Zeuxine boninensis* and *Zeuxine leucochila*, I used the primer set ITS86F/ITS4 (Vancov & Keen, 2009) fused with 3–6-mer Ns, and an Illumina forward/reverse-sequencing primer was used. Polymerase chain reaction (PCR) was conducted using the following program: 98°C for 3 min, followed by 35 cycles at 98°C for 10 s, 65°C for 20 s, 72° C for 20 s, and a final extension at 72°C for 10 min. To address the issue of sequence loss due to amplification of host plant DNA, I used KOD ONE PCR Master Mix (Toyobo, Osaka, Japan) for other species (Table 3.2) and performed nested PCR to enhance specificity for fungal sequences. Nested PCR involved an initial round using ITS1OF/ITS4OF primers followed by a second round using ITS86F/ITS4 primers. The PCR primers and program for nested PCR were as follows: 35 cycles at 98°C for 10 s, 54°C for 5 s, and 68 °C for 1 s with the ITS1OF/ITS4OF (Taylor & McCormick, 2008) primer set for the 1st PCR, and 35 cycles at 98°C for 10 s, 55°C for 5 s, and 68 °C for 1s with the ITS86F/ITS4 primer set fused with 3–6-mer Ns and an Illumina forward/reverse-sequencing primer for the 2nd PCR. The supplemental PCR was then conducted to add Illumina sequencing adapters, using a forward/reverse fusion primer set comprising the P5/P7 Illumina sequencing adaptor, 8-mer indices for sample identification, and a partial sequence of the ITS86F/ITS4 primer.

Post-PCR, the amplicon libraries were purified using the AMPure XP kit (Beckman Coulter, CA, USA) to remove primer dimers and adjusted to a concentration of 8 pM for sequencing on the Illumina MiSeq platform using the MiSeq Reagent Micro Kit v2 (300 cycles) with a 10% Phix spike-in. The sequencing data were deposited in the Sequence

Read Archive of the DNA Data Bank of Japan (accession number: DRAXXXXXX). After sequencing, raw data were processed using Claident v0.9.2023.12.05 (Tanabe, 2023), as described by Suetsugu & Okada (2021) and Suetsugu *et al.* (2022b).

In brief, the forward and reverse primer positions and sequencing reads with low-quality scores (i.e. *Q*-score <30) were eliminated using the clsplitseq command in Claident. The denoising of erroneous sequences was performed using DADA2 package (Callahan *et al.*, 2016), which was implemented in the cldenoiseseqd command of Claident. Subsequently, the sequences that could have originated from PCR chimaera and index-hopping were removed via the clremovechimev and clremovecontam commands in Claident (Esling *et al.*, 2015; Nilsson *et al.*, 2019). The remaining sequencing reads were clustered into OTUs (threshold similarity of 97%) using VSEARCH v2.8.0 (Rognes *et al.*, 2016), and the most abundant sequence in each OTU cluster was selected as the representative sequence.

Taxonomic assignment of the OTUs was performed based on the query-centric auto-k-nearest-neighbor (QCauto) algorithm (Tanabe & Toju, 2013) and the lowest common ancestor (LCA) algorithms (Huson *et al.*, 2007), via the clmakecachedb, clidentseq, and classingtax commands. Relaxed LCA, which tolerates a proportion of 5% unmatched neighborhood sequences and provides the 95% majority-rule consensus of neighborhood sequences, was applied. After identification, the functional guild of each fungal OTU was estimated based on the FUNGuild database (Nguyen *et al.*, 2016). To concentrate on potential orchid mycorrhizal fungi, I omitted OTUs not belonging to the fungal phyla Basidiomycota or Ascomycota, and OTUs identified as animal pathogens in the guild

information from the FUNGuild database.

Because it is difficult to estimate the functional guilds of rhizoctonia based solely on the FUNGuild database, the phylogenetic tree was constructed to evaluate the functional guilds of the Ceratobasidiaceae and Sebacinales. The sequences obtained in this study were integrated into downloaded sequence datasets, including Ceratobasidiaceae from Suetsugu *et al.* (2021), and Sebacinales (including ectomycorrhizal Sebacinaceae and saprotrophic/endophytic Serendipitaceae) from Fritsche *et al.* (2021). Subsequently, they underwent maximum likelihood (ML) analysis with 1000 bootstrap values (Felsenstein, 1985) using MEGA X (Kumar *et al.*, 2018). Since it is challenging to phylogenetically estimate the functional guilds of Tulasnellaceae fungi due to their high variability in the ITS region (Taylor & McCormick, 2008), the functional guilds of a Tulasnellaceae OTU were estimated by examining the host information from BLAST searches. Subsequently, OTUs identified as non-ECM Ceratobasidiaceae, Tulasnellaceae, or Serendipitaceae were categorized as 'non-ECM rhizoctonia', and the OTUs phylogenetically assigned to ECM (i.e., Sebacinaceae) were classified as 'ECM'. For the remaining OTUs, those assigned to both ectomycorrhizal and saprotrophic were categorized as 'ECM/SAP', while those assigned to either were categorized as 'ECM' or 'SAP', respectively. Additionally, OTUs not falling into these categories were classified as 'Other fungi'.

Stable isotope analysis

All stable isotope ratio and nitrogen concentration measurements were conducted at the

Research Institute for Humanity and Nature (Kyoto, Japan). Leaf samples were dried at 65°C overnight, ground with an agate mortar and pestle, and stored in glass vials until analysis. Approximately 0.3–3 mg of samples were weighed into tin capsules, and the relative abundances of ^{13}C and ^{15}N, as well as nitrogen concentrations, were measured using the Delta V Advantage mass spectrometer connected to a Flash EA 1112 elemental analyzer via the ConFlo IV interface (all from Thermo Fisher Scientific, Waltham, Massachusetts, USA). For the relative abundance of ^{2}H, approximately 0.2 mg of samples were weighed into silver capsules. These capsules were wrapped loosely to allow water vapor to enter and tightly to prevent sample loss. Subsequently, weighed capsules were freeze-dried overnight, and exchangeable hydrogens within the samples were equilibrated with atmospheric vapor in the laboratory for one week. After another round of freeze-drying, samples were quickly set into the Costech Zero Blank Autosampler (Pelican Scientific Ltd., Alford, UK), which was coupled to TC/EA. Due to potential post-wrap bias from atmospheric vapor, orchids, and their autotrophic references were analyzed together in the same batches whenever possible. The Cr reactor method was used to minimize the bias of $\delta^{2}H$ caused by nitrogen or halogen in organic samples (Gehre *et al.*, 2015). The temperatures of the gas chromatography column and Cr reactor were set to 90 and 1250 ℃, respectively. Each sample was analyzed only once per batch because my preliminary experiments did not show a noticeable memory bias of $\delta^{2}H$ from previous samples (Olsen *et al.*, 2006) under my experimental conditions.

The C and N isotopic ratios were calibrated using laboratory standards: CERKU-02 (*L*-alanine, $\delta^{13}C = -19.04‰$, $\delta^{15}N = 22.71‰$), CERKU-03 (glycine, $\delta^{13}C = -34.92‰$,

$\delta^{15}N$ = 2.18‰), and CERKU-05 (threonine, $\delta^{13}C$ = −9.45‰, $\delta^{15}N$ = −2.88‰), which are traceable to international standards (Tayasu *et al.*, 2011). I employed IAEA-CH-7 and USGS 61-62 (Coplen, 2019) as international standard materials for the calibration of H isotopic ratios. The difference in exchangeable hydrogen fractions between bulk leaf samples and international standard materials may cause imperfect calibration of $\delta^{2}H$. However, I utilized those standards for calibration because the difference in exchangeable hydrogens is reported not to significantly affect the statistical analysis (Yagi *et al*., 2024). The relative abundances of the stable isotopes were calculated as $\delta^{13}C$, $\delta^{15}N$ or $\delta^{2}H$ = (R_{sample} /$R_{standard}$ − 1) × 1000 [‰], where R_{sample} represents the $^{13}C/^{12}C$, $^{15}N/^{14}N$, or ^{2}H /^{1}H ratio of the sample, and $R_{standard}$ represents the $^{13}C/^{12}C$ ratio of Vienna Pee Dee Belemnite, $^{15}N/^{14}N$ ratio of atmospheric N_2, or the ^{2}H /^{1}H ratio of VSMOW-SLAP.

Statistical analyses described below were performed using R v.4.3.1 (R Development Core Team, 2023). I conducted comparisons of the relative abundances of ^{13}C, ^{15}N, ^{2}H, and the nitrogen concentration between orchids and their autotrophic references using the lmer function (implemented in the lme4 package), including 'plot' as the random effect of my model. *P*-values were calculated using a post-hoc *t*-test with Satterthwaite's approximation using the R package lmerTest (Kuznetsova *et al.*, 2017).

In addition, enrichment factors (ε) *sensu* (Preiss & Gebauer, 2008)were calculated from the δ values of each plant group based on $\varepsilon X = \delta X_S - \delta X_{REF}$, where δX_S represents $\delta^{13}C$, $\delta^{15}N$, or the $\delta^{2}H$ of each orchid, and δX_{REF} represents the mean $\delta^{13}C$, $\delta^{15}N$, or $\delta^{2}H$ of all autotrophic reference plants from a specific sampling plot, to facilitate the visualization of data from multiple species.

Result

Molecular identification of mycobionts

After the bioinformatics filtering process and phylogenetic analysis, I acquired 583,351 reads (82 OTUs). Among the detected sequences, 482,381 (25 OTUs) were assigned as rhizoctonia, 70,059 reads (31 OTUs) were SAP, 29820 reads (22 OTUs) were ECM, and 1,058 reads (3 OTUs) were other fungi (Fig. 3.1.a). Only 33 reads (1 OTU) were categorized as ECM/SAP. Phylogenetic analysis and BLAST search showed that all Ceratobasidiaceae and Tulasnellaceae fungi detected in this study were not ectomycorrhizal (Fig. 3.2, Table 3.3), and 4 of 10 OTUs identified as Sebacinales were assigned to Serendipitaceae clades (Fig. 3.3). The detected number of OTUs and sequence counts for rhizoctonia were as follows: Ceratobasidiaceae comprised 443,044 reads (20 OTUs, Fig. 3.1.b), Tulasnellaceae comprised 32,770 reads (1 OTU, Fig. 3.1.b), and Serendipitaceae comprised 6,567 reads (4 OTUs, Fig. 3.1.b).

The OTU and read numbers of each orchid species are shown in Table 3.4. The proportion of sequences derived from rhizoctonia varied between orchid species (Fig. 3.4). In *Z. strateumatica*, all reads were derived from rhizoctonia (Fig. 3.4). Among other species, the proportion of rhizoctonia-derived reads sequentially decreased as follows: *Odontochilus yakushimensis* with 99.89%, *Z. boninensis* with 96.45%, *Z. leucochila* with 95.67%, *Odontochilus tashiroi* with 95.35%, *Z. affinis* with 91.7%, *C. tashiroi* with 82.35%, *Goodyera hachijoensis* var. *matsumurana* with 62.72%, and *M. unifolia* with

61.54% (Fig. 3.4). In *Goodyera procera* and *H. lepida*, the rhizoctonia-derived reads accounted for less than half of the total sequence count (43.61% and 21.24%, respectively, Fig. 3.4). I acquired no amplicon sequences derived from mycobionts of *T. laxiflora*.

Among the 13 orchid species examined in this study, ectomycorrhizal fungi were detected in four orchids (Fig. 3.4). The proportion of reads derived from ectomycorrhizal fungi was 36.65% in *G. procera*, 7.7% in *Z. affinis*, 1.7% in *Z. boninensis*, and 1.46 % in *Z. leucochila*.

Although I detected various non-rhizoctonia saprotrophic fungal OTUs, in most orchids, except for *H. lepida*, the proportion of reads attributed to SAP fungi was less than half (up to 38.46% in *M. unifolia*, Fig. 3.4). In *H. lepida*, 70.04% of all reads originated from SAP fungi. Among these, the most dominant reads were from Psathyrellaeae (46.73%), followed by Sporormiaceae (16.33%), Chaetomiaceae (8.73%), and Halosphaeriaceae (6.98%) (Fig. 3.4).

Stable isotope analysis

The mean ± SD and results of the lmer function of $\delta^{13}C$, $\delta^{15}N$, and $\delta^{2}H$, as well as the enrichment factors and nitrogen concentrations of all plant species collected in this study, are summarized in Table 3.5, Table S3.1, and Fig. 3.5. Among the orchids investigated in this study, *C. takeoi* displayed significantly higher values for all isotope ratios and nitrogen concentrations than the autotrophs. Similarly, *Z. affinis* also exhibited significantly higher $\delta^{13}C$ and $\delta^{2}H$ values, and nitrogen concentrations than the autotrophs, although $\delta^{15}N$ was not significantly different. No significant differences in $\delta^{13}C$ were

observed for the other species.

Among the remaining 11 species, the following five species showed significantly higher δ^{15}N and δ^{2}H than those of autotrophs: *G. procera*, *O. yakushimensis*, *Z. leucochila*, *Z. strateumatica*, and *Nervilia aragoana*. *Z. leucochila*, *Z. strateumatica*, and *N. aragoana* also exhibited significantly higher nitrogen concentrations than autotrophs. Other than these species, *T. laxiflora* showed significantly higher δ^{2}H and nitrogen concentrations but not in δ^{13}C and δ^{15}N. *Goodyera hachijoensis* var. *matsumurana* showed higher δ^{15}N than that of surrounding autotrophs, but not in other stable isotope ratios or nitrogen concentrations. *Z. boninensis*, *O. tashiroi*, and *H. lepida* showed higher values than autotrophs only in nitrogen concentration. *M. unifolia* did not show significantly higher values for any of the responsible variables than autotrophs.

Discussion

Community profiling based on the metabarcoding technique revealed that rhizoctonia fungi predominated in ten of the thirteen orchid species (*C. takeoi, G. hachijoensis* var. *matsumurana*, *M. unifolia*, *N. aragoana*, *O. tashiroi*, *O. yakushimensis*, *Z. affnis*, *Z. boninesis*, *Z. leucochila*, *Z. strateumatica*), with prevalence rates ranging from 61.5% to 100%. This finding supports the hypothesis that these ten species are likely associated with rhizoctonia as their main mycorrhizal fungi.

A considerable number of sequences of ECM fungi or non-rhizoctonia SAP fungi were found in *G. procera* and *H. lepida*, respectively. In *G. procera*, 43.6% of the sequencing reads were attributed to rhizoctonia, while ECM fungi from the family

Sebacinaceae accounted for 36.7% of the reads in this species. Additionally, 70.0% of the total sequencing reads in *H. lepida* were identified as non-rhizoctonia SAP fungi, predominantly Psathyrellaceae fungi, which are known to be recruited as mycorrhizal fungi in some orchids with a high degree of mycoheterotrophy (Ogura-Tsujita & Yukawa, 2008; Yagame *et al.*, 2013; Bayman *et al.*, 2016; Suetsugu *et al.*, 2022a).

However, these orchids are not enriched in ^{13}C, despite these mycobionts being highly enriched in ^{13}C (Kohzu *et al.*, 1999; Gebauer & Meyer, 2003). Thus, my results do not support the heterotrophic utilization of ECM or non-rhizoctonia SAP fungi. A similar pattern has been observed in *Goodyera velutina* (subfamily Orchidoideae) and *Neottia ovata* (subfamily Epidendroideae) (Suetsugu *et al.*, 2019; Wang *et al.*, 2023). Additionally, although I detected some sequences of ECM fungi from *Z. affinis*, *Z. boninensis*, and *Z. leucochila*, these orchids also appear to rely on carbon from rhizoctonia rather than ECM fungi. Thus, the ECM and non-rhizoctonia SAP fungi detected in this study likely function simply as endophytes (Selosse *et al.*, 2022).

Stable isotope analysis indicated that *C. takeoi* and *Z. affinis* displayed significantly higher $\delta^{13}C$ values than autotrophs. These species also exhibited enrichment in $\delta^{15}N$ and $\delta^{2}H$, along with high nitrogen concentrations, although the $\delta^{2}H$ enrichment in *Z. affinis* was not significant. Meanwhile, five other orchids (*G. procera, N. aragoana, O. yakushimensis, Z. leucochila,* and *Z. strateumatica*) exhibited higher $\delta^{15}N$ and $\delta^{2}H$ than those of autotrophs, whereas their $\delta^{13}C$ were similar or significantly lower than those of autotrophic plants. The enrichment of $\delta^{15}N$ and $\delta^{2}H$ suggests partial mycoheterotrophy in these species, as the lower $\delta^{13}C$ does not necessarily negate mycoheterotrophic activity.

For instance, *Goodyera velutina* associated with rhizoctonia fungi, exhibits higher carbon isotope ratios in its albino individuals than autotrophic plants (Suetsugu *et al.*, 2019). The survival of albino individuals indicates some degree of mycoheterotrophy even under normal green conditions (Selosse *et al.*, 2004). Nonetheless, green *Goodyera velutina* individuals exhibit lower $\delta^{13}C$ than autotrophic plants (Suetsugu *et al.*, 2019). These findings suggest that the photosynthetic products of orchids presumably have low ^{13}C signatures, resulting in lower $\delta^{13}C$ values for green orchids with a low level of mycoheterotrophy. The difficulty in detecting ^{13}C enrichment in many rhizoctonia-associated orchids is likely amplified by the notably low ^{13}C enrichments of rhizoctonia with possibly endophytic lifestyles (Selosse & Martos, 2014). Notably, pelotons extracted from some rhizoctonia-associated orchids exhibit lower ^{13}C enrichments compared to autotrophic reference plants, with values ranging from 1.4–2.4‰ in pelotons of the genera *Anoectochilus*, *Epipactis*, *Ophrys*, and *Orchis* (Gomes *et al.*, 2023; Zahn *et al.*, 2023).

Consequently, via ^{2}H enrichment, along with another indirect evidence for mycoheterotrophy (^{15}N enrichment), my study proposes partial mycoheterotrophy in seven rhizoctonia-associated orchid species belonging to the genera *Cheirostylis*, *Nervilia*, and *Zeuxine* in subtropical or *Odontochilus* and *Zeuxine* in warm temperate regions of Japan. Along with two Asian *Cheirostylis* species, *C. liukiuensis,* and *C. montana* (Roy *et al.*, 2009; Yagi *et al.*, 2022), my study suggests partial mycoheterotrophy in *C. takeoi*. I also suggest partial mycoheterotrophy in *N. aragoana*, although the degree of mycoheterotrophy in *N. aragoana* is probably lower than that in *N. nipponica* associated with non-rhizoctonia fungi (Gale *et al.*, 2021). Meanwhile, I provided evidence for partial

mycoheterotrophy in three *Zeuxine* species. while at least some species (e.g., *Z. boninensis*) may behave autotrophically under certain environmental conditions. These results indicate partial mycoheterotrophy is common in rhizoctonia-associated orchids in Asia.

Notably, six out of seven species with significant ^{2}H and ^{15}N enrichment were collected from the forest understory, while only one species (*Z. strateumatica*) was from grasslands. My results largely align with previous notions that partial mycoheterotrophy is an adaption in shaded environments (Bidartondo *et al.*, 2004; Preiss *et al.*, 2010). On the other hand, partial mycoheterotrophy in *Z. strateumatica*, along with other grassland species (Schweiger *et al.*, 2018; Suetsugu *et al.*, 2020), suggests that this nutritional mode can be influenced by factors beyond light availability. Importantly, mixotrophy is known to have evolved frequently among parasitic and carnivorous plants that inhabit nutrient-poor open habitats (Selosse & Roy, 2009; Selosse *et al.*, 2017). This indicates a scenario where carbon flow occurs primarily to meet mineral needs, and the resulting mixotrophy may in turn promote further dependence on carbon obtained through these interactions (Selosse *et al.*, 2017; Suetsugu *et al.*, 2020). Thus, partial mycoheterotrophy in grassland species like *Z. strateumatica* may have evolved as a byproduct of the acquisition of nitrogen or other minerals, rather than primarily for carbon (Selosse *et al.*, 2017; Suetsugu *et al.*, 2020).

In conclusion, my data strongly suggest that partial mycoheterotrophy is common among rhizoctonia-associated orchids in the warm and humid regions of Asia. Previously, documented cases of partial mycoheterotrophic rhizoctonia-associated orchids in these

regions were primarily limited to specific species such as *Stigmatodactylus sikokianus* that has highly reduced leaves (Suetsugu *et al.*, 2021a), *Platanthera hondoensis* and *Cypripedium debile* that produces albino mutants (Suetsugu *et al.*, 2021c; Suetsugu & Matsubayashi, 2022), and *Cheirostylis liukiuensis* that possesses mycorrhizal rhizomes (Yagi *et al.*, 2022). For example, it was discovered that mature Taiwanese *C. appendiculata* individuals with well-developed leaves are fully autotrophic even based on ^{2}H enrichment pattern, while its seedlings associated with the saprotrophic non-rhizoctonia Psathyrellaceae were found to be partially mycoheterotrophic (Zahn *et al.*, 2022). This study, similar to recent research in Europe (Gebauer *et al.*, 2016; Schiebold *et al.*, 2018; Schweiger *et al.*, 2018, 2019), indicates that partial mycoheterotrophy is not uncommon in rhizoctonia-associated orchids with normal, well-developed leaves. The widespread partial mycoheterotrophic nature in rhizoctonia-associated orchids likely served as a preadaptation for the repeated evolution of full mycoheterotrophy within the family Orchidaceae.

Figures

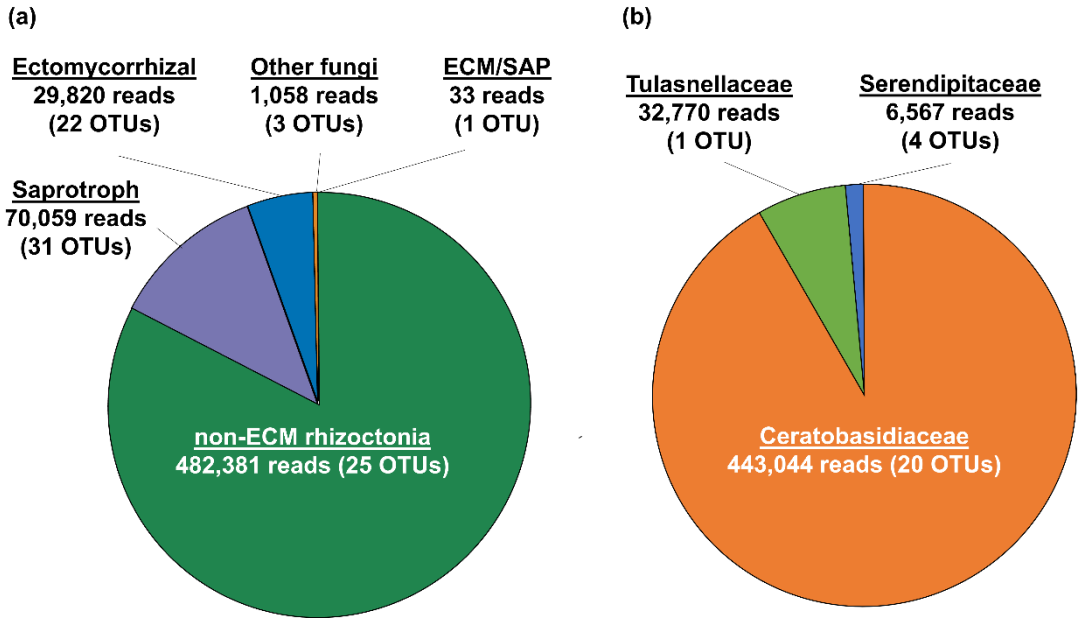

Figure 3.1. The numbers of OTUs and sequence reads detected from orchid species investigated in this study. (a) A pie graph segmented by fungal categories, and (b) segmented by fungal family within the rhizoctonia fungal sequences.

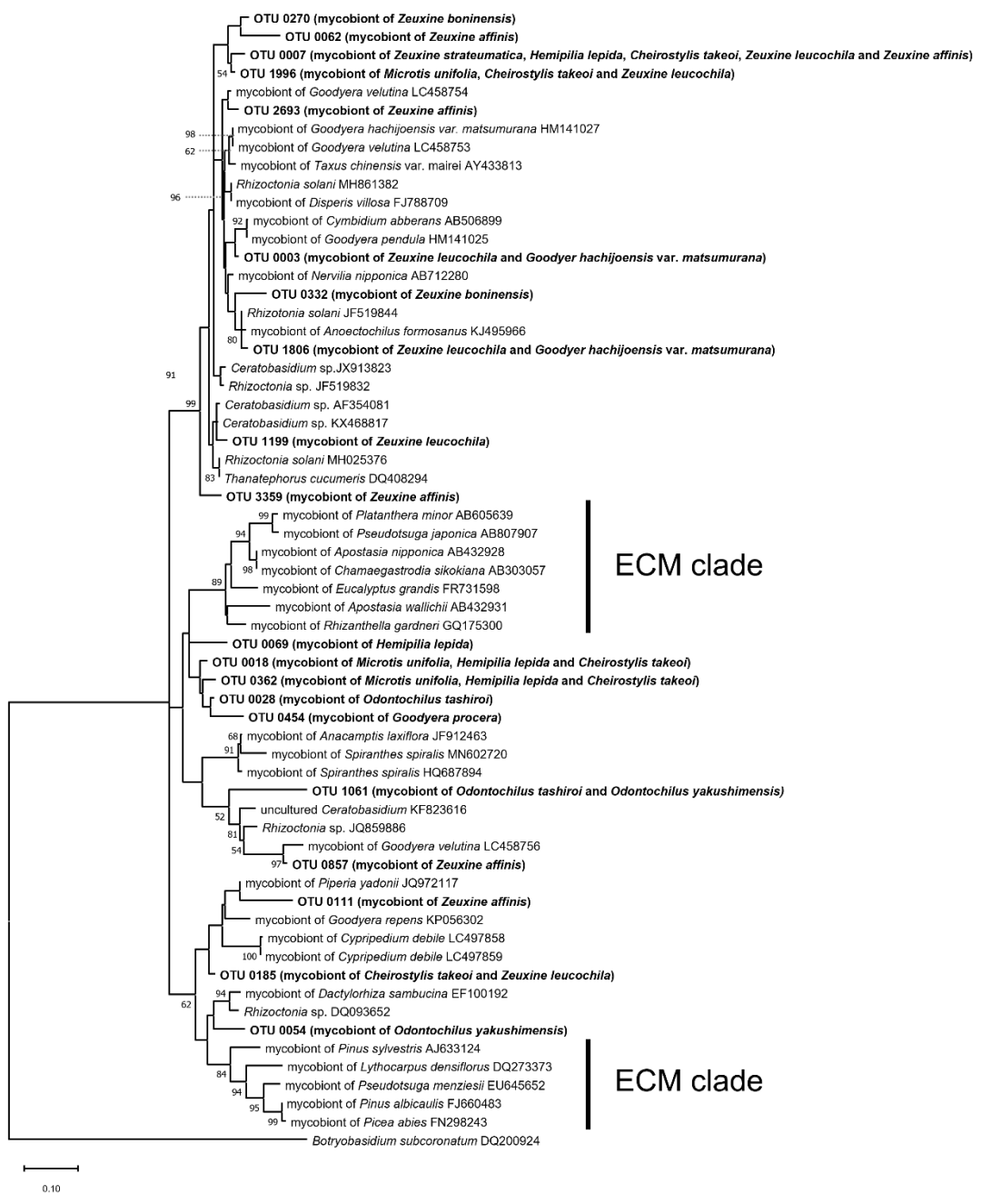

Figure 3.2. Phylogenetic tree of Ceratobasidiaceae based on maximum likelihood analysis. Sequences obtained in this study (ITS2 region; 230 bp) and partial internal transcribed spacer (ITS) region (530–557 bp) from International Nucleotide Sequence Database Collaboration (INSDC) used in Suetsugu et al. (2021) were analyzed. The tree is rooted using *Botryobasidium subcoronatum* (accession number DQ200924). Bootstrap values (1000 replicates, only >50%) are shown at each node. Scale bar indicates the number of substitutions per site. Putative fungal functional guilds (ECM, ectomycorrhizal) are indicated on the corresponding clades.

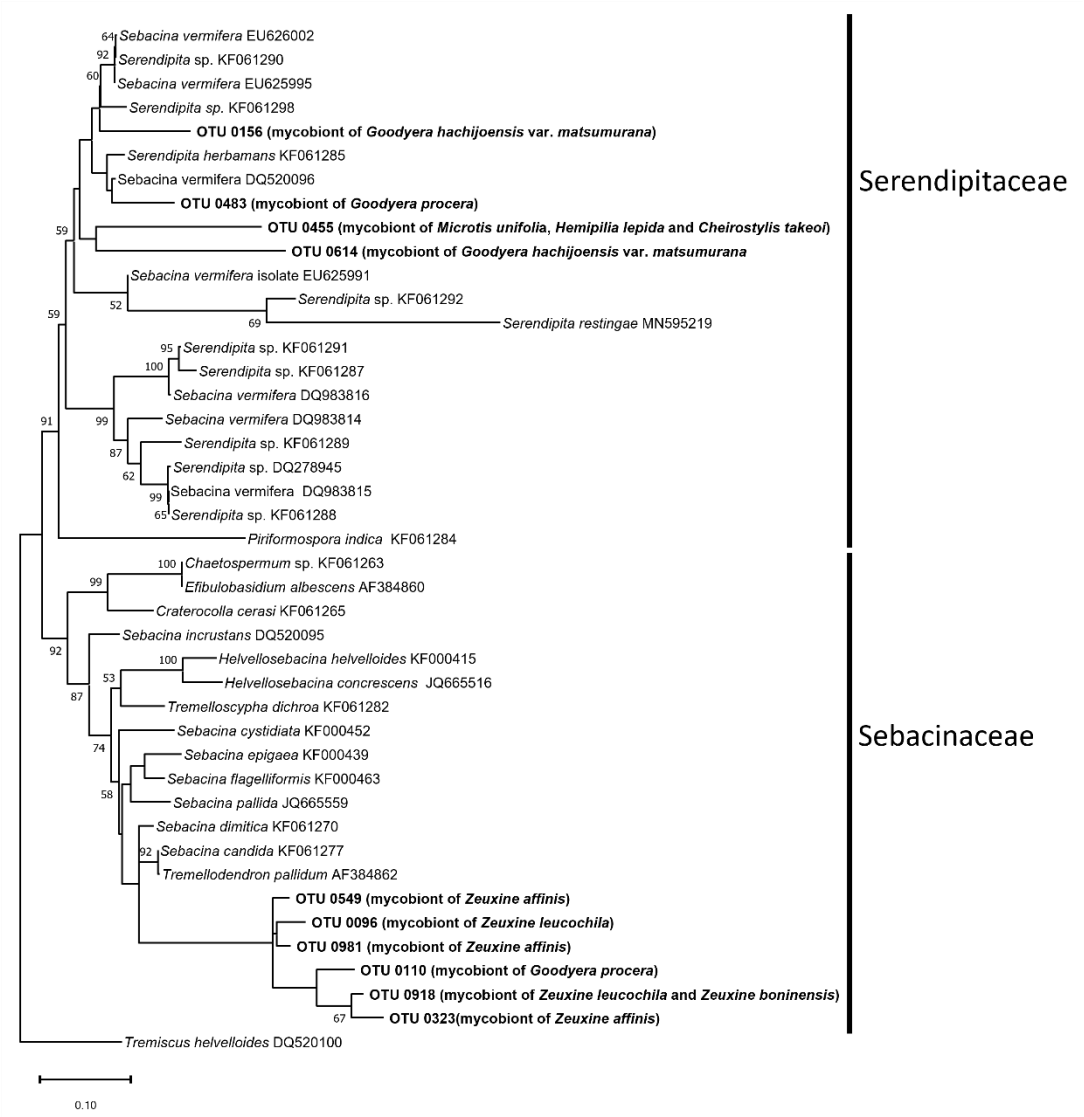

Figure 3.3. Phylogenetic tree of Sebacinales based on maximum likelihood analysis. Sequence obtained in this study (ITS2 region; 230 bp) and internal transcribed spacer (ITS) region (613–3049 bp) from International Nucleotide Sequence Database Collaboration (INSDC) used in Fritsche et al. (2021) were analyzed. The tree is rooted using *Tremiscus helvelloides* (accession number DQ520100). Bootstrap values (1000 replicates, only >50%) are shown at each node. Scale bar indicates the number of substitutions per site. Fungal families (Sebacinaceae or Serendipitaceae) are indicated on the corresponding clades.

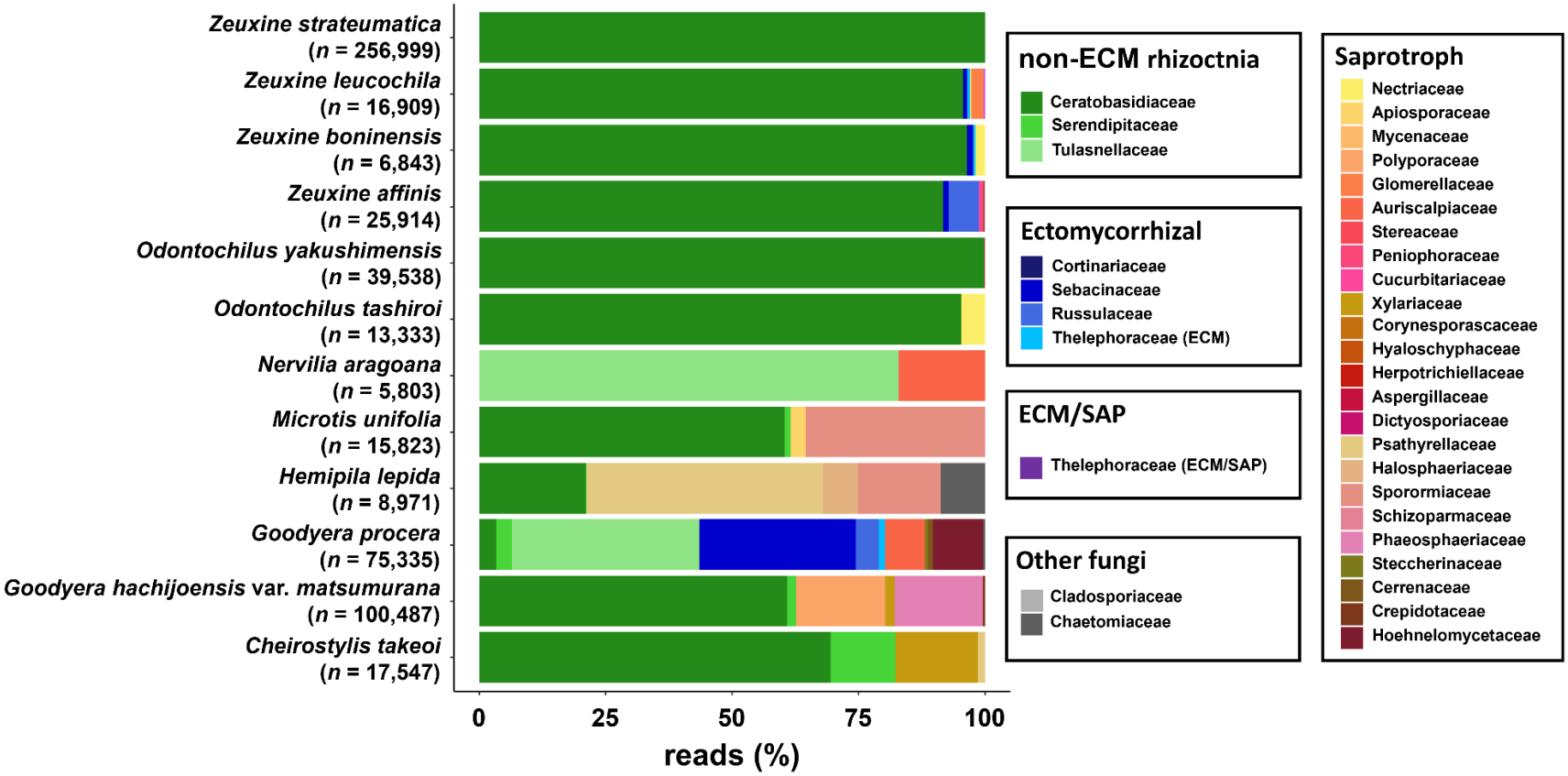

Figure 3.4. Read numbers and proportions of sequences detected from orchid species investigated in this study.

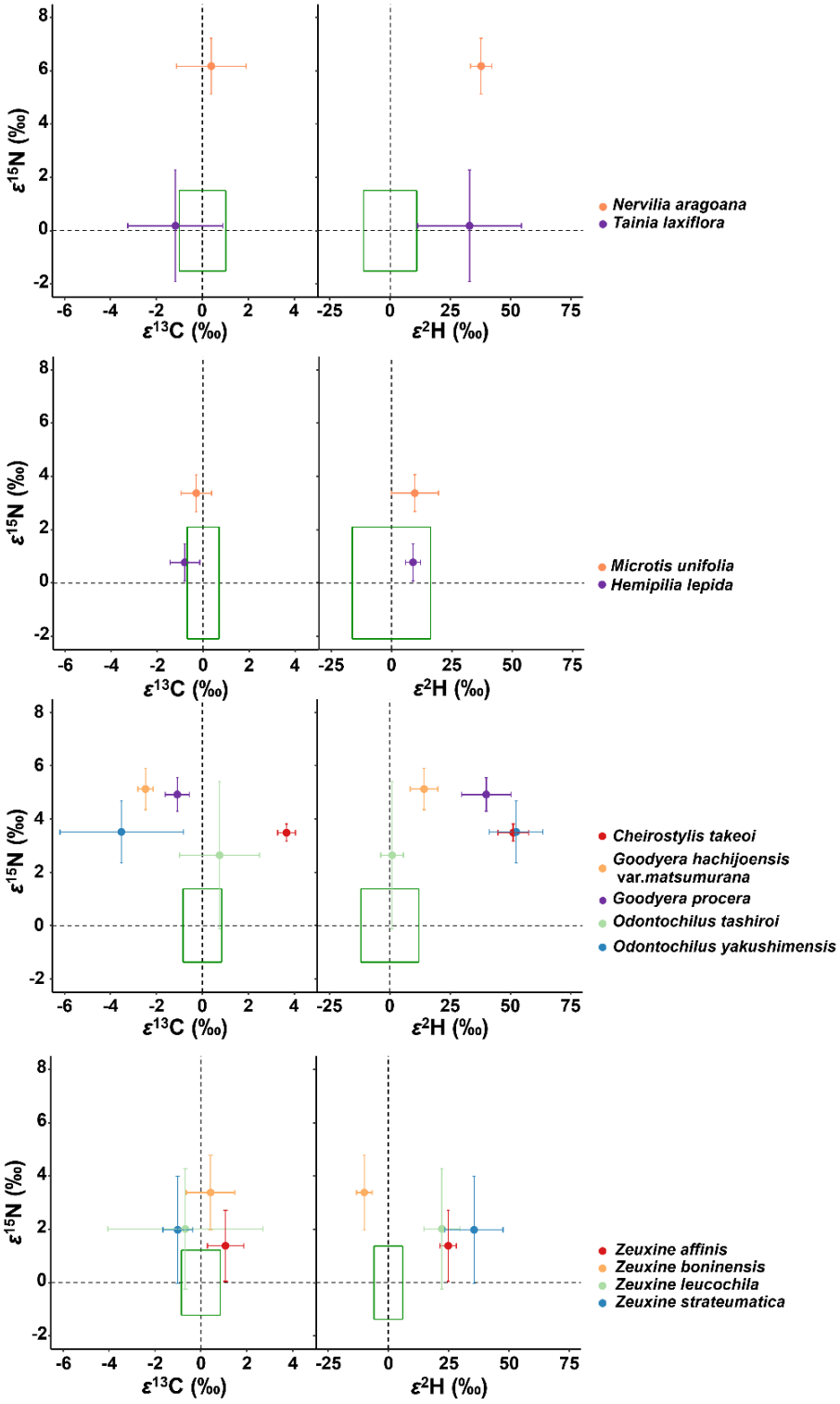

Figure 3.5. $\varepsilon^{13}C$, $\varepsilon^{15}N$, and $\varepsilon^{2}H$ values of orchids investigated in this study: (a) Orchids within Epidendroideae, (b) Orchidoideae (excluding Goodyerinae species), (c) Goodyerinae species other than *Zeuxine*, and (d) *Zeuxine* species. Green boxes represent ± SD of autotrophic references.

Table 3.1. Sample infromation investigated in this study.

Orchidoideae

Orchid species	Tribe	Subtribe	Sample n	Sampling sites	Climate	Sampling date	Species n of surrounding autotrophs	Sample n of surrounding autotrophs
Zeuxine affinis	Cranichideae	Goodyerinae	6	Awa, Kunigami-son, Kunigami-gun, Okinawa Pref., Japan	subtropical	2019.03.13	2	12
Odontochilus tashiroi	Cranichideae	Goodyerinae	5	Benoki, Kunigami-son, Kunigami-gun, Okinawa Pref., Japan	subtropical	2016.06.05	2	10
Zeuxine boninensis	Cranichideae	Goodyerinae	4		subtropical			
Zeuxine strateumatica	Cranichideae	Goodyerinae	5	Shimonaka, Sadowara-cho, Miyazaki City, Mayazaki Pref., Japan	warm temperate	2019.03.27	4	16
Zeuxine leucochila	Cranichideae	Goodyerinae	4	Sate, Kunigami-son, Kunigami-gun, Okinawa Pref., Japan	subtropical	2019.03.13	2	7
Cheirostylis takeoi	Cranichideae	Goodyerinae	3	Nerome, Oogimi-son, Kunigami-gun, Okinawa Pref. Japan	subtropical	2016.06.05	2	6
Goodyera hachijoensis var. *matsumurana*	Cranichideae	Goodyerinae	3	Haiminaka, Taketomi-cho, Yaeyama-gun, Okinawa Pref., Japan	subtropical	2022.3.25	3	9
Odontochilus yakushimensis	Cranichideae	Goodyerinae	4	Hina, Fuji City, Shizuoka Pref., Japan	warm temperate	2015.09.11	2	8
Goodyera procera	Cranichideae	Goodyerinae	3	Hiji, Kunigami-son, Kunigami-gun, Okinawa Pref., Japan	subtropical	2022.03.12	3	8
Microtis unifolia	Diurideae	Prasophyllinae	5	Ada, Kunigami-son, Kunigami-gun, Okinawa Pref., Japan	subtropical	2019.03.14	3	15
Hemipilia lepida	Orchideae	Orchidineae	5					

Epidendroideae

Orchid species	Tribe	Subtribe	Sample n	Sampling sites	Climate	Sampling date	Species n of surrounding autotrophs	Sample n of surrounding autotrophs
Nervilia aragoana	Nervillieae	Nervillinae	5	Uehara, Taketomi-cho, Yaeyama-gun, Okinawa Pref., Japan	subtropical	2019.07.20	3	15
Tainia laxiflora	Collabieae	Collabiinae	4	Sate, Kunigami-son, Kunigami-gun, Okinawa Pref., Japan	subtropical	2019.03.13	2	8

Table 3.2. Sample type (root or rhizome), number of individuals or mycorrhizal fragments, polymerase and primer set information used in this study.

Orchidoideae

Orchid species	sample type	individual number	mycorrhizal fragment *n*	Used polymerase	Used primer set
Cheirostylis takeoi	rhizome	3	12	KOD ONE	ITS1OF-ITS4OF, ITS86F/ITS4
Goodyera hachijoensis var. *matsumurana*	root	3	12	KOD ONE	ITS1OF-ITS4OF, ITS86F/ITS4
Goodyera procera	root	3	12	KOD ONE	ITS1OF-ITS4OF, ITS86F/ITS4
Hemipilia lepida	root	3	12	KOD ONE	ITS1OF-ITS4OF, ITS86F/ITS4
Microtis unifolia	root	3	12	KOD ONE	ITS1OF-ITS4OF, ITS86F/ITS4
Odontochilus tashiroi	rhizome	4	8	KOD ONE	ITS1OF-ITS4OF, ITS86F/ITS4
Odontochilus yakushimensis	rhizome	4	5	KOD ONE	ITS1OF-ITS4OF, ITS86F/ITS4
Zeuxine affinis	root	6	24	KOD ONE	ITS1OF-ITS4OF, ITS86F/ITS4
Zeuxine boninensis	root	3	8	Q5	ITS86F/ITS4
Zeuxine leucochila	root	3	8	Q5	ITS86F/ITS4
Zeuxine strateumatica	root	4	12	KOD ONE	ITS1OF-ITS4OF, ITS86F/ITS4

Epidendroideae

Orchid species	sample type	individual number	mycorrhizal fragment *n*	Used polymerase	Used primer set
Nervilia aragoana	root	3	9	KOD ONE	ITS1OF-ITS4OF, ITS86F/ITS4
Tainia laxiflora	root	4	12	KOD ONE	ITS1OF-ITS4OF, ITS86F/ITS4

Table 3.3. Result of BLAST search on the sequence identified as Tulasnellaceae fungi.

OTU name	Sequence	Accession of BLAST hit	Organism	Isolation source information
OTU 0083	CGCACCTTGCGCCCTCTGGTATTCCGGAGGGCATGCCCGGTTGAGTGTCATGAATATCTCAACTCTAACATTTTGTTAACGGTCTTGTGGGTGAAGGCTGCGGTCTAGCGAGATCGCAGGTTGTAATCCTTAGGGCTAAAGTGTTAGAGATTGGACTTGAGTTCTGTTGGCCCGCTAGGTCGACTGACTTGAAATTGATTAGCGATGCGTGATCCATTGGGTCCACCTCG	OQ678389	Tulasnellaceae sp.	roots of *Paphiopedilum armeniacum*

Table 3.4. Mycobiont OTUs and their read numbers detected from each orchid species.

Orchid species	non-ECM rhizoctonia		Saprotroph		Ectomycorrhizal		ECM/SAP		other fungi		Total read
	OTU *n*	read *n*	OTU *n*	read *n*	OTU *n*	read *n*	OTU *n*	read *n*	OTU *n*	read *n*	*n*
Cheirostylis takeoi	6	14450	3	3097	0	0	0	0	0	0	17547
Goodyera hachijoensis var. *matsumurana*	4	63023	4	37464	0	0	0	0	0	0	100487
Goodyera procera	3	32851	4	14626	3	27614	0	0	1	244	75335
Hemipilia lepida	5	1905	4	6283	0	0	0	0	1	783	8971
Microtis unifolia	3	9737	3	6086	0	0	0	0	0	0	15823
Nervilia aragoana	1	4815	1	988	0	0	0	0	0	0	5803
Odontochilus tashiroi	2	12713	1	620	0	0	0	0	0	0	13333
Odontochilus yakushimensis	1	39493	2	45	0	0	0	0	0	0	39538
Zeuxine affinis	6	23790	10	276	6	1845	0	0	1	31	25942
Zeuxine boninensis	2	6600	1	127	3	116	0	0	0	0	6843
Zeuxine leucochila	5	16005	5	447	11	245	1	33	0	0	16730
Zeuxine strateumatica	1	256999	0	0	0	0	0	0	0	0	256999

Table 3.5. The stable isotope ratios and nitrogen concentrations with summary of comparison between orchids and autotrophs. This comparison is based on Linear Mixed Model (LMM) fitting with plot as a random effect, and post-hoc t-tests using Satterthwaite's approximation.

Orchid (*Cheirostylis takeoi*) vs. Autotrophs							
	Orchid	Autotrophs	Estimates	Std. Error	df	t	*p*-value
$\delta^{13}C$ (‰)	−28.9 ± 0.4	−32.6 ± 1.3	3.7	0.8	7.0000	4.801	< 0.001
$\delta^{15}N$ (‰)	3.0 ± 0.3	−0.5 ± 1.3	3.5	0.8	7	4.336	< 0.01
N mmol/g	1.6 ± 0.5	1.1 ± 0.1	0.5	0.5	7	2.564	< 0.05
$\delta^{2}H$ (‰)	−10.3 ± 4.2	−61.4 ± 25.4	51.2	15.3	7	3.352	< 0.05

Orchid (*Goodyera hachijoensis var. matumurana*) vs. Autotrophs							
	Orchid	Autotrophs	Estimates	Std. Error	df	t	*p*-value
$\delta^{13}C$ (‰)	−36.7 ± 0.6	−34.3 ± 0.6	−2.4778	0.5	8.0000	−4.631	< 0.01
$\delta^{15}N$ (‰)	1.3 ± 0.7	−3.9 ± 2.3	5.1	1.4	10	3.713	< 0.01
N mmol/g	1.4 ± 0.2	1.4 ± 0.1	−0.04444	0.1	10.00000	−0.573	0.580
$\delta^{2}H$ (‰)	−38.2 ± 3.7	−52.5 ± 15.3	14.2	9.2	8.000	1.539	0.162

Orchid (*Goodyera procera*) vs. Autotrophs							
	Orchid	Autotrophs	Estimates	Std. Error	df	t	*p*-value
$\delta^{13}C$ (‰)	−34.8 ± 0.3	−33.7 ± 0.8	−1.1583	0.5	9.0000	−2.342	< 0.05
$\delta^{15}N$ (‰)	−0.1 ± 1.9	−4.9 ± 1.5	4.9	0.6	7	8.459	< 0.001
N mmol/g	0.8 ± 0.3	1.3 ± 0.3	−0.4229	0.2	7.1395	−2.71	0.030
$\delta^{2}H$ (‰)	−29.5 ± 7.9	−69.5 ± 11.4	40.0	3.9	5.000	10.26	< 0.001

Orchid (*Hemipilia lepida*) vs. Autotrophs							
	Orchid	Autotrophs	Estimates	Std. Error	df	t	*p*-value

$\delta^{13}C$ (‰)	31.4 ± 0.5	31.1 ± 0.7	−0.3	0.3	22.0000	−0.885	0.3857
$\delta^{15}N$ (‰)	0.1 ± 0.1	−2.9 ± 2.3	3.1	1.2	19.000	2.511	< 0.05
N mmol/g	1.8 ± 0.1	1.4 ± 0.5	0.4	0.2	22.0000	1.891	0.0719
$\delta^{2}H$ (‰)	−80.5 ± 8.3	−90.2 ± 16.7	9.7	7.3	21.000	1.318	0.202

Orchid (*Microtis unifolia*) vs. Autotrophs							
	Orchid	Autotrophs	Estimates	Std. Error	df	t	*p*-value
$\delta^{13}C$ (‰)	−31.9 ± 0.5	−31.1 ± 0.7	−0.8	0.3	22.0000	−2.360	< 0.05
$\delta^{15}N$ (‰)	−2.1 ± 0.4	−2.9 ± 2.3	0.5	1.1	19	0.432	0.6705
N mmol/g	1.2 ± 0.1	1.4 ± 0.5	−0.3	0.2	22.0000	−1.271	0.217
$\delta^{2}H$ (‰)	−81.4 ± 5.1	−90.2 ± 16.7	8.7	8.0	21.000	1.092	0.287

Orchid (*Nervilia aragoana*) vs. Autotrophs							
	Orchid	Autotrophs	Estimates	Std. Error	df	t	*p*-value
$\delta^{13}C$ (‰)	−34.2 ± 0.9	−34.5 ± 1.4	0.4	0.7	18	0.568	0.577
$\delta^{15}N$ (‰)	3.9 ± 0.9	−2.3 ± 0.8	6.2	0.4	18	14.850	< 0.001
N mmol/g	1.8 ± 0.7	1.2 ± 0.3	0.6	0.2	18	2.686	< 0.05
$\delta^{2}H$ (‰)	−24.1 ± 11.3	−62.0 ± 12.8	37.8	6.7	14.062	5.67	< 0.001

Orchid (*Odontochilus tashiroi*) vs. Autotrophs							
	Orchid	Autotrophs	Estimates	Std. Error	df	t	*p*-value
$\delta^{13}C$ (‰)	−35.5 ± 1.7	−36.2 ± 1.1	0.8	0.7	16.0000	1.097	0.289
$\delta^{15}N$ (‰)	3.7 ± 2.2	1.0 ± 1.1	2.6	0.8	15.000	3.317	< 0.01
N mmol/g	2.8 ± 0.4	2.2 ± 0.6	0.6	0.3	16.0000	1.934	0.07096
$\delta^{2}H$ (‰)	−35.8 ± 2.8	−36.8 ± 4.9	1.0	2.2	11.367	0.445	0.664404

Orchid (*Odontochilus yakushimensis*) vs. Autotrophs

	Orchid	Autotrophs	Estimates	Std. Error	df	t	*p*-value
$\delta^{13}C$ (‰)	−37.3 ± 2.2	−33.8 ± 1.1	−3.525	0.9	10	−3.832	< 0.01
$\delta^{15}N$ (‰)	−2.3 ± 0.5	−5.8 ± 2.0	3.5	1.0	10	3.396	< 0.01
N mmol/g	1.5 ± 0.2	1.2 ± 0.5	0.3	0.2	7.000	1.207	0.267
$\delta^{2}H$ (‰)	−31.7 ± 0.9	−85.8 ± 11.9	54.0	6.0	4.989	8.979	< 0.001

Orchid (*Tainia laxiflora*) vs. Autotrophs							
	Orchid	Autotrophs	Estimates	Std. Error	df	t	*p*-value
$\delta^{13}C$ (‰)	−35.2 ± 0.9	−34.1 ± 1.5	−1.175	0.8	7.0000	−1.4	0.199
$\delta^{15}N$ (‰)	−3.1 ± 0.8	−3.2 ± 2.9	0.2	1.5	10.0	0.124	0.904
N mmol/g	1.8 ± 0.3	0.8 ± 0.2	1.0	0.1	7.00000	9.859	< 0.001
$\delta^{2}H$ (‰)	−35.8 ± 23.9	−68.7 ± 12.6	32.9	9.9	7.000	3.319	< 0.05

Orchid (*Zeuxine affinis*) vs. Autotrophs							
	Orchid	Autotrophs	Estimates	Std. Error	df	t	*p*-value
$\delta^{13}C$ (‰)	−33.4 ± 0.6	−34.5 ± 0.7	1.1	0.3	11.0000	3.434	< 0.01
$\delta^{15}N$ (‰)	-2.2 ± 0.9	−3.6 ± 1.9	1.4	0.8	16.0000	1.641	0.120
N mmol/g	2.3 ± 0.3	0.9 ± 0.2	1.4	0.1	16.00000	11.88	< 0.001
$\delta^{2}H$ (‰)	--31.7 ± 5.0	−56.6 ± 8.4	24.9	3.4	11.000	7.355	< 0.001

Orchid (*Zeuxine boninensis*) vs. Autotrophs							
	Orchid	Autotrophs	Estimates	Std. Error	df	t	*p*-value
$\delta^{13}C$ (‰)	−35.9 ± 1.0	−36.2 ± 1.1	0.4	0.7	16.0000	0.515	0.614
$\delta^{15}N$ (‰)	4.1 ± 0.5	1.0 ± 1.1	3.0	1.0	15	3.185	< 0.01
N mmol/g	3.2 ± 0.6	2.2 ± 0.6	1.0	0.3	16.0000	3.119	0.007
$\delta^{2}H$ (‰)	−48.1 ± 2.1	−36.8 ± 4.9	−11.214	2.3	12.253	-4.8	< 0.001

Orchid (*Zeuxine leucochila*) vs. Autotrophs							
	Orchid	Autotrophs	Estimates	Std. Error	df	t	*p*-value
$\delta^{13}C$ (‰)	−35.1 ± 2.8	−34.6 ± 2.8	−0.4357	1.1	9	−0.387	0.708
$\delta^{15}N$ (‰)	1.2 ± 0.9	−1.1 ± 1.1	2.3	0.8	6	3.018	< 0.05
N mmol/g	3.4 ± 1.5	1.5 ± 0.6	1.9	0.4	6.1543	4.439	< 0.01
$\delta^{2}H$ (‰)	−32.5 ± 3.0	−53.3 ± 9.2	20.8	4.8	9	4.327	< 0.01

Orchid (*Zeuxine strateumatica*) vs. Autotrophs							
	Orchid	Autotrophs	Estimates	Std. Error	df	t	*p*-value
$\delta^{13}C$ (‰)	−30.0 ± 0.4	−29.1 ± 1.2	−0.917	0.6	19	−1.619	0.122
$\delta^{15}N$ (‰)	−0.1 ± 1.5	−2.1 ± 1.7	2.0	0.8	14	2.512	< 0.05
N mmol/g	0.9 ± 0.1	1.7 ± 0.6	−0.8313	0.3	19	−3.237	< 0.01
$\delta^{2}H$ (‰)	−33.8 ± 5.6	−70.1 ± 9.0	36.4	4.5	13.000	8.158	< 0.001

Table S3.1 Stable isotope ratios, enrichment factors, and nitrogen concentrations of each sample.

Taketomi-cho, Yaeyama-gun, Okinawa Pref., Japan, collected on 2019.07.20

Sample species	Plot	$\delta^{13}C$	$\delta^{15}N$	N mmol/g	$\delta^{2}H$	$\varepsilon^{13}C$	$\varepsilon^{15}N$	$\varepsilon^{2}H$	Analysis date: $\delta^{13}C$ and nitrogen concentration	Analysis date: $\delta^{15}N$	Analysis date: $\delta^{2}H$	Type
Nervilia aragoana	A	−34.9	4.3	2.4	−30.9	−1.1	7.1	37.2	2019.08.28	2019.09.05	2022.11.16	orchid
Nervilia aragoana	B	−32.7	4.9	1.2	NA	2.5	7.0	NA	2019.08.28	2019.09.05	2022.11.16	orchid
Nervilia aragoana	C	−34.7	4.1	1.6	−27.1	−1.1	6.6	34.3	2019.08.28	2019.09.05	2022.11.16	orchid
Nervilia aragoana	D	−33.8	2.8	1.3	−7.4	0.6	4.7	44.1	2019.08.28	2019.09.05	2022.11.16	orchid
Nervilia aragoana	E	−34.7	3.2	2.7	−31.1	1.0	5.5	35.2	2019.08.28	2019.09.05	2022.11.16	orchid
Diospyros maritima	A	−34.4	−2.8	1.4	−54.7	−0.6	0.0	13.4	2019.08.28	2019.09.05	2022.11.16	autotroph
Diospyros maritima	B	−35.3	−2.1	1.0	−77.2	−0.1	0.0	−14.6	2019.08.28	2019.09.05	2022.11.16	autotroph
Diospyros maritima	C	−35.3	−1.6	1.0	−68.5	−1.7	0.9	−7.1	2019.08.28	2019.09.05	2022.11.16	autotroph
Diospyros maritima	D	−33.8	−1.5	1.4	−43.9	0.6	0.4	7.6	2019.08.28	2019.09.05	2022.11.16	autotroph
Diospyros maritima	E	−35.5	−2.6	1.1	−64.8	0.2	−0.3	1.5	2019.08.28	2019.09.05	2022.11.16	autotroph
Machilus thunbergii	A	−31.7	−1.5	0.8	−78.6	2.1	1.3	−10.5	2019.08.28	2019.09.05	2022.11.16	autotroph
Machilus thunbergii	B	−35	−2.2	1.6	−73.4	0.2	−0.1	−10.8	2019.08.28	2019.09.05	2022.11.16	autotroph
Machilus thunbergii	C	−32.2	−2.6	1.1	−58.6	1.4	−0.1	2.8	2019.08.28	2019.09.05	2022.11.16	autotroph
Machilus thunbergii	D	−35.8	−2.8	1.0	−66.6	−1.4	−0.9	−15.1	2019.08.28	2019.09.05	2022.11.16	autotroph
Machilus thunbergii	E	−37	−2.9	0.8	−73.4	−1.3	−0.6	−7.1	2019.08.28	2019.09.05	2022.11.16	autotroph
Alpinia zerumbet	A	−35.4	−4.1	1.8	−71.1	−1.6	−1.3	−3.0	2019.08.28	2019.09.05	2022.11.16	autotroph
Alpinia zerumbet	B	−35.4	−2.9	1.9	−37.2	−0.2	0.1	25.4	2019.08.28	2019.09.05	2022.11.16	autotroph
Alpinia zerumbet	C	−33.4	−3.3	1.3	−57.1	0.2	−0.8	4.3	2019.08.28	2019.09.05	2022.11.16	autotroph
Alpinia zerumbet	D	−33.5	−1.4	1.1	−44	0.9	0.5	7.5	2019.08.28	2019.09.05	2022.11.16	autotroph

Alpinia zerumbet	E	−34.5	−1.4	1.3	−60.7	1.2	0.9	5.6	2019.08.28	2019.09.05	2022.11.16	autotroph

Awa, Kunigami-son, Kunigami-gun, Okinawa Pref., Japan, collected on 2019.03.13

Sample species	Plot	$\delta^{13}C$	$\delta^{15}N$	N mmol/g	$\delta^{2}H$	$\varepsilon^{13}C$	$\varepsilon^{15}N$	$\varepsilon^{2}H$	Analysis date: $\delta^{13}C$ and nitrogen concentration	Analysis date: $\delta^{15}N$	Analysis date: $\delta^{2}H$	Type
Zeuxine affinis	A	−33.8	−0.7	2.3	−32	1.5	2.5	27.0	2019.08.28	2019.11.05	2023.05.31	orchid
Zeuxine affinis	B	−33.4	−3.2	2.0	−37.2	0.5	−0.6	20.7	2019.08.28	2019.11.05	2023.05.31	orchid
Zeuxine affinis	C	−32.4	−3.2	2.3	−35.8	2.5	0.1	25.1	2019.08.28	2019.11.05	2023.05.31	orchid
Neolitsea sericea	A	−34.5	−5.2	1.1	−59	0.8	−2.1	−0.1	2019.08.28	2019.11.05	2023.05.31	autotroph
Neolitsea sericea	B	−34.4	−5	1.1	−59.4	−0.5	−2.4	−1.5	2019.08.28	2019.11.05	2023.05.31	autotroph
Neolitsea sericea	C	−34.4	−5.3	0.9	−59.9	0.5	−2.1	1.0	2019.08.28	2019.11.05	2023.05.31	autotroph
Castanopsis sieboldii	A	−36	−1.1	0.9	−58.9	−0.8	2.1	0.1	2019.08.28	2019.11.05	2023.05.31	autotroph
Castanopsis sieboldii	B	−33.4	−0.3	1.1	−56.4	0.5	2.4	1.5	2019.08.28	2019.11.05	2023.05.31	autotroph
Castanopsis sieboldii	C	−35.3	−1.2	0.7	−61.8	−0.5	2.1	−1.0	2019.08.28	2019.11.05	2023.05.31	autotroph
Zeuxine affinis	D	−33.8	−2.0	3.0	−23.4	0.4	1.7	22.2	2019.09.05	2019.11.05	2024.01.15	orchid
Zeuxine affinis	E	−33	−1.8	2.2	−29	1.1	1.9	30.1	2019.09.05	2019.11.05	2024.01.15	orchid
Zeuxine affinis	F	−33.9	−2.4	2.2	−32.9	0.6	2.8	24.2	2019.06.14	2019.11.05	2024.01.15	orchid
Neolitsea sericea	D	−34.2	−4.8	0.8	−30.7	−0.1	−1.1	14.9	2019.09.05	2019.11.05	2024.01.15	autotroph
Neolitsea sericea	E	−34.2	−5	0.8	−61.3	−0.1	−1.3	−2.2	2019.09.05	2019.11.05	2024.01.15	autotroph
Neolitsea sericea	F	−34.2	−5	1.1	−58.6	0.3	0.2	−1.6	2019.06.14	2019.11.05	2024.01.15	autotroph
Castanopsis sieboldii	D	−34.1	−2.6	0.7	−60.5	0.1	1.1	−14.9	2019.09.05	2019.11.05	2024.01.15	autotroph
Castanopsis sieboldii	E	−34	−2.4	0.6	−56.9	0.1	1.3	2.2	2019.09.05	2019.11.05	2024.01.15	autotroph
Castanopsis sieboldii	F	−34.8	−5.3	0.9	−55.5	−0.3	−0.2	1.6	2019.06.14	2019.11.05	2024.01.15	autotroph

Benoki, Kunigami-son, Kunigami-gun, Okinawa Pref., Japan, collected on 2016.06.05

Sample species	Plot	$\delta^{13}C$	$\delta^{15}N$	N mmol/g	$\delta^{2}H$	$\varepsilon^{13}C$	$\varepsilon^{15}N$	$\varepsilon^{2}H$	Analysis date: $\delta^{13}C$ and	Analysis date: $\delta^{15}N$	Analysis date: $\delta^{2}H$	Type

									nitrogen concentration			
Odontochilus tashiroi	A	−38	4.0	2.9	−37.9	−1.8	2.2	3.5	2019.09.05	2019.11.05	2023.05.31	orchid
Odontochilus tashiroi	B	−33.2	7.1	2.8	−37.8	3.1	6.7	−2.6	2019.09.05	2019.11.05	2023.05.31	orchid
Odontochilus tashiroi	C	−35.8	3.3	2.5	−31.1	0.7	3.5	6.2	2019.09.05	2019.11.05	2023.05.31	orchid
Odontochilus tashiroi	D	−35.6	1.1	3.3	−35.9	0.6	−1.0	3.0	2019.09.05	2019.11.05	2023.05.31	orchid
Odontochilus tashiroi	E	−34.8	2.8	2.4	−36.4	1.3	1.8	−5.2	2019.06.14	2019.11.05	2023.05.31	orchid
Zeuxine boninensis	A	−36.2	3.8	3.1	−49.4	0.0	2.0	−8.1	2019.09.05	2019.11.05	2023.05.31	orchid
Zeuxine boninensis	B	−35.4	3.8	3.0	−48	0.9	3.4	−12.8	2019.09.05	2019.11.05	2023.05.31	orchid
Zeuxine boninensis	C	−34.8	4.6	4.1	−49.9	1.7	4.8	−12.6	2019.09.05	2019.11.05	2023.05.31	orchid
Zeuxine boninensis	D	−37	NA	2.7	−45.2	−0.8	NA	−6.4	2019.06.14	2019.11.05	2023.05.31	orchid
Piper kadsura	A	−37.3	2.9	2.6	−41.5	−1.1	1.1	−0.2	2019.09.05	2019.11.05	2023.05.31	autotroph
Piper kadsura	B	−37.4	−0.2	2.6	−36.5	−1.2	−0.7	−1.3	2019.09.05	2019.11.05	2023.05.31	autotroph
Piper kadsura	C	−37.8	−0.7	2.7	−41.1	−1.35	−0.5	−3.8	2019.09.05	2019.11.05	2023.05.31	autotroph
Piper kadsura	D	−36.6	2.8	3.2	−33.1	−0.4	0.8	5.8	2019.09.05	2019.11.05	2023.05.31	autotroph
Piper kadsura	E	−36.7	0.9	2.1	−31.6	−0.7	−0.1	−0.4	2019.06.14	2019.11.05	2023.05.31	autotroph
Damnacanthus indicus	A	−35.1	0.7	1.4	−41.2	1.1	−1.1	0.2	2019.09.05	2019.11.05	2023.05.31	autotroph
Damnacanthus indicus	B	−35.1	1.1	1.4	−33.9	1.2	0.7	1.3	2019.09.05	2019.11.05	2023.05.31	autotroph
Damnacanthus indicus	C	−35.1	0.3	2.3	−33.5	1.4	0.5	3.8	2019.09.05	2019.11.05	2023.05.31	autotroph
Damnacanthus indicus	D	−35.8	1.3	2.1	−44.6	0.4	−0.8	−5.8	2019.09.05	2019.11.05	2023.05.31	autotroph
Damnacanthus indicus	E	−35.4	1.1	1.4	−30.8	0.7	0.1	0.4	2019.06.14	2019.11.05	2023.05.31	autotroph

Shimonaka, Sadowara-cho, Miyazaki City, Mayazaki Pref., Japan, collected on 2019.03.27

Sample species	Plot	$\delta^{13}C$	$\delta^{15}N$	N mmol/g	$\delta^{2}H$	$\varepsilon^{13}C$	$\varepsilon^{15}N$	$\varepsilon^{2}H$	Analysis date: $\delta^{13}C$ and nitrogen concentration	Analysis date: $\delta^{15}N$	Analysis date: $\delta^{2}H$	Type
Zeuxine strateumatica	A	−29.8	−1	1.0	−27.6	−0.2	0.1	42.3	2019.09.05	2019.11.05	2024.01.15	orchid
Zeuxine strateumatica	B	−30.6	0.5	0.8	−37.4	−1.3	3.9	33.4	2019.09.05	2019.11.05	2024.01.15	orchid
Zeuxine strateumatica	C	−30.2	0.0	0.8	−41	−0.9	0.6	19.6	2019.09.05	2019.11.05	2024.01.15	orchid
Zeuxine strateumatica	D	−29.7	2.1	1.1	−33.7	−1.9	4.4	NA	2019.09.05	2019.11.05	2024.01.15	orchid
Zeuxine strateumatica	E	−29.6	−1.9	0.8	−29.1	−0.8	0.9	47.0	2019.09.05	2019.11.05	2024.01.15	orchid
Kummerowia striata	A	−29.1	−1.4	1.8	−65.2	0.5	−0.3	4.7	2019.09.05	2019.11.05	2024.01.15	autotroph
Kummerowia striata	B	−28.5	−2.6	1.5	−72.6	0.8	0.8	−1.8	2019.09.05	2019.11.05	2024.01.15	autotroph
Kummerowia striata	C	−28.5	−2.7	1.9	NA	0.9	−2.13	NA	2019.09.05	2019.11.05	NA	autotroph
Kummerowia striata	D	−28.5	−2.7	1.8	NA	−0.7	−0.4	NA	2019.09.05	2019.11.05	NA	autotroph
Kummerowia striata	E	−28.6	−2.2	2.0	−66.4	0.3	0.6	9.7	2019.09.05	2019.11.05	2024.01.15	autotroph
Trifolium repens	A	−28.8	−0.8	2.5	NA	0.8	0.3	NA	2019.09.05	2019.11.05	NA	autotroph
Trifolium repens	C	−29.6	−0.6	2.2	NA	−0.3	0.0	NA	2019.09.05	2019.11.05	NA	autotroph
Trifolium repens	E	−29.4	−1.5	2.2	−91.2	−0.6	1.3	−15.1	2019.09.05	2019.11.05	2024.01.15	autotroph
Ophioglossum thermale	B	−29.4	−2.1	1.1	−66.3	−0.1	1.3	4.5	2019.09.05	2019.11.05	2024.01.15	autotroph
Ophioglossum thermale	C	−28	1.6	1.8	−57.4	1.4	2.2	3.2	2019.09.05	2019.11.05	2024.01.15	autotroph
Ophioglossum thermale	D	−27.1	−1.9	2.2	NA	0.7	0.4	NA	2019.09.05	2019.11.05	NA	autotroph
Ophioglossum thermale	E	−26.9	−3.9	2.6	NA	2.0	−1.1	NA	2019.09.05	2019.11.05	NA	autotroph
Hydrocotyle maritima	A	−30.9	NA	0.9	−74.5	−1.3	NA	−4.7	2019.09.05	2019.11.05	2024.01.15	autotroph
Hydrocotyle maritima	B	−29.9	−5.5	1.2	−73.4	−0.6	−2.1	−2.6	2019.09.05	2019.11.05	2024.01.15	autotroph

Hydrocotyle maritima	C	−31.3	NA	0.8	−63.7	−20	NA	−3.2	2019.09.05	2019.11.05	2024.01.15	autotroph
Hydrocotyle maritima	E	−30.5	−3.7	1.2	−70.7	−1.7	−0.9	5.4	2019.09.05	2019.11.05	2024.01.15	autotroph

Sate, Kunigami-son, Kunigami-gun, Okinawa Pref., Japan, collected on 2019.03.13

Sample species	Plot	$\delta^{13}C$	$\delta^{15}N$	N mmol/g	$\delta^{2}H$	$\varepsilon^{13}C$	$\varepsilon^{15}N$	$\varepsilon^{2}H$	Analysis date: $\delta^{13}C$ and nitrogen concentration	Analysis date: $\delta^{15}N$	Analysis date: $\delta^{2}H$	Type
Tainia laxiflora	A	−34	−1.9	1.4	−47.3	1.5	2.9	15.8	2019.09.05	2019.11.05	2023.06.01	orchid
Tainia laxiflora	B	−35.9	−3.5	2.0	−48.7	−3.45	−0.4	26.5	2019.09.05	2019.11.05	2023.06.01	orchid
Tainia laxiflora	C	−35.1	−3.1	1.7	−47.3	−1.85	−2.2	25.0	2019.09.05	2019.11.05	2023.06.01	orchid
Tainia laxiflora	D	−35.9	−3.7	1.9	0.0	−0.9	0.4	64.4	2019.06.14	2019.11.05		orchid
Smilax china	A	−34.8	−2.2	0.7	−80.8	0.7	2.6	−17.7	2019.09.05	2019.11.05	2023.06.01	autotroph
Smilax china	B	−32.9	−0.5	0.7	−78.5	−0.45	2.7	−3.4	2019.09.05	2019.11.05	2023.06.01	autotroph
Smilax china	C	−33.7	0.5	0.6	−82.8	−0.45	1.5	−10.5	2019.09.05	2019.11.05	2023.06.01	autotroph
Smilax china	D	−33.9	−1.7	1.1	−68.9	1.1	2.4	−4.5	2019.06.14	2019.11.05	2023.06.01	autotroph
Neolitsea sericea	A	−36.2	−7.4	0.8	−45.4	−0.7	−2.6	17.7	2019.09.05	2019.11.05	2023.06.01	autotroph
Neolitsea sericea	B	−32	−5.8	1.0	−71.8	0.5	−2.6	3.4	2019.09.05	2019.11.05	2023.06.01	autotroph
Neolitsea sericea	C	−32.8	−2.4	0.6	−61.8	0.5	−1.5	10.5	2019.09.05	2019.11.05	2023.06.01	autotroph
Neolitsea sericea	D	−36.1	−6.4	0.9	−59.9	−1.1	−2.4	4.5	2019.09.05	2019.11.05	2023.06.01	autotroph
Zeuxine leucochila	A	−31.9	2.3	5.6	−34.1	3.2	4.2	16.0	2019.09.05	2019.11.05	2024.01.15	orchid
Zeuxine leucochila	B	−33.7	0.9	3.2	−28.4	1.2	2.2	22.9	2019.09.05	2019.11.05	2024.01.15	orchid
Zeuxine leucochila	C	−38	NA	2.3	−35.3	−3.1	NA	17.5	2019.09.05	2019.11.05	2024.01.15	orchid
Zeuxine leucochila	D	−36.6	0.5	2.6	−32	−3.9	−0.3	32.6	2019.06.14	2019.11.05	2024.01.15	orchid
Smilax china	A	−35.8	−1.9	2.3	−57.3	−0.75	0.0	−7.3	2019.09.05	2019.11.05	2024.01.15	autotroph
Smilax china	B	−33.3	−1.2	2.0	−58.5	−0.45	0.1	−7.2	2019.09.05	2019.11.05	2024.01.15	autotroph
Smilax china	C	−33.3	NA	1.4	−61	−0.4	NA	−8.3	2019.06.14	2019.11.05	2024.01.15	autotroph
Castanopsis sieboldii	A	−34.3	−1.9	2.1	−42.8	0.8	0.0	7.3	2019.09.05	2019.11.05	2024.01.15	autotroph

Castanopsis sieboldii	B	−34.4	−1.3	0.8	−44.1	0.5	−0.1	7.2	2019.09.05	2019.11.05	2024.01.15	autotroph
Castanopsis sieboldii	C	−34.5	NA	0.8	−44.5	0.4	NA	8.3	2019.09.05	2019.11.05	2024.01.15	autotroph
Castanopsis sieboldii	D	−32.7	0.8	1.3	−64.6	0.0	0.0	0.0	2019.06.14	2019.11.05	2024.01.15	autotroph

Nerome, Oogimi-son, Kunigami-gun, Okinawa Pref. Japan, collected on 2016.06.05

Sample species	Plot	$\delta^{13}C$	$\delta^{15}N$	N mmol/g	$\delta^{2}H$	$\varepsilon^{13}C$	$\varepsilon^{15}N$	$\varepsilon^{2}H$	Analysis date: $\delta^{13}C$ and nitrogen concentration	Analysis date: $\delta^{15}N$	Analysis date: $\delta^{2}H$	Type
Cheirostylis takeoi	A	−28.6	3.2	2.2	−6.1	3.6	3.8	57.7	2022.08.24	2022.08.26	2023.07.27	orchid
Cheirostylis takeoi	B	−29.3	3.0	1.3	−10.2	3.4	3.5	50.8	2022.08.24	2022.08.26	2023.07.27	orchid
Cheirostylis takeoi	C	−28.9	2.7	1.3	−14.5	4.1	3.2	45.1	2022.08.24	2022.08.26	2023.07.27	orchid
Hedera rhombea	A	−33.5	−1.8	1.1	−84.3	−1.4	−1.2	−20.5	2022.08.24	2022.08.26	2023.07.27	autotroph
Hedera rhombea	B	−33.4	−1.7	1.2	−84.0	−0.8	−1.2	−23.1	2022.08.24	2022.08.26	2023.07.27	autotroph
Hedera rhombea	C	−34.1	−1.7	1.0	−85.1	−1.1	−1.3	−25.6	2022.08.24	2022.08.26	2023.07.27	autotroph
Trachelospermum asiaticum	A	−30.8	0.6	1.0	−43.3	1.4	1.2	20.5	2022.08.24	2022.08.26	2023.07.27	autotroph
Trachelospermum asiaticum	B	−31.9	0.7	1.1	−37.9	0.8	1.2	23.1	2022.08.24	2022.08.26	2023.07.27	autotroph
Trachelospermum asiaticum	C	−31.9	0.8	1.1	−34.0	1.1	1.3	25.6	2022.08.24	2022.08.26	2023.07.27	autotroph

Haiminaka, Taketomi-cho, Yaeyama-gun, Okinawa Pref., Japan, collected on 2022.03.25

Sample species	Plot	$\delta^{13}C$	$\delta^{15}N$	N mmol/g	$\delta^{2}H$	$\varepsilon^{13}C$	$\varepsilon^{15}N$	$\varepsilon^{2}H$	Analysis date: $\delta^{13}C$ and nitrogen concentration	Analysis date: $\delta^{15}N$	Analysis date: $\delta^{2}H$	Type
Goodyera hachijoensis var. *matsumurana*	A	−37.4	0.7	1.2	−42	−2.73	4.3	8.4	2022.08.24	2022.08.26	2023.07.27	orchid

Goodyera hachijoensis var. *matsumurana*	B	−36.3	2.0	1.4	−38	−2.6	5.3	14.4	2022.08.24	2022.08.26	2023.07.27	orchid
Goodyera hachijoensis var. *matsumurana*	C	−36.5	1.1	1.5	−34.7	−2.1	5.8	19.9	2022.08.24	2022.08.26	2023.07.27	orchid
Dioscorea pseudojaponica	A	−33.3	−1.9	1.4	−30.9	1.4	1.7	19.5	2022.08.24	2022.08.26	2023.07.27	autotroph
Dioscorea pseudojaponica	B	−33.3	−0.1	1.5	−34.3	0.4	3.2	18.1	2022.08.24	2022.08.26	2023.07.27	autotroph
Dioscorea pseudojaponica	C	−34.5	−3.5	1.6	−57	−0.1	1.2	−2.5	2022.08.24	2022.08.26	2023.07.27	autotroph
Oplismenus undulatifolius	A	−34.4	−5.1	1.5	−69.9	0.3	−1.5	−19.5	2022.08.24	2022.08.26	2023.07.27	autotroph
Oplismenus undulatifolius	B	−33.9	−6	1.3	−69.4	−0.2	−2.7	−17.0	2022.08.24	2022.08.26	2023.07.27	autotroph
Oplismenus undulatifolius	C	−34.1	−7.9	1.3	NA	0.3	−3.2	NA	2022.08.24	2022.08.26	2023.07.27	autotroph
Alpinia intermedia	A	−36.3	−3.7	1.4	NA	−1.6	−0.1	NA	2022.08.24	2022.08.26	2023.07.27	autotroph
Alpinia intermedia	B	−33.9	−3.8	1.3	−53.6	−0.2	−0.5	−1.2	2022.08.24	2022.08.26	2023.07.27	autotroph
Alpinia intermedia	C	−34.6	−2.7	1.4	−52.1	−0.2	2.0	2.5	2022.08.24	2022.08.26	2023.07.27	autotroph

Hina, Fuji City, Shizuoka Pref., Japan, collected on 2015.09.11

Sample species	Plot	$\delta^{13}C$	$\delta^{15}N$	N mmol/g	$\delta^{2}H$	$\varepsilon^{13}C$	$\varepsilon^{15}N$	$\varepsilon^{2}H$	Analysis date: $\delta^{13}C$ and nitrogen concentration	Analysis date: $\delta^{15}N$	Analysis date: $\delta^{2}H$	Type
Odontochilus yakushimensis	A	−37.4	−2.2	1.7	−31.5	−2.3	1.8	59.0	2022.08.24	2022.08.26	2023.07.27	orchid
Odontochilus yakushimensis	B	−40.3	−2	1.3	−32.7	−7.6	4.2	51.5	2022.08.24	2022.08.26	2023.07.27	orchid

Odontochilus yakushimensis	C	−36.4	−2	1.4	−32	−2.6	4.3	62.1	2022.08.24	2022.08.26	2023.07.27	orchid
Odontochilus yakushimensis	D	−35.2	−3	1.6	−30.5	−1.7	3.8	37.2	2022.08.24	2022.08.26	2023.07.27	orchid
Rubus buergeri	A	−34.2	−6.9	1.4	−90.5	−2.9	0.9	0.0	2022.08.24	2022.08.26	2023.07.27	autotroph
Rubus buergeri	B	−33.2	−6.5	1.5	−86.1	−0.5	−0.3	−2.0	2022.08.24	2022.08.26	2023.07.27	autotroph
Rubus buergeri	C	−33.7	−7.2	1.1	−104.4	0.2	−0.9	−10.3	2022.08.24	2022.08.26	2023.07.27	autotroph
Rubus buergeri	D	−33	−6.5	1.4	NA	0.5	0.3	NA	2022.08.24	2022.08.26	2023.07.27	autotroph
Eurya japonica var. *japonica*	A	−36	−1.1	2.1	NA	−0.9	2.9	NA	2022.08.24	2022.08.26	2023.07.27	autotroph
Eurya japonica var. *japonica*	B	−32.3	−5.9	0.7	−82.2	0.5	0.3	2.0	2022.08.24	2022.08.26	2023.07.27	autotroph
Eurya japonica var. *japonica*	C	−34	−5.4	0.9	−83.8	−0.2	0.9	10.3	2022.08.24	2022.08.26	2023.07.27	autotroph
Eurya japonica var. *japonica*	D	−34	−7	0.8	−67.7	−0.5	−0.3	0.0	2022.08.24	2022.08.26	2023.07.27	autotroph

Hiji, Kunigami-son, Kunigami-gun, Okinawa Pref., Japan, collected on 2022.03.12

Sample species	Plot	$\delta^{13}C$	$\delta^{15}N$	N mmol/g	$\delta^{2}H$	$\varepsilon^{13}C$	$\varepsilon^{15}N$	$\varepsilon^{2}H$	Analysis date: $\delta^{13}C$ and nitrogen concentration	Analysis date: $\delta^{15}N$	Analysis date: $\delta^{2}H$	Type
Goodyera procera	A	−35.1	−1.3	0.5	−38.7	−1.5	4.3	38.8	2022.08.24	2022.08.26	2024.01.15	orchid
Goodyera procera	B	−34.8	−1.2	0.9	−25.3	−0.5	5.0	50.8	2022.08.24	2022.08.26	2024.01.15	orchid
Goodyera procera	C	−34.6	2.1	1.1	−24.6	−1.3	5.5	30.5	2022.08.24	2022.08.26	2024.01.15	orchid
Rubus nesiotes	A	−34	−6.3	1.0	−75.3	−0.4	−0.7	2.2	2022.08.24	2022.08.26	2024.01.15	autotroph
Rubus nesiotes	B	−34	−6.6	0.9	−76.9	0.3	−0.5	−0.9	2022.08.24	2022.08.26	2024.01.15	autotroph
Rubus nesiotes	C	−33.5	−3.5	1.3	−56.1	−0.2	−0.1	−1.1	2022.08.24	2022.08.26	2024.01.15	autotroph
Styrax japonicus	A	−34.3	−6.2	1.3	−79.7	−0.7	−0.6	−2.2	2022.08.24	2022.08.26	2024.01.15	autotroph

Styrax japonicus	B	−34.6	−5.7	1.3	−75.2	−0.3	0.5	0.9	2022.08.24	2022.08.26	2024.01.15	autotroph
Styrax japonicus	C	−34.1	−2.6	1.8	NA	−0.8	0.8	NA	2022.08.24	2022.08.26	NA	autotroph
Melastoma candidum	A	−32.5	−4.2	1.2	NA	1.1	1.4	NA	2022.08.24	2022.08.26	NA	autotroph
Melastoma candidum	C	−32.4	−4.2	1.3	−54	0.9	−0.8	1.1	2022.08.24	2022.08.26	2024.01.15	autotroph

Ada, Kunigami-son, Kunigami-gun, Okinawa Pref., Japan, collected on 2019.03.14

Sample species	Plot	$\delta^{13}C$	$\delta^{15}N$	N mmol/g	$\delta^{2}H$	$\varepsilon^{13}C$	$\varepsilon^{15}N$	$\varepsilon^{2}H$	Analysis date: $\delta^{13}C$ and nitrogen concentration	Analysis date: $\delta^{15}N$	Analysis date: $\delta^{2}H$	Type
Microtis unifolia	A	−32.4	−2.9	1.1	−86.3	−1.4	−0.1	6.0	2019.09.05	2019.11.05	2023.07.26	orchid
Microtis unifolia	B	−32.4	−2.8	1.1	−85	−1.4	1.4	8.2	2019.09.05	2019.11.05	2023.07.26	orchid
Microtis unifolia	C	−31.2	−2.2	1.3	−79	0	0.6	13.4	2019.09.05	2019.11.05	2023.07.26	orchid
Microtis unifolia	D	−31.7	−2	1.1	−75.4	−0.9	1.3	8.0	2019.09.05	2019.11.05	2023.07.26	orchid
Microtis unifolia	E	−31.6	NA	1.2	NA	−0.3	NA	NA	2019.06.14	NA	NA	orchid
Hemipilia lepida	A	−30.9	0.2	1.8	−68.2	0.1	3.0	24.1	2019.09.05	2019.11.05	2023.07.26	orchid
Hemipilia lepida	B	−31.4	0.0	2.0	−87.2	−0.4	4.2	6.0	2019.09.05	2019.11.05	2023.07.26	orchid
Hemipilia lepida	C	−30.9	0.2	1.8	−86	0.3	3.0	6.4	2019.09.05	2019.11.05	2023.07.26	orchid
Hemipilia lepida	D	−32.2	NA	1.7	−85.5	−1.4	NA	−2.1	2019.09.05	NA	2023.07.26	orchid
Hemipilia lepida	E	−31.4	NA	1.9	−75.5	−0.1	NA	13.8	2019.06.14	NA	2023.07.26	orchid
Curculigo orchioides	A	−31.4	−3.2	1.1	−84.8	−0.4	−0.4	7.5	2019.09.05	2019.11.05	2023.07.26	autotroph
Curculigo orchioides	B	−30.9	−4.6	0.9	−77.5	0.1	−0.4	15.7	2019.09.05	2019.11.05	2023.07.26	autotroph
Curculigo orchioides	C	−30.9	−5.6	1.1	−80.4	0.3	−2.8	12.	2019.09.05	2019.11.05	2023.07.26	autotroph
Curculigo orchioides	D	−30.4	−5.9	0.9	−76	0.4	−2.6	7.4	2019.09.05	2019.11.05	2023.07.26	autotroph
Curculigo orchioides	E	−31.5	−3.1	1.2	−63.3	−0.2	−1.3	26.0	2019.06.14	2019.11.05	2023.07.26	autotroph
Bidens pilosa	A	−32	−4.3	0.9	−95.1	−1	−1.5	−2.8	2019.09.05	2019.11.05	2023.07.26	autotroph
Bidens pilosa	B	−32.1	−6.1	1.5	−102.2	−1.1	−1.9	−9.0	2019.09.05	2019.11.05	2023.07.26	autotroph

Bidens pilosa	C	−31.9	−3	1.1	−85.4	−0.7	−0.2	7.0	2019.09.05	2019.11.05	2023.07.26	autotroph
Bidens pilosa	D	−31.1	−4.2	1.2	−63.2	−0.3	−0.9	20.2	2019.09.05	2019.11.05	2023.07.26	autotroph
Bidens pilosa	E	−31	−2.7	2.2	−87.8	0.3	−0.9	1.5	2019.06.14	2019.11.05	2023.07.26	autotroph
Polygala paniculata	A	−29.6	−0.8	2.1	−97.1	1.4	2.0	−4.8	2019.09.05	2019.11.05	2023.07.26	autotroph
Polygala paniculata	B	−29.9	−1.8	1.3	−100	1.1	2.4	−6.8	2019.09.05	2019.11.05	2023.07.26	autotroph
Polygala paniculata	C	−30.8	0.3	2.1	−111.5	0.4	3.1	−19.1	2019.09.05	2019.11.05	2023.07.26	autotroph
Polygala paniculata	D	−30.9	0.3	2.4	−111.1	−0.1	3.6	−27.7	2019.09.05	2019.11.05	2023.07.26	autotroph
Polygala paniculata	E	−31.5	0.5	1.5	−116.9	−0.17	2.3	−27.6	2019.06.14	2019.11.05	2023.07.26	autotroph

Table S3.2. Details of comparison of stable isotope ratios and nitrogen concentrations between plant type (Orchid vs autotrophs) using linear mixed model and post-hoc t-test with Satterthwaite's approximation.

Orchid (*Hemipilia lepida* and *Microtis unifolia)* vs. Autotrophs					
$\delta^{13}C$ (‰)					
Fixed effects	Estimates	Std. Error	df	t	p-value
(Intercept)	−31.06	0.170	22.0000	183.254	<2e-16 ***
H. lepida	−0.3	0.339	22.0000	−0.885	0.3857
M. unifolia	−0.8	0.339	22.0000	−2.360	0.0276 *
Random effects	σ^2	N		Marginal R^2	0.191
plot	0.0000	5		AICc	62.997
$\delta^{15}N$ (‰)					
Fixed effects	Estimates	Std. Error	df	t	p-value
(Intercept)	−2.9467	0.501	19.000	−5.883	1.15e-05 ***
H. lepida	3.080	1.227	19.000	2.511	0.0213 *
M. unifolia	0.472	1.092	19	0.432	0.6705
Random effects	σ^2	N		Marginal R^2	0.231
plot	0.000	5		AICc	98.040
N mmol/g					
Fixed effects	Estimates	Std. Error	df	t	p-value
(Intercept)	1.4333	0.1076	22.0000	13.327	5.17e-12 ***
H. lepida	0.4067	0.2151	22.0000	1.891	0.0719
M. unifolia	−0.2733	0.2151	22.0000	−1.271	0.217
Random effects	σ^2	N		Marginal R^2	0.221

plot	0.000	5		AICc	42.985
δ^2H (‰)					
Fixed effects	Estimates	Std. Error	df	t	p-value
(Intercept)	−90.153	3.669		−24.574	<2e-16 ***
H. lepida	9.673	7.337	21.000	1.318	0.202
M. unifolia	8.728	7.996	21.000	1.092	0.287
Random effects	σ^2	N		Marginal R^2	0.094
plot	0.000	5		AICc	190.095

Orchid (*Goodyera hachijoensis* var. *matumurana*) vs. Autotrophs					
δ^{13}C (‰)					
Fixed effects	Estimates	Std. Error	df	t	p-value
(Intercept)	−34.2556	0.319	2.9104	−107.335	2.5e-06
G. hachijoensis var. *matumurana*	−2.4778	0.5351	8.0000	−4.631	0.002
Random effects	σ^2	N		Marginal R^2	0.631
plot	0.3014	3		AICc	41.886
δ^{15}N (‰)					
Fixed effects	Estimates	Std. Error	df	t	p-value
(Intercept)	−3.8556	0.690	10.000	−5.59	0.000231

G. hachijoensis var. *matumurana*	5.122	1.379	10	3.713	0.004018
Random effects	σ^2	N		Marginal R^2	0.556
plot	0.000	3		AICc	59.931
N mmol/g					
Fixed effects	Estimates	Std. Error	df	t	p-value
(Intercept)	1.41111	0.03881	10.00000	36.36	5.89e-12
G. hachijoensis var. *matumurana*	−0.04444	0.07762	10.00000	−0.573	0.580
Random effects	σ^2	N		Marginal R^2	0.029
plot	0.0000	3		AICc	2.379
δ^2H (‰)					
Fixed effects	Estimates	Std. Error	df	t	p-value
(Intercept)	−52.457	5.061	8.000	−10.364	6.49e-06
G. hachijoensis var. *matumurana*	14.224	9.241	8.000	1.539	0.162
Random effects	σ^2	N		Marginal R^2	0.208
plot	0.0000	3		AICc	83.261

Orchid (*Odontchilus yakushimensis*) vs. Autotrophs

$\delta^{13}C$ (‰)					
Fixed effects	Estimates	Std. Error	df	t	p-value
(Intercept)	−33.8	0.531	10	−63.639	***
O. yakushimensis	−3.525	0.919	10	−3.832	**
Random effects	σ^2	N		Marginal R^2	0.572
plot	0.0	4		AICc	53.698
$\delta^{15}N$ (‰)					
Fixed effects	Estimates	Std. Error	df	t	p-value
(Intercept)	−5.812	0.597	10.000	−9.733	***
O. yakushimensis	3.513	1.034	10	3.396	**
Random effects	σ^2	N		Marginal R^2	
plot	0.0	4		AICc	
N mmol/g					
Fixed effects	Estimates	Std. Error	df	t	p-value
(Intercept)	1.2375	0.1568	4.7041	7.893	***
O. yakushimensis	0.2625	0.2175	7.000	1.207	0.267
Random effects	σ^2	N		Marginal R^2	0.094
plot	0.1878	4		AICc	26.682
$\delta^{2}H$ (‰)					
Fixed effects	Estimates	Std. Error	df	t	p-value
(Intercept)	−85.706	3.907	5.362	−21.935	***

O. yakushimensis	54.031	6.017	4.989	8.979	***
Random effects	σ^2	N		Marginal R^2	0.897
plot	1.719	4		AICc	77.822

Orchid (*Tainia laxiflora*) vs. Autotrophs					
$\delta^{13}C$ (‰)					
Fixed effects	Estimates	Std. Error	df	t	p-value
(Intercept)	−34.05	0.500	5.7290	−68.09	1.49e-09
T. laxiflora	−1.175	0.8276	7.0000	−1.4	0.199
Random effects	σ^2	N		Marginal R^2	0.149
plot	0.295	4		AICc	51.983
$\delta^{15}N$ (‰)					
Fixed effects	Estimates	Std. Error	df	t	p-value
(Intercept)	−3.2375	0.876	10.0	−3.694	0.00415
T. laxiflora	0.1875	1.518	10.0	0.124	0.904
Random effects	σ^2	N		Marginal R^2	0.001
plot	0.0	4		AICc	63.715
N mmol/g					
Fixed effects	Estimates	Std. Error	df	t	p-value
(Intercept)	0.8	0.09336	3.82999	8.569	0.00123
T. laxiflora	0.95000	0.09636	7.00000	9.859	***
Random effects	σ^2	N		Marginal R^2	0.822
plot	0.1500	4		AICc	12.519
$\delta^{2}H$ (‰)					

Fixed effects	Estimates	Std. Error	df	t	p-value
(Intercept)	−68.738	6.211	5.473	−11.066	***
T. laxiflora	32.912	9.917	7.000	3.319	*
Random effects	σ^2	N		Marginal R^2	0.479
plot	4.817	4		AICc	101.958

Orchid (*Zeuxine strateumtacia*) vs. Autotrophs					
$\delta^{13}C$ (‰)					
Fixed effects	Estimates	Std. Error	df	t	p-value
(Intercept)	−29.0625	0.277	19	−105.099	***
Z. strateumatica	−0.917	0.5667	19	−1.619	0.122
Random effects	σ^2	N		Marginal R^2	0.116
plot	0.0	5		AICc	72.633
$\delta^{15}N$ (‰)					
Fixed effects	Estimates	Std. Error	df	t	p-value
(Intercept)	−2.0956	0.492	6.303	−4.264	**
Z. strateumatica	2.036	0.811	14	2.512	*
Random effects	σ^2	N		Marginal R^2	0.236
plot	0.576	5		AICc	79.953
N mmol/g					
Fixed effects	Estimates	Std. Error	df	t	p-value
(Intercept)	1.7313	0.1253	19	13.815	***

Z. strateumatica	−0.8313	0.2568	19	−3.237	**
Random effects	σ^2	N		Marginal R^2	0.344
plot	0.0	5		AICc	42.559
δ^2H (‰)					
Fixed effects	Estimates	Std. Error	df	t	p-value
(Intercept)	−70.140	2.575	13.000	−27.242	***
Z. strateumatica	36.380	4.459	13.000	8.158	***
Random effects	σ^2	N		Marginal R^2	0.826
plot	0.0	5		AICc	107.327

Orchid (*Odontochilus tashiroi* and *Zeuxine boninensis*) vs. Autotrophs					
δ^{13}C (‰)					
Fixed effects	Estimates	Std. Error	df	t	p-value
(Intercept)	−36.23	0.395	16.0000	−91.804	<2e-16
O. tashiroi	0.750	0.684	16.0000	1.097	0.289
Z. boninensis	0.38	0.7383	16.0000	0.515	0.614
Random effects	σ^2	N		Marginal R^2	0.064
plot	0.0000	5		AICc	72.408
δ^{15}N (‰)					
Fixed effects	Estimates	Std. Error	df	t	p-value
(Intercept)	1.020	0.460	15.000	2.220	0.04228
O. tashiroi	2.640	0.796	15.000	3.317	0.00469

Z. boninensis	3.047	0.957	15	3.185	0.00615
Random effects	σ^2	N		Marginal R^2	0.493
plot	0.0000	5		AICc	73.791
N mmol/g					
Fixed effects	Estimates	Std. Error	df	t	p-value
(Intercept)	2.18	0.1791	16.0000	12.173	1.67e-09
O. tashiroi	0.6	0.3102	16.0000	1.934	0.07096
Z. boninensis	1.0450	0.335	16.0000	3.119	0.007
Random effects	σ^2	N		Marginal R^2	0.374
plot	0.0000	5		AICc	47.125
δ^2H (‰)					
Fixed effects	Estimates	Std. Error	df	t	p-value
(Intercept)	−36.780	1.315	9.280	−27.970	2.81e-10
O. tashiroi	0.960	2.155	11.367	0.445	0.664404
Z. boninensis	−11.214	2.336	12.253	−4.8	0.000409
Random effects	σ^2	N		Marginal R^2	0.589
plot	0.9501	5		AICc	109.949

Orchid (*Goodyera procera*) vs. Autotrophs					
δ^{13}C (‰)					
Fixed effects	Estimates	Std. Error	df	t	p-value
(Intercept)	−33.675	0.258	9.0000	−130.4	4.66e-16

G. procera	−1.1583	0.4945	9.0000	−2.342	0.044
Random effects	σ^2	N		Marginal R^2	0.354
plot	0.0000	3		AICc	37.731
δ^{15}N (‰)					
Fixed effects	Estimates	Std. Error	df	t	p-value
(Intercept)	−5.0361	0.909	2.138	−5.54	0.0267
G. procera	4.903	0.580	7	8.459	6.28e-05
Random effects	σ^2	N		Marginal R^2	0.642
plot	1.483	3		AICc	45.484
N mmol/g					
Fixed effects	Estimates	Std. Error	df	t	p-value
(Intercept)	1.2563	0.126	2.6468	9.972	0.00358
G. procera	−0.4229	0.1561	7.1395	−2.71	0.030
Random effects	σ^2	N		Marginal R^2	0.327
plot	0.1657	3		AICc	19.046
δ^2H (‰)					
Fixed effects	Estimates	Std. Error	df	t	p-value
(Intercept)	−69.533	6.006	2.199	−11.58	0.005177
G. procera	40.000	3.900	5.000	10.26	0.000151
Random effects	σ^2	N		Marginal R^2	
plot	9.644	3		AICc	

Orchid (*Cheirostylis takeoi*) vs. Autotrphs

$\delta^{13}C$ (‰)					
Fixed effects	Estimates	Std. Error	df	t	p-value
(Intercept)	−32.6	0.441	7.0000	−73.93	***
C. takeoi	3.7	0.7638	7.0000	4.801	***
Random effects	σ^2	N		Marginal R^2	0.742
plot	0.0	3		AICc	41.835

$\delta^{15}N$ (‰)					
Fixed effects	Estimates	Std. Error	df	t	p-value
(Intercept)	−0.5167	0.464	7.000	−1.114	0.30208
C. takeoi	3.483	0.803	7	4.336	0.00341
Random effects	σ^2	N		Marginal R^2	0.702
plot	0.000	3		AICc	42.542

N mmol/g					
Fixed effects	Estimates	Std. Error	df	t	p-value
(Intercept)	1.0833	0.1163	7	9.313	***
C. takeoi	0.5167	0.5167	7	2.564	*
Random effects	σ^2	N		Marginal R^2	0.451
plot	0.0	3		AICc	23.179

$\delta^{2}H$ (‰)					
Fixed effects	Estimates	Std. Error	df	t	p-value
(Intercept)	−61.433	8.814	7	−6.970	0.000217
C. takeoi	51.167	15.266	7	3.352	0.012223
Random effects	σ^2	N		Marginal R^2	0.584
plot	0.0	3		AICc	83.766

Orchid (*Zeuxine leucochila*) vs. Autotrophs					
$\delta^{13}C$ (‰)					
Fixed effects	Estimates	Std. Error	df	t	p-value
(Intercept)	−34.6143	0.679	9	−51.002	***
Z. leucochila	−0.4357	1.1255	9	−0.387	0.708
Random effects	σ^2	N		Marginal R^2	0.015
plot	0.0	4		AICc	54.076
$\delta^{15}N$ (‰)					
Fixed effects	Estimates	Std. Error	df	t	p-value
(Intercept)	−1.1	0.474	6.000	−23.23	0.0592
Z. leucochila	2.333	0.773	6	3.018	0.0235
Random effects	σ^2	N		Marginal R^2	0.565
plot	0.000	3		AICc	41.755
N mmol/g					
Fixed effects	Estimates	Std. Error	df	t	p-value
(Intercept)	1.4788	0.4565	3.9524	3.24	0.03224
Z. leucochila	1.9462	0.4385	6.1543	4.439	0.004
Random effects	σ^2	N		Marginal R^2	0.483
plot	0.7401	4		AICc	41.188
$\delta^{2}H$ (‰)					
Fixed effects	Estimates	Std. Error	df	t	p-value
(Intercept)	−53.257	2.9	9	−18.365	***

Z. leucochila	20.807	4.809	9	4.327	**
Random effects	σ^2	N		Marginal R^2	0.652
plot	0.000	4		AICc	80.217

Orchid (*Nervilia aragoana*) vs. Autotroph					
$\delta^{13}C$ (‰)					
Fixed effects	Estimates	Std. Error	df	t	p-value
(Intercept)	−34.5467	0.340	18	101.482	***
N. aragoana	0.3867	0.6808	18	0.568	0.577
Random effects	σ^2	N		Marginal R^2	0.017
plot	0.0	5		AICc	76.018
$\delta^{15}N$ (‰)					
Fixed effects	Estimates	Std. Error	df	t	p-value
(Intercept)	−2.32	0.208	18.000	−11.15	1.64e-09
N. aragoana	6.180	0.416	18	14.850	1.53e-11
Random effects	σ^2	N		Marginal R^2	0.921
plot	0.000	5		AICc	58.306
N mmol/g					
Fixed effects	Estimates	Std. Error	df	t	p-value
(Intercept)	1.24	0.1117	18	11.102	***
N. aragoana	0.6000	0.2234	18	2.686	*
Random effects	σ^2	N		Marginal R^2	0.275
plot	0.0	5		AICc	35.897

δ^2H (‰)					
Fixed effects	Estimates	Std. Error	df	t	p-value
(Intercept)	−61.987	3.644	5.706	−17.01	***
N. aragoana	37.815	6.669	14.062	5.67	***
Random effects	σ^2	N		Marginal R^2	0.613
plot	4.508	5		AICc	148.740

Chapter 4

General discussion

The effectiveness of δ^2H analysis on the estimation of nutritional mode in green orchids

Recent research has utilized hydrogen stable isotope ratios to assess the nutritional modes of orchids (Gebauer *et al.*, 2016; Schiebold *et al.*, 2018; Schweiger *et al.*, 2018, 2019), based on the premise that heterotrophic organic compounds, such as plant storage carbohydrates or fungi-derived compounds, exhibit ^{2}H enrichment (Yakir, 1992). Although this application has provided new insights into the nutritional modes of green orchids, prior studies have not adequately addressed exchangeable hydrogen. Inter-species variations in the exchangeable hydrogen fractions are largely mitigated by the nitration of extracted cellulose (e.g., Epstein *et al.*, 1976; Sternberg *et al.*, 1984; Luo & Sternberg, 1992). In Chapter 2, I explored the influence of exchangeable hydrogen on estimating plant nutritional modes by analyzing the δ^2H of samples with manipulated exchangeable hydrogen fractions. The findings revealed that the exchangeable hydrogen fractions do not significantly affect the estimation of nutritional modes. The findings suggest that using even the simplest bulk sample is feasible for estimating nutritional modes, thereby potentially accelerating progress in this research area.

Furthermore, even in instances where no ^{13}C enrichment is observed, I pointed out partial mycoheterotrophy can be estimated based on the significant enrichment of ^{15}N and ^{2}H compared to those of autotrophic plants. The ^{13}C depletion observed in rhizoctonia-associated orchids may be partially explained by the uptake of carbon from endophytic rhizoctonia, which is presumably ^{13}C-depleted compared to saprotrophic fungi (Gomes *et al.*, 2023; Zahn *et al.*, 2023). Conversely, Suetsugu *et al.* (2019) observed that the green

individuals of *Goodyera velutina*, which associate with supposedly-^{13}C enriched saprotrophic rhizoctonia, show depleted δ^{13}C, while the albino variant individuals of the species show ^{13}C enrichment (ε^{13}C = 8.8 ‰). This observation suggests that orchids may accumulate photosynthates, that are significantly more ^{13}C-depleted compared to other autotrophs. Therefore, even when the δ^{13}C of these orchids is similar to or lower than that of autotrophic plants, the acquisition of organic matter from fungi is not ruled out (Fig. 4.1). Consequently, the nutritional modes of rhizoctonia-associated orchids should be assessed in a phased manner — first comparing δ^{13}C, followed by δ^{15}N and δ^{2}H.

The nutritional mode of orchids investigated and its insights into the possible nature of partial mycoheterotrophy

Building on the findings from Chapter 2, which demonstrated the effectiveness of bulk δ^{2}H analysis in estimating the nutritional modes of green orchids, Chapter 3 further explored the fungal communities and nutritional modes of 13 orchid species by combining ^{2}H, ^{13}C, and ^{15}N stable isotope analysis with DNA barcoding. The analysis revealed that seven orchid species are associated with rhizoctonia and exhibit partial mycoheterotrophy. However, species such as *H. lepida* showed no significant differences in any stable isotope ratios compared to autotrophic plants, suggesting that some rhizoctonia-associated orchids may exhibit autotrophic behavior under certain conditions.

The current findings also point to the evolution of partial mycoheterotrophy in genera not previously recognized for this nutritional mode, including *Calanthe, Goodyera*, *Odontochilus*, and *Zeuxine*, in addition to genera *Cheirostylis* (Roy *et al.*, 2009; Yagi *et*

al., 2022) and *Nervilia* (Gale *et al.*, 2021), known for harboring partially mycoheterotrophic species. Therefore, my findings suggest a relatively widespread acquisition of this nutritional mode in orchids associated with rhizoctonia, at least within the two subfamilies investigated (Epidendroideae and Orchidoideae, Fig.4.2).

The prevalence of partial mycoheterotrophy among rhizoctonia-associated orchids in the other three subfamilies (Apostasioideae, Cypripedioideae, Vanilloideae) remains uncertain. In Apostasioideae, *Apostasia nipponica* is known to be partially mycoheterotrophic, depending on ectomycorrhizal fungi (Suetsugu & Matsubayashi, 2021a), although partial mycoheterotrophic species dependent on non-ECM rhizoctonia have not been reported within this subfamily. Similarly, while full mycoheterotrophy has frequently evolved in Vanilloideae (Cameron, 2009), the existence of partially mycoheterotrophic species in this subfamily has yet to be identified. In Cypripedioideae, two species, *Cypripedium debile* and *Cypripedium calceolus*, also associate with non-ECM rhizoctonia and show partial mycoheterotrophy (Gebauer *et al.*, 2016; Suetsugu *et al.*, 2021c); research on stable isotope signatures in more species from this subfamily is required to discuss their evolutionary history of mycoheterotrophy.

While many rhizoctonia-associated orchids have traditionally been considered autotrophic (Cameron *et al.*, 2006, 2008; Hynson *et al.*, 2009), several European species were suggested to be partially mycoheterotrophic based on earlier studies (Girlanda *et al.*, 2011; Gebauer *et al.*, 2016; Schiebold *et al.*, 2018; Schweiger *et al.*, 2018, 2019). On the other hand, recent research on the nutritional modes of Asian orchids has documented partial mycoheterotrophy in additional rhizoctonia-associated species (Suetsugu *et al.*,

2021a,c; Suetsugu & Matsubayashi, 2022), although research on the stable isotope signatures of rhizoctonia-associated orchids distributed in the Asian region is still limited. Given that the environmental factors of Asia, such as dark forest floors, warm temperatures, and high humidity, may more readily facilitate the evolution of mycoheterotrophy than those of the European region (Roy *et al.*, 2009; Lee *et al.*, 2015), a greater number of partial mycoheterotrophic orchids utilizing saprotrophic rhizoctonia as a nutritional source should be discovered from Asia. Indeed, the discovery of multiple partially mycoheterotrophic rhizoctonia-associated orchids in my study, conducted in the temperate and subtropical regions of Japan, also indicates the possible widespread nature of partial mycoheterotrophy in other green orchids.

Future directions in the research fields of orchid nutritional strategies

The present study, aligning with findings from Gebauer *et al.* (2016), supports the notion that partial mycoheterotrophy is relatively common among rhizoctonia-associated orchids. Nonetheless, given that Orchidaceae is a diverse family comprising over 28,000 species (Givnish *et al.*, 2015), and nutritional mode has been investigated in only dozens of species (Hynson *et al.*, 2013; Stöckel *et al.*, 2014; Liebel *et al.*, 2015; Gebauer *et al.*, 2016; Schiebold *et al.*, 2018; Schweiger *et al.*, 2018, 2019; Suetsugu *et al.*, 2021a,c; Jacquemyn *et al.*, 2021; Suetsugu & Matsubayashi, 2022; Yagi *et al.*, 2022; Gomes *et al.*, 2023; Zahn *et al.*, 2023; Wang *et al.*, 2023), further research is essential to elucidate the distribution of partial mycoheterotrophy within the family.

The utility of the hydrogen stable isotope analysis method, using bulk samples in

my study, has proven significant in addressing this research issue. However, for an accurate interpretation of ^{2}H enrichment in orchids, it is crucial to understand how factors other than partial mycoheterotrophy influence this enrichment. Investigating hydrogen isotope fractionation from water to sugars via photosynthesis and determining the stable hydrogen ratios of amino acids in fungal hyphae or plant leaves through compound-specific analysis could greatly enhance our understanding of these processes. Determining the hydrogen stable isotope ratios of rhizoctonia could also improve the accuracy of interpreting isotopic signatures in orchids. While the stable isotope ratios of rhizoctonia have long been elusive, recent research has begun to report the carbon and nitrogen stable isotope ratios of pelotons extracted from orchid root cells (Gomes *et al.*, 2023; Zahn *et al.*, 2023). However, data on the hydrogen stable isotope ratio of rhizoctonia fungi, which is expected to be higher than that of autotrophic plants (Yakir, 1992; Gebauer *et al.*, 2016; Cormier *et al.*, 2019), remain unreported. Since fungal bodies may exhibit exchangeable hydrogen fractions different from those of plants, comparisons with plants should employ techniques such as hot vapor equilibration (Filot *et al.*, 2006; Wassenaar *et al.*, 2015; Schuler *et al.*, 2022).

Beyond stable isotope analysis, alternative approaches could be employed to investigate the nutritional modes of orchids. Other techniques, such as the quantitative assessment of carbon and mineral nutrients transfer using radioactive or stable isotope tracers (Cameron *et al.*, 2006, 2008; Field *et al.*, 2015), may provide a more accurate understanding of the nutritional interactions between orchids and rhizoctonia, opening new avenues for comprehensive exploration in orchid ecology and evolution.

Figure

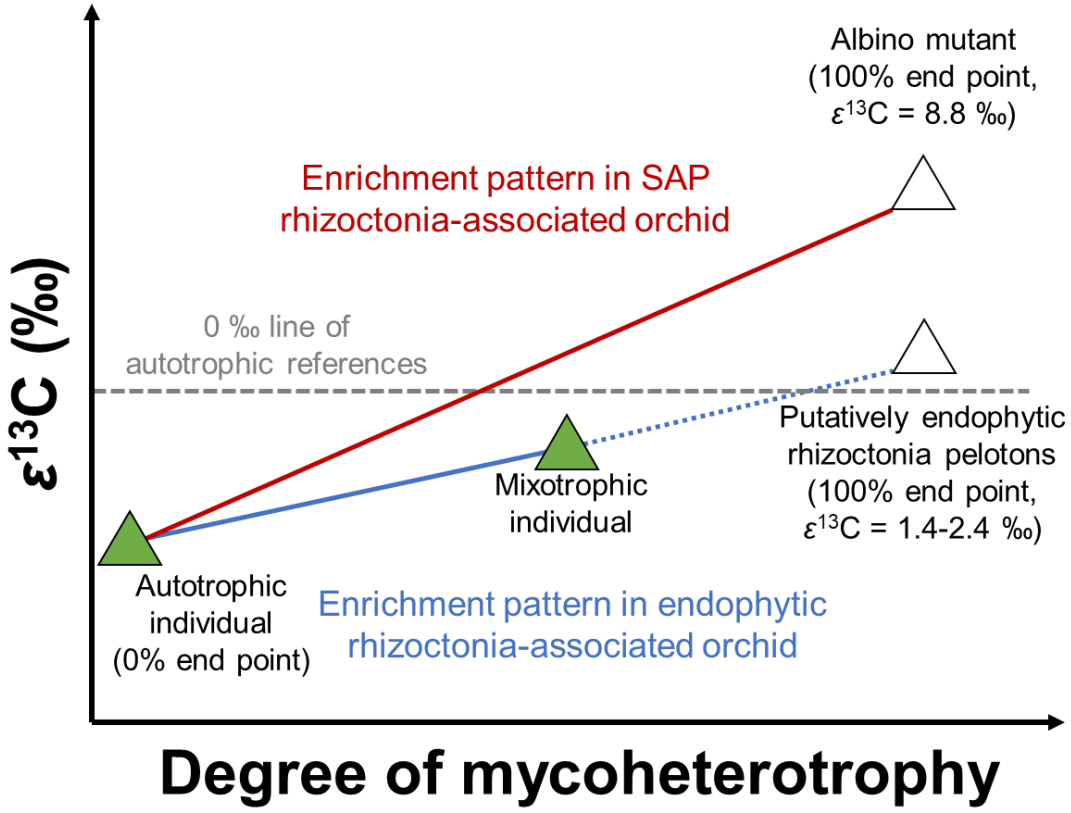

Figure 4.1. Schematic graph explaining the ^{13}C enrichment pattern in green/albino individuals of rhizoctonia-associated orchids.

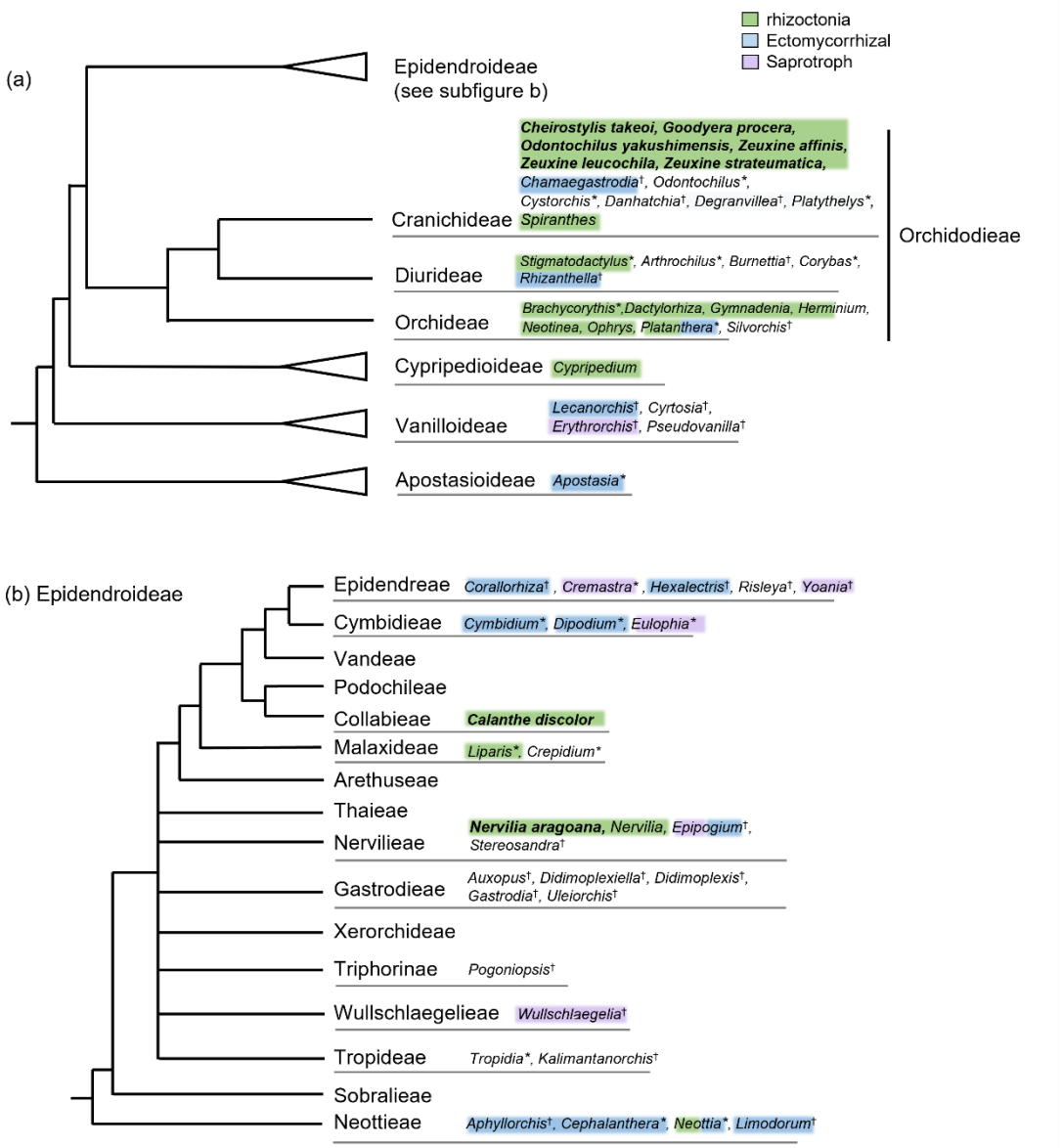

Figure 4.2. Phylogenetic tree of Orchidaceae (Chase *et al.*, 2015) and distribution of mycoheterotrophy within the tree. Mycorrhizal information reported in previous research is presented in green (rhizoctonia), blue (ectomycorrhizal fungi), or purple (saprotrophic fungi). Genera that include mycoheterotrophic species, and bolded species suggested to be partially mycoheterotrophic in this study, are listed. Stars indicate that both leafy and leafless species are included in the genus. Daggers indicate that the genus is composed of only fully mycoheterotrophic species.

Acknowledgements

I express sincere gratitude to Professor Kenji Suetsugu for providing me the opportunity to study interesting and challenging subjects and for the invaluable guidance and assistance throughout my research activities. I am thankful to Professor Kimitsune Ishizaki, Associate Professor Kaoru Tsuji, and Lecturer Ryo Onuma for reviewing the manuscript and providing comments. I thank Associate Professor Akiyo Naiki (Ryukyu University), Mr. Shigeki Fukushima (Chiba Prefectural Agriculture and Forestry Research Center), and Mr. Kaiji Umeki for their help with plant sampling. Professor Ichiro Tayasu, Dr. Chikage Yoshimizu (both from the Research Institute of Humanity and Nature), and Dr. Takashi F. Haraguchi (Research Institute of Environment, Agriculture, and Fisheries, Osaka Prefecture), as well as Associate Professor Jun Matsubayashi (University of Fukui), assisted with experimental designs and interpretation in stable isotope analysis. For the analysis of mycorrhizal fungal communities, Mr. Hidehito Okada (Suetsugu Laboratory) and Dr. Makoto Taniguchi (Genome Read Co., Ltd.) assisted with data acquisition and analysis. This study was financially supported by JSPS KAKENHI, the Joint Research Grant for Environmental Isotope Study of Research Institute for Humanity and Nature, the Fujiwara Natural History Foundation, and the JST Support for Pioneering Research Initiated by the Next Generation. I also thank all the current and past members of Suetsugu Laboratory for helpful discussions and support. Dr. Wataru Fujibuchi (Nippon Shinyaku Co., Ltd., and the University of Tokyo) provided the determination and spiritual guidance necessary to embark on the doctoral course. Finally, heartfelt appreciation is extended to my parents for their support in daily life.

References

Alexander WJ, Mitchell RL. **1949**. Rapid measurement of cellulose viscosity by the nitration method. *Analytical Chemistry* **21**: 1497–1500.

Bayman P, Mosquera-Espinosa AT, Saladini-Aponte CM, Hurtado-Guevara NC, Viera-Ruiz NL. **2016**. Age-dependent mycorrhizal specificity in an invasive orchid, *Oeceoclades maculata*. *American Journal of Botany* **103**: 1880–1889.

Bidartondo MI. **2005**. The evolutionary ecology of myco-heterotrophy. *New Phytologist* **167**: 335–352.

Bidartondo MI, Burghardt B, Gebauer G, Bruns TD, Read DJ. **2004**. Changing partners in the dark: isotopic and molecular evidence of ectomycorrhizal liaisons between forest orchids and trees. *Proceedings of the Royal Society of London. Series B: Biological Sciences* **271**: 1799–1806.

Bougoure J, Ludwig M, Brundrett M, Cliff J, Clode P, Kilburn M, Grierson P. **2014**. High-resolution secondary ion mass spectrometry analysis of carbon dynamics in mycorrhizas formed by an obligately myco-heterotrophic orchid. *Plant, Cell & Environment* **37**: 1223–1230.

Callahan BJ, McMurdie PJ, Rosen MJ, Han AW, Johnson AJA, Holmes SP. **2016**. DADA2: high-resolution sample inference from Illumina amplicon data. *Nature Methods* **13**: 581–583.

Cameron KM. **2009**. On the value of nuclear and mitochondrial gene sequences for reconstructing the phylogeny of vanilloid orchids (Vanilloideae, Orchidaceae). *Annals of Botany* **104**: 377–385.

Cameron DD, Johnson I, Read DJ, Leake JR. **2008**. Giving and receiving: measuring the carbon cost of mycorrhizas in the green orchid, *Goodyera repens*. *New Phytologist* **180**: 176–184.

Cameron DD, Leake JR, Read DJ. **2006**. Mutualistic mycorrhiza in orchids: evidence from plant–fungus carbon and nitrogen transfers in the green-leaved terrestrial orchid *Goodyera repens*. *New Phytologist* **171**: 405–416.

Chase MW, Cameron KM, Freudenstein JV, Pridgeon AM, Salazar G, Van den Berg C, Schuiteman A. **2015**. An updated classification of Orchidaceae. *Botanical Journal of the Linnean Society* **177**: 151–174.

Coplen TB. **2019**. *RSIL: Report of Stable Isotopic Composition for reference materials USGS61 USGS62 and USGS63 | U.S. Geological Survey*. Virginia: Reston Stable Isotope Laboratory.

Cormier MA, Werner RA, Leuenberger MC, Kahmen A. **2019**. ^{2}H-enrichment of cellulose and n-alkanes in heterotrophic plants. *Oecologia* **189**: 365–373.

Dearnaley JDW, Martos F, Selosse MA. **2012**. Orchid mycorrhizas: Molecular ecology, physiology, evolution and conservation aspects. In: Hock B, ed. The Mycota. Fungal associations. Berlin, Germany: Springer, 207–230. **Eastmond PJ, Astley HM, Parsley K, Aubry S, Williams BP, Menard GN, Craddock**

CP, Nunes-Nesi A, Fernie AR, Hibberd JM. 2015. *Arabidopsis* uses two gluconeogenic gateways for organic acids to fuel seedling establishment. *Nature Communications* **6**: 6659.

Epstein S, Yapp CJ, Hall JH. **1976**. The determination of the D/H ratio of non-exchangeable hydrogen in cellulose extracted from aquatic and land plants. *Earth and Planetary Science Letters* **30**: 241–251.

Esling P, Lejzerowicz F, Pawlowski J. **2015**. Accurate multiplexing and filtering for high-throughput amplicon-sequencing. *Nucleic Acids Research* **43**: 2513–2524.

Felsenstein J. **1985**. Confidence limits on phylogenies: an approach using the bootstrap. *Evolution* **39**: 783–791.

Field KJ, Leake JR, Tille S, Allinson KE, Rimington WR, Bidartondo MI, Beerling DJ, Cameron DD. **2015**. From mycoheterotrophy to mutualism: mycorrhizal specificity and functioning in *Ophioglossum vulgatum* sporophytes. *New Phytologist* **205**: 1492–1502.

Filot MS, Leuenberger M, Pazdur A, Boettger T. **2006**. Rapid online equilibration method to determine the D/H ratios of non-exchangeable hydrogen in cellulose. *Rapid Communications in Mass Spectrometry* **20**: 3337–3344.

Fochi V, Chitarra W, Kohler A, Voyron S, Singan VR, Lindquist EA, Barry KW, Girlanda M, Grigoriev IV, Martin F. **2017**. Fungal and plant gene expression in the *Tulasnella calospora–Serapias vomeracea* symbiosis provides clues about nitrogen pathways in orchid mycorrhizas. *New Phytologist* **213**: 365–379.

Fritsche Y, Lopes ME, Selosse M-A, Stefenon VM, Guerra MP. **2021**. *Serendipita restingae* sp. nov. (Sebacinales): an orchid mycorrhizal agaricomycete with wide host range. *Mycorrhiza* **31**: 1–15.

Gale SW, Maeda A, Miyashita A, Sugiura D, Ogura-Tsujita Y, Kinoshita A, Fujimori S, Hutchings MJ, Yukawa T. **2021**. International Biological Flora: *Nervilia nipponica*. *Journal of Ecology* **109**: 2780–2799.

Gaudinski JB, Dawson TE, Quideau S, Schuur EAG, Roden JS, Trumbore SE, Sandquist DR, Oh S-W, Wasylishen RE. **2005**. Comparative analysis of cellulose preparation techniques for use with ^{13}C, ^{14}C, and ^{18}O isotopic measurements. *Analytical Chemistry* **77**: 7212–7224.

Gebauer G, Meyer M. **2003**. ^{15}N and ^{13}C natural abundance of autotrophic and myco-heterotrophic orchids provides insight into nitrogen and carbon gain from fungal association. *New Phytologist* **160**: 209–223.

Gebauer G, Preiss K, Gebauer AC. **2016**. Partial mycoheterotrophy is more widespread among orchids than previously assumed. *New Phytologist* **211**: 11–15.

Gehre M, Renpenning J, Gilevska T, Qi H, Coplen TB, Meijer HAJ, Brand WA, Schimmelmann A. **2015**. On-line hydrogen-isotope measurements of organic samples using elemental chromium: an extension for high temperature elemental-analyzer techniques. *Analytical Chemistry* **87**: 5198–5205.

Giesemann P, Rasmussen HN, Liebel HT, Gebauer G. **2020**. Discreet heterotrophs: green plants that

receive fungal carbon through *Paris*-type arbuscular mycorrhiza. *New Phytologist* **226**: 960–966.

Girlanda M, Segreto R, Cafasso D, Liebel HT, Rodda M, Ercole E, Cozzolino S, Gebauer G, Perotto S. **2011**. Photosynthetic Mediterranean meadow orchids feature partial mycoheterotrophy and specific mycorrhizal associations. *American Journal of Botany* **98**: 1148–1163.

Givnish TJ, Spalink D, Ames M, Lyon SP, Hunter SJ, Zuluaga A, Iles WJD, Clements MA, Arroyo MTK, Leebens-Mack J, *et al.* 2015. Orchid phylogenomics and multiple drivers of their extraordinary diversification. *Proceedings of the Royal Society B: Biological Sciences* **282**: 20151553.

Gomes SIF, Giesemann P, Klink S, Hunt C, Suetsugu K, Gebauer G. **2023**. Stable isotope natural abundances of fungal hyphae extracted from the roots of arbuscular mycorrhizal mycoheterotrophs and rhizoctonia-associated orchids. *New Phytologist* **239**: 1166–1172.

Gonneau C, Jersáková J, de Tredern E, Till-Bottraud I, Saarinen K, Sauve M, Roy M, Hájek T, Selosse MA. **2014**. Photosynthesis in perennial mixotrophic *Epipactis* spp. (Orchidaceae) contributes more to shoot and fruit biomass than to hypogeous survival. *Journal of Ecology* **102**: 1183–1194.

Green JW. **1963**. Wood cellulose. In: Whistler RL, ed. Methods in Carbohydrate Chemistry. New York, USA: Academic Press, 9–21.

Halbwachs H, Dentinger BT, Detheridge AP, Karasch P, Griffith GW. **2013**. Hyphae of waxcap fungi colonise plant roots. *Fungal Ecology* **6**: 487–492.

Hobbie EA, Sánchez FS, Rygiewicz PT. **2012**. Controls of isotopic patterns in saprotrophic and ectomycorrhizal fungi. *Soil Biology and Biochemistry* **48**: 60–68.

Holloway-Phillips M, Baan J, Nelson DB, Lehmann MM, Tcherkez G, Kahmen A. **2022**. Species variation in the hydrogen isotope composition of leaf cellulose is mostly driven by isotopic variation in leaf sucrose. *Plant, Cell & Environment* **45**: 2636–2651.

Huson DH, Auch AF, Qi J, Schuster SC. **2007**. MEGAN analysis of metagenomic data. *Genome Research* **17**: 377–386.

Hynson NA, Madsen TP, Selosse MA, Adam IKU, Ogura-Tsujita Y, Roy M, Gebauer G. **2013**. The physiological ecology of mycoheterotrophy. In: Merckx VSFT, ed. Mycoheterotrophy: The biology of plants living on fungi. Berlin, Germany: Springer, 297–342.

Hynson NA, Preiss K, Gebauer G. **2009**. Is it better to give than to receive? A stable isotope perspective on orchid-fungal carbon transport in the green orchid species *Goodyera repens* and *Goodyera oblongifolia*. *New Phytologist* **182**: 8–11.

IAEA. **2007**. NBS 22, IAEA-CH-3, IAEA-CH-6, IAEA-CH-7, USGS24 reference sheet issue date: 3 August 2007.

Jacquemyn H, Brys R, Waud M, Busschaert P, Lievens B. **2015**. Mycorrhizal networks and coexistence in species-rich orchid communities. *New Phytologist* **206**: 1127–1134.

Jacquemyn H, Brys R, Waud M, Evans A, Figura T, Selosse M-A. **2021**. Mycorrhizal communities and isotope signatures in two partially mycoheterotrophic orchids. *Frontiers in Plant Science* **12**: 618140.

Jacquemyn H, Waud M, Lievens B, Brys R. **2016**. Differences in mycorrhizal communities between *Epipactis palustris*, *E. helleborine* and its presumed sister species *E. neerlandica*. *Annals of Botany* **118**: 105–114.

Jae-Young Y, Han-Kyeol H, Jae-Min C, Yong-Chan C, Byung-Chun L, Ahn-Heum E. **2012**. Identification of orchid mycorrhizal fungi isolated from five species of terrestrial orchids in Korea. *Korean Journal of Mycology* **40**: 132–135.

Kinoshita A, Ogura-Tsujita Y, Umata I, Sato H, Hashimoto T, Yukawa T. **2016**. How do fungal partners affect the evolution and habitat preferences of mycoheterotrophic plants? A case study in *Gastrodia*. *American Journal of Botany* **103**: 207–220.

Kohzu A, Yoshioka T, Ando T, Takahashi M, Koba K, Wada E. **1999**. Natural ^{13}C and ^{15}N abundance of field-collected fungi and their ecological implications. *New Phytologist* **144**: 323–330.

Kumar S, Stecher G, Li M, Knyaz C, Tamura K. **2018**. MEGA X: Molecular evolutionary genetics analysis across computing platforms. *Molecular Biology and Evolution* **35**: 1547–1549.

Kuznetsova A, Brockhoff PB, Christensen RHB. **2017**. LmerTest package: Tests in linear mixed effects models. *Journal of Statistical Software* **82**: 1–26.

Lallemand F, Puttsepp Ü, Lang M, Luud A, Courty P-E, Palancade C, Selosse M-A. **2017**. Mixotrophy in Pyroleae (Ericaceae) from Estonian boreal forests does not vary with light or tissue age. *Annals of Botany* **120**: 361–371.

Leake JR. **1994**. The biology of myco-heterotrophic ('saprophytic') plants. *New Phytologist* **127**: 171–216.

Leake JR, Cameron DD. **2010**. Physiological ecology of mycoheterotrophy. *New Phytologist* **185**: 601–605.

Lee YI, Yang CK, Gebauer G. **2015**. The importance of associations with saprotrophic non-*Rhizoctonia* fungi among fully mycoheterotrophic orchids is currently under-estimated: Novel evidence from sub-tropical Asia. *Annals of Botany* **116**: 423–435.

Liebel HT, Bidartondo MI, Gebauer G. **2015**. Are carbon and nitrogen exchange between fungi and the orchid *Goodyera repens* affected by irradiance? *Annals of Botany* **115**: 251–261.

Loader NJ, Robertson I, Barker AC, Switsur VR, Waterhouse JS. **1997**. An improved technique for the batch processing of small wholewood samples to α-cellulose. *Chemical Geology* **136**: 313–317.

Luo Y-H, Sternberg LO. **1992**. Hydrogen and oxygen isotopic fractionation during heterotrophic cellulose synthesis. *Journal of Experimental Botany* **43**: 47–50.

Merckx VSFT. **2013**. *Mycoheterotrophy: The biology of plants living on fungi*. Berlin, Germany:

Springer.

Merckx V, Freudenstein JV. **2010**. Evolution of mycoheterotrophy in plants: a phylogenetic perspective. *New Phytologist* **185**: 605–609.

Merckx VS, Freudenstein JV, Kissling J, Christenhusz MJ, Stotler RE, Crandall-Stotler B, Wickett N, Rudall PJ, Maas-van de Kamer H, Maas PJ. **2013a**. Taxonomy and classification. In: Merckx VSFT, ed. Mycoheterotrophy: The biology of plants living on fungi. Berlin, Germany: Springer, 19–101.

Merckx VS, Mennes CB, Peay KG, Geml J. **2013b**. Evolution and diversification. In: Merckx VSFT, ed. Mycoheterotrophy: The biology of plants living on fungi. Berlin, Germany: Springer, 215–244.

Merckx VSFT, Merckx VSFT. **2013**. Mycoheterotrophy: an introduction. In: Mycoheterotrophy: The biology of plants living on fungi. New York, USA: Springer, 1–17.

Nguyen NH, Song Z, Bates ST, Branco S, Tedersoo L, Menke J, Schilling JS, Kennedy PG. **2016**. FUNGuild: an open annotation tool for parsing fungal community datasets by ecological guild. *Fungal Ecology* **20**: 241–248.

Nilsson RH, Larsson K-H, Taylor AFS, Bengtsson-Palme J, Jeppesen TS, Schigel D, Kennedy P, Picard K, Glöckner FO, Tedersoo L. **2019**. The UNITE database for molecular identification of fungi: handling dark taxa and parallel taxonomic classifications. *Nucleic Acids Research* **47**: D259–D264.

Ogura-Tsujita Y, Yokoyama J, Miyoshi K, Yukawa T. **2012**. Shifts in mycorrhizal fungi during the evolution of autotrophy to mycoheterotrophy in *Cymbidium* (Orchidaceae). *American Journal of Botany* **99**: 1158–1176.

Ogura-Tsujita Y, Yukawa T. **2008**. High mycorrhizal specificity in a widespread mycoheterotrophic plant, *Eulophia zollingeri* (Orchidaceae). *American Journal of Botany* **95**: 93–97.

Ogura-Tsujita Y, Yukawa T, Kinoshita A. **2021**. Evolutionary histories and mycorrhizal associations of mycoheterotrophic plants dependent on saprotrophic fungi. *Journal of Plant Research* **134**: 19–41.

Olsen J, Seierstad I, Vinther B, Johnsen S, Heinemeier J. **2006**. Memory effect in deuterium analysis by continuous flow isotope ratio measurement. *International Journal of Mass Spectrometry* **254**: 44–52.

Preiss K, Adam IK, Gebauer G. **2010**. Irradiance governs exploitation of fungi: fine-tuning of carbon gain by two partially myco-heterotrophic orchids. *Proceedings of the Royal Society B: Biological Sciences* **277**: 1333–1336.

Preiss K, Gebauer G. **2008**. A methodological approach to improve estimates of nutrient gains by partially myco-heterotrophic plants. *Isotopes in Environmental and Health Studies* **44**: 393–401.

Qi H, Coplen TB, Jordan JA. **2016**. Three whole-wood isotopic reference materials, USGS54, USGS55, and USGS56, for δ^{2}H, δ^{18}O, δ^{13}C, and δ^{15}N measurements. *Chemical Geology* **442**: 47–53.

R Development Core Team. **2023**. *R: A language and environment for statistical computing, v.4.3.1.*

Vienna, Austria: R foundation for Statistical Computing.

Rasmussen HN, Rasmussen FN. **2009**. Orchid mycorrhiza: implications of a mycophagous life style. *Oikos* **118**: 334–345.

Rognes T, Flouri T, Nichols B, Quince C, Mahé F. **2016**. VSEARCH: a versatile open source tool for metagenomics. *PeerJ* **4**: e2584.

Roy M, Watthana S, Stier A, Richard F, Vessabutr S, Selosse M-A. **2009**. Two mycoheterotrophic orchids from Thailand tropical dipterocarpacean forests associate with a broad diversity of ectomycorrhizal fungi. *BMC Biology* **7**: 51.

Sakamoto Y, Ogura-Tsujita Y, Ito K, Suetsugu K, Yokoyama J, Yamazaki J, Yukawa T, Maki M. **2016**. The tiny-leaved orchid *Cephalanthera subaphylla* obtains most of its carbon via mycoheterotrophy. *Journal of Plant Research* **129**: 1013–1020.

Schiebold JMI, Bidartondo MI, Karasch P, Gravendeel B, Gebauer G. **2017**. You are what you get from your fungi: Nitrogen stable isotope patterns in *Epipactis* species. *Annals of Botany* **119**: 1085–1095.

Schiebold JMI, Bidartondo MI, Lenhard F, Makiola A, Gebauer G. **2018**. Exploiting mycorrhizas in broad daylight: Partial mycoheterotrophy is a common nutritional strategy in meadow orchids. *Journal of Ecology* **106**: 168–178.

Schuler P, Cormier M-A, Werner RA, Buchmann N, Gessler A, Vitali V, Saurer M, Lehmann MM. **2022**. A high-temperature water vapor equilibration method to determine non-exchangeable hydrogen isotope ratios of sugar, starch and cellulose. *Plant, Cell & Environment* **45**: 12–22.

Schuler P, Vitali V, Saurer M, Gessler A, Buchmann N, Lehmann MM. **2023**. Hydrogen isotope fractionation in carbohydrates of leaves and xylem tissues follows distinct phylogenetic patterns: a common garden experiment with 73 tree and shrub species. *New Phytologist* **239**: 547–561.

Schweiger JMI, Bidartondo MI, Gebauer G. **2018**. Stable isotope signatures of underground seedlings reveal the organic matter gained by adult orchids from mycorrhizal fungi. *Functional Ecology* **32**: 870–881.

Schweiger JMI, Kemnade C, Bidartondo MI, Gebauer G. **2019**. Light limitation and partial mycoheterotrophy in rhizoctonia-associated orchids. *Oecologia* **189**: 375–383.

Selosse MA, Charpin M, Not F. **2017**. Mixotrophy everywhere on land and in water: the grand écart hypothesis. *Ecology Letters* **20**: 246–263.

Selosse MA, Faccio A, Scappaticci G, Bonfante P. **2004**. Chlorophyllous and achlorophyllous specimens of *Epipactis microphylla* (Neottieae, Orchidaceae) are associated with ectomycorrhizal septomycetes, including truffles. *Microbial Ecology* **47**: 416–426.

Selosse M-A, Martos F. **2014**. Do chlorophyllous orchids heterotrophically use mycorrhizal fungal carbon? *Trends in Plant Science* **19**: 683–685.

Selosse M-A, Petrolli R, Mujica MI, Laurent L, Perez-Lamarque B, Figura T, Bourceret A, Jacquemyn H, Li T, Gao J, *et al.* 2022. The Waiting Room Hypothesis revisited by orchids: were orchid mycorrhizal fungi recruited among root endophytes? *Annals of Botany* **129**: 259–270.

Selosse M-A, Roy M. **2009**. Green plants that feed on fungi: facts and questions about mixotrophy. *Trends in plant science* **14**: 64–70.

Smith FA, Grace EJ, Smith SE. **2009**. More than a carbon economy: nutrient trade and ecological sustainability in facultative arbuscular mycorrhizal symbioses. *New Phytologist* **182**: 347–358.

Sternberg LO, Deniro MJ, Johnson HB. **1984**. Isotope ratios of cellulose from plants having different photosynthetic pathways. *Plant Physiology* **74**: 557–561.

Stöckel M, Těšitelová T, Jersáková J, Bidartondo MI, Gebauer G. **2014**. Carbon and nitrogen gain during the growth of orchid seedlings in nature. *New Phytologist* **202**: 606–615.

Suetsugu K, Haraguchi TF, Okada H, Tayasu I. **2021a**. *Stigmatodactylus sikokianus* (Orchidaceae) mainly acquires carbon from decaying litter through association with a specific clade of Serendipitaceae. *New Phytologist* **231**: 1670–1675.

Suetsugu K, Haraguchi TF, Tanabe AS, Tayasu I. **2021b**. Specialized mycorrhizal association between a partially mycoheterotrophic orchid *Oreorchis indica* and a *Tomentella* taxon. *Mycorrhiza* **31**: 243–250.

Suetsugu K, Haraguchi TF, Tayasu I. **2022a**. Novel mycorrhizal cheating in a green orchid: *Cremastra appendiculata* depends on carbon from deadwood through fungal associations. *New Phytologist* **235**: 333–343.

Suetsugu K, Matsubayashi J. **2021a**. Evidence for mycorrhizal cheating in *Apostasia nipponica*, an early-diverging member of the Orchidaceae. *New Phytologist* **229**: 2302–2310.

Suetsugu K, Matsubayashi J. **2021b**. Subterranean morphology modulates the degree of mycoheterotrophy in a green orchid *Calypso bulbosa* exploiting wood-decaying fungi. *Functional Ecology* **35**: 2305–2315.

Suetsugu K, Matsubayashi J. **2022**. Foliar chlorophyll concentration modulates the degree of fungal exploitation in a rhizoctonia-associated orchid. *Journal of Experimental Botany* **73**: 4204–4213.

Suetsugu K, Matsubayashi J, Ogawa NO, Murata S, Sato R, Tomimatsu H. **2020**. Isotopic evidence of arbuscular mycorrhizal cheating in a grassland gentian species. *Oecologia* **192**: 929–937.

Suetsugu K, Ohta T, Tayasu I. **2018**. Partial mycoheterotrophy in the leafless orchid *Cymbidium macrorhizon*. *American Journal of Botany* **105**: 1595–1600.

Suetsugu K, Okada H. **2021**. Symbiotic germination and development of fully mycoheterotrophic plants convergently targeting similar Glomeraceae taxa. *Environmental Microbiology* **23**: 6328–6343.

Suetsugu K, Okada H, Hirota SK, Suyama Y. **2022b**. Evolutionary history of mycorrhizal associations

between Japanese *Oxygyne* (Thismiaceae) species and Glomeraceae fungi. *New Phytologist* **235**: 836–841.

Suetsugu K, Yamato M, Matsubayashi J, Tayasu I. **2019**. Comparative study of nutritional mode and mycorrhizal fungi in green and albino variants of *Goodyera velutina*, an orchid mainly utilizing saprotrophic rhizoctonia. *Molecular Ecology* **28**: 4290–4299.

Suetsugu K, Yamato M, Matsubayashi J, Tayasu I. **2021c**. Partial and full mycoheterotrophy in green and albino phenotypes of the slipper orchid *Cypripedium debile*. *Mycorrhiza* **31**: 301–312.

Tanabe AS. **2018**. 'Claident v0.2.2018.05.29' A program distributed by the author. Available online at: http://www.fifthdimension.jp/. *Claident v0.2.2015*.

Tanabe AS, Toju H. **2013**. Two new computational methods for universal DNA barcoding: A benchmark using barcode sequences of bacteria, archaea, animals, fungi, and land plants. *PLoS ONE* **8**: e76910.

Tayasu I, Hirasawa R, Ogawa NO, Ohkouchi N, Yamada K. **2011**. New organic reference materials for carbon- and nitrogen-stable isotope ratio measurements provided by Center for Ecological Research, Kyoto University, and Institute of Biogeosciences, Japan Agency for Marine-Earth Science and Technology. *Limnology* **12**: 261–266.

Taylor AFS, Högbom L, Högberg M, Lyon AJE, Näsholm T, Högberg P. **1997**. Natural ^{15}N abundance in fruit bodies of ectomycorrhizal fungi from boreal forests. *New Phytologist* **136**: 713–720.

Taylor DL, McCormick MK. **2008**. Internal transcribed spacer primers and sequences for improved characterization of basidiomycetous orchid mycorrhizas. *New Phytologist* **177**: 1020–1033.

Valladares F, Niinemets Ü. **2008**. Shade tolerance, a key plant feature of complex nature and consequences. *Annual Review of Ecology, Evolution and Systematics* **39**: 237–257.

Vancov T, Keen B. **2009**. Amplification of soil fungal community DNA using the ITS86F and ITS4 primers. *FEMS Microbiology Letters* **296**: 91–96.

Veldre V, Abarenkov K, Bahram M, Martos F, Selosse M-A, Tamm H, Kõljalg U, Tedersoo L. **2013**. Evolution of nutritional modes of Ceratobasidiaceae (Cantharellales, Basidiomycota) as revealed from publicly available ITS sequences. *Fungal Ecology* **6**: 256–268.

Wang D, Gebauer G, Jacquemyn H, Zahn FE, Gomes SIF, Lorenz J, Van Der Hagen H, Schilthuizen M, Merckx VSFT. **2023**. Variation in mycorrhizal communities and the level of mycoheterotrophy in grassland and Forest populations of *Neottia ovata* (Orchidaceae). *Functional Ecology* **37**: 1948–1961.

Wang D, Jacquemyn H, Gomes SIF, Vos RA, Merckx VSFT. **2021**. Symbiont switching and trophic mode shifts in Orchidaceae. *New Phytologist* **231**: 791–800.

Wassenaar LI, Hobson KA, Sisti L. **2015**. An online temperature-controlled vacuum-equilibration preparation system for the measurement of δ^2H values of non-exchangeable-H and of $\delta^{18}O$ values in

organic materials by isotope-ratio mass spectrometry. *Rapid Communications in Mass Spectrometry* **29**: 397–407.

Xiang X-G, Jin W-T, Li D-Z, Schuiteman A, Huang W-C, Li J-W, Jin X-H, Li Z-Y. **2014**. Phylogenetics of tribe Collabieae (Orchidaceae, Epidendroideae) based on four chloroplast genes with morphological appraisal. *PLOS ONE* **9**: e87625.

Yagame T, Funabiki E, Nagasawa E, Fukiharu T, Iwase K. **2013**. Identification and symbiotic ability of Psathyrellaceae fungi isolated from a photosynthetic orchid, *Cremastra appendiculata* (Orchidaceae). *American Journal of Botany* **100**: 1823–1830.

Yagame T, Orihara T, Selosse M, Yamato M, Iwase K. **2012**. Mixotrophy of *Platanthera minor*, an orchid associated with ectomycorrhiza-forming Ceratobasidiaceae fungi. *New Phytologist* **193**: 178–187.

Yagi R, Tayasu I, Suetsugu K. **2022**. Partial mycoheterotrophy in rhizoctonia-associated orchid *Cheirostylis liukiuensis*. *Plant Species Biology* **37**: 257–264.

Yagi R, Haraguchi TF, Tayasu I, Suetsugu K. **2024**. Do exchangeable hydrogens affect the evaluation of partial mycoheterotrophy in orchids?: Insights from δ2H analysis in bulk, α-cellulose, and cellulose nitrate samples. *New Phytologist* https://doi.org/10.1111/nph.19998

Yakir D. **1992**. Variations in the natural abundance of oxygen-18 and deuterium in plant carbohydrates. *Plant, Cell & Environment* **15**: 1005–1020.

Yuan Y, Jin X, Liu J, Zhao X, Zhou J, Wang X, Wang D, Lai C, Xu W, Huang J. **2018**. The *Gastrodia elata* genome provides insights into plant adaptation to heterotrophy. *Nature Communications* **9**: 1–11.

Zahn FE, Lee Y-I, Gebauer G. **2022**. Fungal association and root morphology shift stepwise during ontogenesis of orchid *Cremastra appendiculata* towards autotrophic nutrition. *AoB Plants* **14**: 1–10.

Zahn FE, Söll E, Chapin TK, Wang D, Gomes SIF, Hynson NA, Pausch J, Gebauer G. **2023**. Novel insights into orchid mycorrhiza functioning from stable isotope signatures of fungal pelotons. *New Phytologist* **239**: 1449–1463.